Development of Novel Catalysts for the Hydrodeoxygenation of Vegetable Oils

A Thesis Submitted to the College of Graduate and Postdoctoral Studies in Partial Fulfillment of the Requirements for the Degree of Doctor of Philosophy in the Department of Chemical and Biological Engineering,

University of Saskatchewan, Saskatoon, SK

Canada

By

Naveenji Arun

PERMISSION TO USE

I grant that the libraries of the University of Saskatchewan may make this thesis available for inspection for free. The permission for using this thesis in any form for scholarly purposes may be granted by Dr. Ajay Dalai and Dr. Yongfeng Hu, who are the supervisors during my PhD study. In the case of their absence, the use of this thesis could be granted by Head of the Department of Chemical and Biological Engineering or the Dean of the College of Engineering.

Any other use of the thesis for financial gain without the University of Saskatchewan and author's permission is prohibited. Also, due recognition shall be given to me and the University of Saskatchewan for any use.

The requests for permission to copy, or use any content in this thesis should be sent to:

Head of the Department

Chemical and Biological Engineering

57 Campus Drive

Saskatoon, Saskatchewan

Canada S7N 5A9

ABSTRACT

Traditional hydrotreating catalysts and NiMo supported on various support materials, were evaluated for their catalytic activity towards HDO of oleic acid. It was concluded that NiMo supported on γ-Al_2O_3 offered better catalytic activity in terms of oleic acid conversion and selectivity towards n-octadecane. Extensive characterization of the NiMo supported on γ-Al_2O_3 was conducted to understand the structure-activity relationship for the NiMo/γ-Al_2O_3 using Raman mapping and X-ray absorption spectroscopy. Raman analysis indicates that the Mo and Ni species are not uniformly distributed on the support material. Raman spectroscopy indicated that Mo is present in the form of clusters and these Mo clusters interact with the support material. Mo L_3-edge clearly indicated that γ-Al_2O_3 and SBA-15 supports offered distorted tetrahedral-octahedral and tetrahedral geometry, respectively. Better catalytic performance of γ-Al_2O_3 supported catalyst was attributed to the occurrence of distorted tetrahedral-octahedral geometry.

NiMo/γ-Al_2O_3 was impregnated with Cu, Cr and Fe to understand the performance of supported trimetallic catalyst systems for HDO of oleic acid. Reactions were carried out at 300°C, hydrogen pressure of 6.89 MPa and agitation speed maintained at 600 rpm. Maximum hydrodeoxygenation conversion of 92% was obtained using CuNiMo/γ-Al_2O_3 followed by FeNiMo/γ-Al_2O_3. It was concluded that Cu and Fe have the potential to actively participate in redox reactions and aid in the removal of oxygen from the feedstock by reverse Mars-van Krevelen mechanism. Optimization of the process parameters (reaction temperature, catalyst loading, hydrogen pressure, reaction time) was performed using orthogonal design matrix (OA_{16} matrix) for the best performing catalyst (CuNiMo/γ-Al_2O_3).

The order of significant factors affecting the conversion of oleic acid was found to be: reaction temperature > catalyst loading > hydrogen pressure > reaction time.

FeCu supported on γ-Al_2O_3 was prepared by impregnation method to evaluate its HDO performance. For comparison, the unsupported mixed metal oxide catalyst, commercial NiMo and FeCu supported catalysts were evaluated for HDO of oleic acid. During hydrodeoxygenation of oleic acid at different reaction temperatures, the conversion obtained using a mixed metal catalyst (MMC) was higher (>90%) in comparison to commercial NiMo/γ-Al_2O_3 (80-85%) and FeCu/γ-Al_2O_3 catalyst (>85%). However, the product selectivity study indicated that FeCu/γ-Al_2O_3 catalyst works better for HDO of oleic acid at similar process conditions. Additionally, the FeCu catalyst systems offered higher HDO conversion (>85%) at less severe operating conditions (T< 320° C; P_{H2} < 8.96 MPa, reaction time < 8 h) and regeneration studies were performed on the same catalyst.

Life cycle and techno-economic assessment of the HDO process were carried out to understand the environmental and economic impact of the HDO process using canola oil as feedstock. It was found that the green diesel production pathway (HDO process) is 95% energy efficient while the biodiesel pathway (transesterification process) is only 85% energy efficient.

ACKNOWLEDGEMENTS

I would like to thank my supervisors Dr. Ajay Dalai, and Dr. Yongfeng Hu for their technical advice and supervision on my research work.

Special thanks to my Ph.D. advisory committee, Dr. Richard Evitts, Dr. Ramaswami Sammynaiken, Dr. Lope Tabil, and Dr. Lee Wilson for evaluating my research progress. Technical support and suggestions from Ms. Heli Eunike, and Mr. Richard B. Prokopishyn are deeply appreciated.

My sincere gratitude to the financial supporters of my research including BioFuelNet Canada, Natural Science and Engineering Research Council of Canada, and the University of Saskatchewan.

I would like to thank my friends (not in any special order), Esther, Marina, Ankita, Manjunathan, Haneesha, Zanil, Sana, Tina, Jeevan, Vamsi, Karthik, Sudhakar, Phani, Venu for their companionship.

Special thanks to Dr. Abraham Ninan and Mrs. Ninan, Mr. James Premkumar, Dr. Kalyani Premkumar for their prayers, food, and moral support.

Above all, I want to thank my family: my parents and my sister for trusting in me through troubled times and supporting me spiritually throughout my Ph.D. program and my life in general.

DEDICATION

My dear parents and sister, V. S. Arun, Jessy Arun and Preethi, who encouraged me throughout my program and supported me in several ways.

My wonderful wife, Gayathri, who shared all the good and tough times with me.

TABLE OF CONTENTS

LIST OF TABLES

LIST OF FIGURES

NOMENCLATURE

Ar	argon
HDO	hydrodeoxygenation
HYD	hydrogenation
H_2	hydrogen
IN	entering the reactor
M	total mass *{g}*
N	normalized
OA	oleic acid
OUT	exiting the reactor
T	temperature *{°C}*

CHAPTER 1

INTRODUCTION AND RESEARCH OVERVIEW

1.1 Introduction

Globally, the outlook and motivation towards the development and usage of cleaner and renewable source of energy are growing due to environmental health hazards associated with the emissions from fossil fuels. Increase in production and consumption of energy are directly related to the growth in population and economic status of the people. Owing to factors such as capital interests, fluctuations in oil prices and other geopolitical issues there is a tremendous growth in biofuel industry globally (Romero et al. 2009). Considerable work has been done on bio-based fuels production from rapeseed oil, soybean oil, palm oil, Karanja oil, waste cooking oil (Kim et al. 2013). According to the prediction by International Energy Agency (IEA), liquid biofuels will dominate the energy sector by 2030.

Fig 1.1. indicates the rise in world energy consumption (quadrillion Btu) from 1990 till date and its future trend (IEA, 2011). It is seen that there will be a constant rise in energy demands in future. Transition in the economy from the dependency on non-renewable fossil fuels to fuels from bio-based renewable resources poses considerable challenges because the energy needs of present generation should be met without altering or depleting the resources for future generations (Azadi et al. 2013). Availability of constant energy source at an affordable price is a key factor for a nation's gross domestic product (GDP) (Miskolczi et al. 2010). Fig. 1.2.a and b indicate the energy consumption in Organization for Economic Co-operation and Development (OECD) region in 2008 and its projection for 2035 (IEA, 2011).

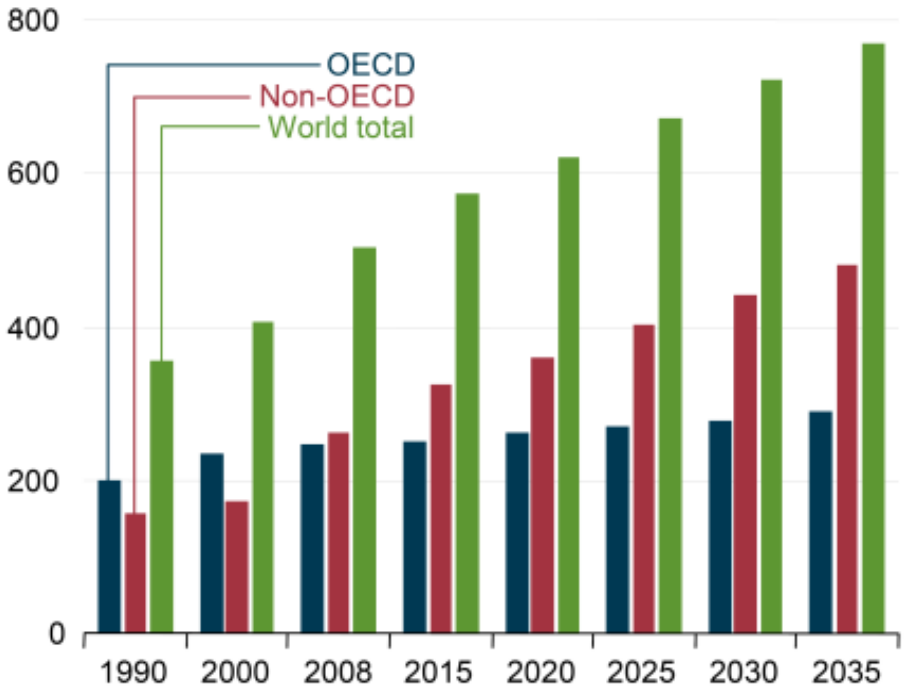

Fig. 1.1 Projected energy consumption (IEA, 2011)

Fig 1.2. c and d indicate the energy consumption in the non-OECD region in 2008 and its projection for 2035 respectively. It could be seen that the energy demands for the Asian countries will rise tremendously in comparison to Americas and the European Union.

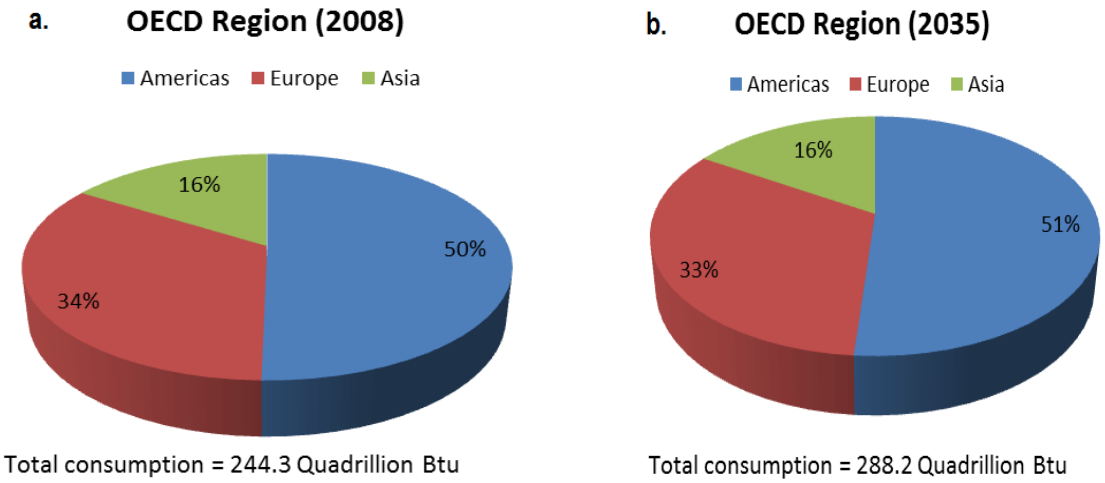

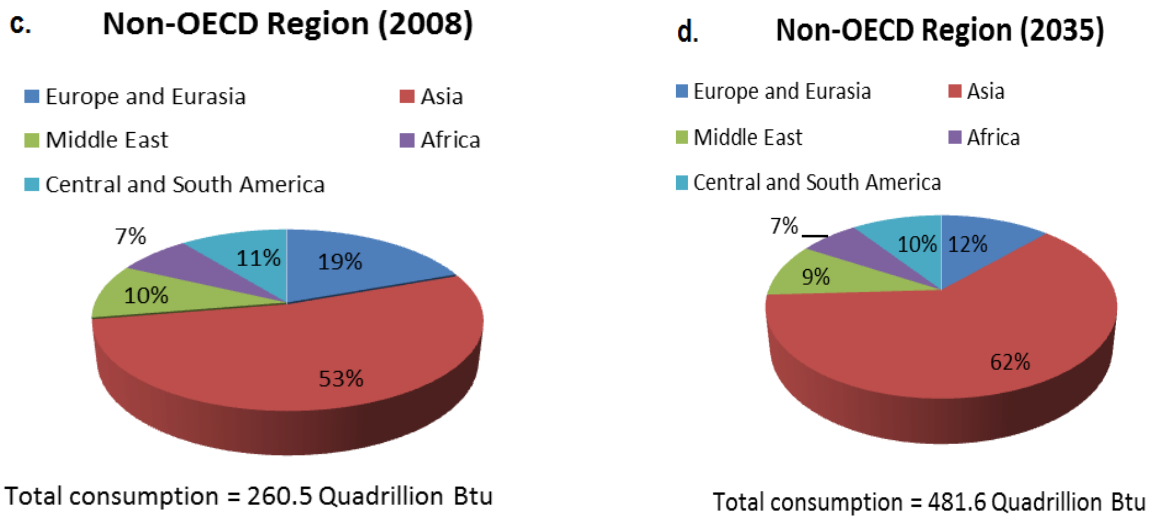

Fig. 1.2 World energy consumption by country grouping (IEA, 2011)

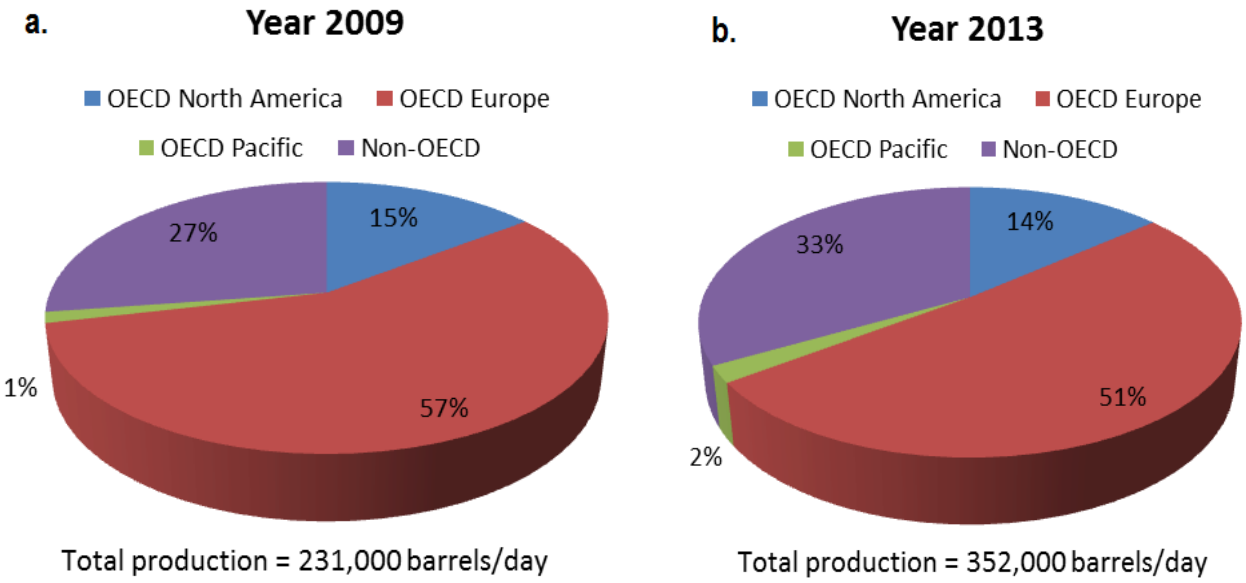

Fig. 1.3 World biodiesel production (IEA, 2009).

From Figs. 1.1 and 1.2, it is evident that an overwhelming demand for alternate fuels will arise and a replacement to fossil fuels is highly essential. Innovations in technology, hike in oil prices, employment effects, reduction in emission of greenhouse gases and continued support from the

government through various policies contribute to the rapid growth of biofuels industry. About 40% of global liquid fuels demand will be met by biofuels after 2020 and it is projected to approach 60% by 2030. Fig. 1.3 represents the growth in biofuel sector from 2009 to 2013 and it confirms the immediate need for alternate fuels across the globe.

First generation fuels primarily involve fossil fuel resources such as coal, petroleum and natural gases. Depletion of fossil fuel resources and the environmental issues associated with their usage resulted in the search for second generation fuels. Production of second generation fuels involves feedstocks such as corn to obtain bio-ethanol and bio-based fuels. However, most of the feed sources are edible and they lead to food vs. fuel problem. Third generation fuel involves usage of sources such as lignocellulosic biomass, waste cooking oil, and non-edible vegetable oils. Biofuels tend to have a high oxygen content that can impart deleterious characteristics such as elevated thermal and chemical instability, lower heating values and higher viscosity in comparison to fossil fuels. Hence, upgrading of biofuels is crucial to producing usable fuels commercially.

Recently, technologies such as biomass to liquid fuels (BTL) and hydrotreatment of vegetable oils to produce green diesel are being focused. Fig. 1.4 represents the trend in the growth of biofuel sector. Presently, fossil fuels and second generation fuels such as biodiesel and bioethanol are being commercially used and it is evident that technologies such as BTL and hydrotreated vegetable oil (HVO) are promising routes to meet the future energy demands. Methods for upgradation of fuels can be broadly classified into chemical and physical methods. Chemical upgrading methods include catalytic esterification (Xu et al. 2008) hydrothermal liquefaction, hydrodeoxygenation and catalytic hydroprocessing (Elliott and Hart, 2009; Donnis et al. 2009).

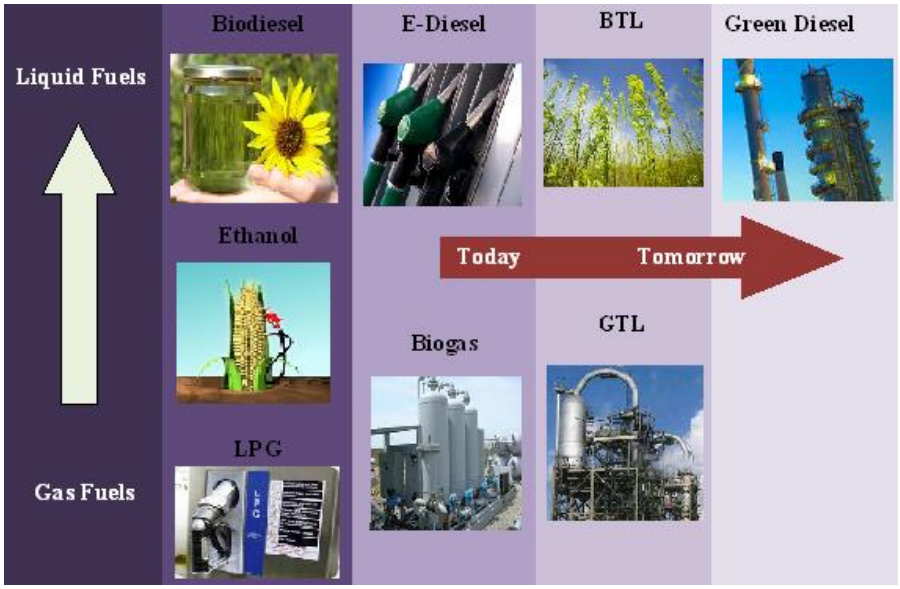

Fig. 1.4 Trend in the growth of biofuel sector (Reproduced from Arun et al. (2015) with permission from Elsevier)

Physical upgrading method includes char removal, hot vapor filtration, solvent addition and extraction of organic acids (Mahfud et al. 2008; Luo et al. 2010). In case of hydrothermal liquefaction, the biomass is converted to fuels and chemicals under a supercritical condition in the presence of water at a temperature of 350-374°C (Toor et al. 2011). Inclusive of hydrodeoxygenation process, other methods such as catalytic cracking (Nokkosmaki et al. 2000; Graca et al. 2011), emulsification (Chiaramonti et al. 2003), steam reforming and esterification (Zhang et al. 2006) have been investigated for upgradation of fuels. Li et al. (2011) reported on upgrading bio-oil, especially the low-boiling fraction using supercritical methanol and it was proven to be an efficient method. Many other methods such as supercritical method (Dickinson et al. 2012; Duan et al. 2011), pyrolysis (Mercader et al. 2010), gasification, Fisher-Tropsch synthesis (Lappas et al. 2009; Damartzis et al. 2011), liquefaction and hydrotreating are also being used to produce liquid fuels (Naik et al. 2010). Biomass-derived feedstocks can be converted into fuels and useful chemicals in three routes: (1) fluid catalytic cracking (FCC), (2)

hydrotreating-hydrocracking, and (3) utilization of biomass-derived synthesis gas (syngas) or hydrogen. Presently, hydrotreating process for converting vegetable oils and animal fats into renewable diesel fuel substitutes is gaining considerable importance.

1.2 Knowledge gaps and Hypotheses

Based on the literature review, the following knowledge gaps were identified.

Knowledge gaps

- Limited literature have reported on the development of nitride catalyst for HDO of oleic acid (model compound) and real feedstocks.
- Studies on the influence of promoter metals such as copper (Cu), iron (Fe) and chromium (Cr) on the performance of $NiMo/Al_2O_3$ catalysts for HDO of oleic acid are not reported in the literature.
- Literature on techno-economic and life cycle analysis of the HDO process are scarce.

Hypothesis

- Metallic nitride catalysts are reported to be efficient for hydrotreating reactions such as hydrodenitrogenation and hydrodesulfurization. Hence, metallic nitride catalysts are suitable for HDO reaction. The acidity of the support material and pore size of mesoporous catalytic materials are crucial factors governing the extent of hydrotreating reaction.
- Transition metallic catalysts promoted with metals such as Cu, Fe, and Cr are efficient in terms of catalytic activity.
- Green diesel produced by the HDO process is energy efficient and its impact on the environment is comparatively lesser than fossil fuels.

1.3 Research objectives

The overall objective of this Ph.D. research work is to develop novel catalysts for the HDO of vegetable oils and evaluate their performance. Following are the specific objectives involved to accomplish the overall objective:

1. Evaluate reduced NiMo catalysts supported on different support materials (Al_2O_3, SBA-15, and HMS) for the HDO of oleic acid;
2. To characterize reduced NiMo catalysts using Raman spectroscopy and X-ray absorption spectroscopy to understand the coordination geometry of the catalyst and develop structure-activity relationship;
3. To investigate the promotional effects of Cu, Cr, and Fe on NiMo/γ-Al_2O_3 for the HDO of oleic acid;
4. To compare commercial NiMo/γ-Al_2O_3, mixed-metal catalyst and FeCu/γ-Al_2O_3 for the HDO of model compound (oleic acid); and
5. To perform techno-economic and life cycle analysis of HDO process.

1.4 Thesis Outline

The thesis titled 'Development of Novel Catalysts for the Hydrodeoxygenation (HDO) of Vegetable Oils' illustrates the transition from traditional NiMo based catalyst to a novel FeCu supported catalyst system for hydrodeoxygenation reactions and environmental impact assessment of hydrodeoxygenation process. The importance of this research work and the literature review that forms the background for this research work are detailed in Chapters 1 and 2. As the acidity of the support material plays a crucial role, NiMo supported on γ-Al_2O_3, SBA-15 and HMS were evaluated and detailed characterization of the catalysts was performed

(Chapter 3 and 4). Based on the findings from the initial experiments, an attempt was made to understand the performance of NiMo/γ-Al_2O_3 catalyst system with promoters such as Cu, Cr, and Fe. NiMo/γ-Al_2O_3 selected from the earlier phases was impregnated with Cu, Cr, and Fe to understand the performance of supported trimetallic catalysts systems for HDO of oleic acid (Chapter 5). Based on the performance of trimetallic catalyst systems, it was planned to develop FeCu based supported catalyst by impregnation method and evaluate its HDO performance. Commercial NiMo/γ-Al_2O_3 catalyst was chosen as the reference material to compare the performance of the synthesized catalysts (Chapter 6). Finally, techno-economic and environmental impact assessment of the HDO process was performed, and its assessment was compared to biodiesel production process (Chapter 7).

The most significant feature of this thesis is the development of novel FeCu supported catalyst system that can actively catalyze HDO reactions at less severe operating conditions and evaluation of techno-economic and life cycle impact of the hydrodeoxygenation process using real feedstock.

CHAPTER 2

LITERATURE REVIEW

This part of the work has been published as research article and was presented at the following conference:

1. N. Arun, R. V. Sharma, A. K. Dalai. Green diesel synthesis by hydrodeoxygenation of bio-based feedstocks: Strategies for catalyst design and development. *Renewable Sustainable Energy Rev.* 48, 240, 2015.
2. N. Arun, R. V. Sharma and A.K. Dalai (Invited talk) "Conversion of agricultural crops to bio-based fuels and chemicals – Technical and Economic challenges in Canadian biofuel Industry", CHEMCON 2013, 66th Annual Session of Indian Institute of Chemical Engineers, India, December 27-30, 2013.

Contribution of the Ph.D. candidate and collaborators

Manuscript writing and revision work were done by Naveenji Arun based on the suggestions from Dr. Ajay K. Dalai and Dr. Rajesh V. Sharma. Dr. R. V. Sharma proofread the manuscript (No.1) before submission.

The contribution of this chapter to the overall Ph. D. work

This chapter focused on understanding the basis of catalyst design and development for hydrodeoxygenation reactions.

Abstract

Biofuels have gained considerable attention as an efficient alternative for fossil fuels to meet the energy demands of the present and future generations. In this review, the chemistry of HDO, strategies for catalyst development, process design and usage of life cycle assessment are focussed to understand the environmental and commercial impact of alternate fuels sector on

global fuel economy. Majorly, the studies that include life-cycle assessment (LCA) are related to the energy efficiency and impact of greenhouse gas (GHG) emissions of alternate biofuels systems. Complete replacement of fossil fuels by biofuels is highly challenging and not feasible. Studies have reported that total substitution of fossil fuels by biofuels will result in negative impacts due to the contamination of water resources by pesticides that are currently used for the cultivation of the crops that acts as feedstocks for the production of alternate fuels. For a successful LCA, understanding the processing system from an integrated and inter-disciplinary perspective covering the social, ecological, economic, legal and geographic outlook is essential. This review work also highlights the importance and techno-economic challenges in commercializing biofuels production from feedstocks such as soybean, canola, and green seed canola oils.

2.1 Introduction on hydrodeoxygenation (HDO)

Hydrotreating process includes hydrodesulphurization (HDS), hydrodenitrogenation (HDN), hydrodeoxygenation (HDO) and hydrodemetallization (HDM) reactions. These reactions can occur simultaneously during a catalytic hydrotreating process and the extent of these chemical reactions depends on the type of feedstock, chemicals, catalysts and operating conditions of the reaction system. The oxygen content of the bio-based fuel plays a major role in assessing the fuel properties. It is desirable to have a low oxygen content in the fuel. The high oxygen content of vegetable oils (up to 50 wt.%) has adverse effects such as low heating value, thermal and chemical instabilities, corrosivity, immiscibility with fossil fuels and increase in the tendency towards polymerization (Wang et al. 2010).

Hydrodeoxygenation can be a promising process to remove oxygen content from the fuels aiding in the production of bio-based transportation fuels (Wang et al. 2012). Bio-oils obtained from

wood and wood residues can be potential feedstocks for HDO reactions due to their high oxygen content (>35 wt.%) and they can be upgraded by physical or chemical methods (Zhang et al. 2013). Research efforts to study the chemistry of hydrodeoxygenation of biomass-derived oil are gaining considerable importance over the last 20 years.

Hydrodeoxygenation of bio-oil is reported to be the most suitable method to upgrade bio-oil (Majhi et al. 2013; Yunquan et al. 2008). Industrialization of HDO process was first done by Neste oil in Porvoo, Finland using vegetable oils as primary feedstocks. Although HDO is an efficient method to obtain fuel from bio-based feedstocks, it has not received considerable importance as the petroleum feeds generally contains 98 wt. % carbon and hydrogen, 1.8 wt. % sulfur and only 0.1 wt. % oxygen (Yunquan et al. 2008). Hydrodeoxygenation of feedstock's that contains triglyceride produces diesel-like deoxygenated hydrocarbons, with high cetane number that is fully compatible with petro-diesel (Sebos et al. 2009). Fig. 2.1 indicates the factors affecting the choice of feed source, reaction conditions, product formation and commercialization of hydrodeoxygenation process. Out of these, optimization of the catalyst can be the most challenging task. Choice of feedstock should be based on the environmental conditions of the locality. In a province like Saskatchewan, canola oil is available abundantly and it can be a promising feed source. For the efficient design of the hydrodeoxygenation process, choice of catalyst, optimization of reaction temperature, hydrogen pressure and catalyst loading is highly essential. The catalyst should be designed to hinder side reactions and have higher selectivity towards desired products. Finally, information on the supply-demand structure for the diesel substitute products in a local community and process economics are mandatory for the commercialization of the hydrodeoxygenation process.

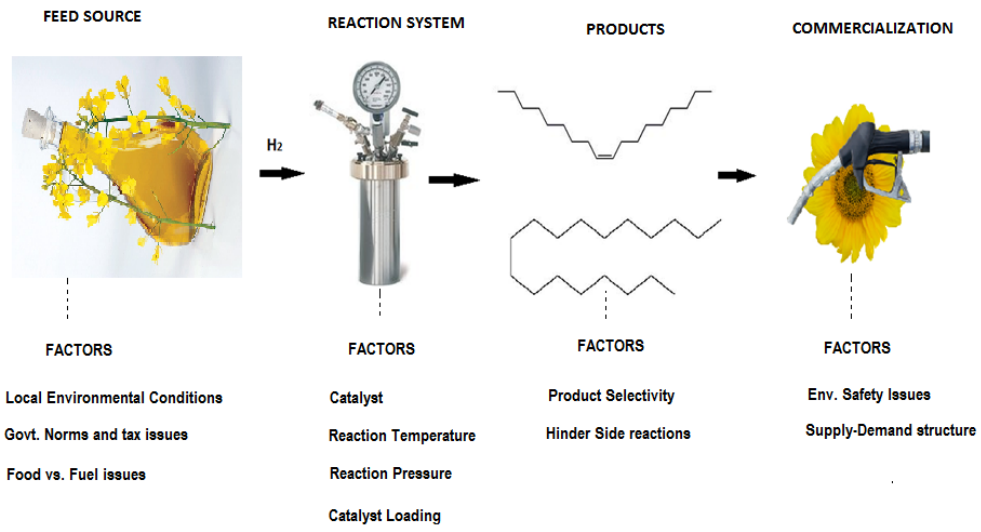

Fig. 2.1 Overall hydrodeoxygenation reaction system (Reproduced from Arun et al. (2015) with permission from Elsevier)

The possible routes for hydrodeoxygenation include direct hydrodeoxygenation, decarbonylation and/or decarboxylation (Dupont et al. 2011). In direct hydrodeoxygenation, organo-oxygen molecules present in feedstocks react with hydrogen at elevated temperature (250-400°C) and pressure (3-10 MPa) and hydrocarbons are obtained as main products with oxygen removed in the form of water. However, most of the times, oxygen is removed in the form of CO_2 (decarboxylation) and CO (decarbonylation) resulting in products with less carbon number.

In the case of direct HDO, the C=O double bond is cleaved first, resulting in the transformation of the carboxylic acid into an alcohol. Then, the attack on the remaining C-O bond continues and the alcohol is further transformed to an alkane. In the case of decarboxylation reaction, the C-C single bond is attacked first and the oxygen atoms are removed directly in the form of CO_2. Reactions involved during hydrodeoxygenation are represented by equations (2.1) & (2.2). Equation (2.1) is the most desired route (direct HDO) as the number of carbons is preserved and the by-product formed is water (Arun et al. 2015).

Reaction Scheme for direct hydrodeoxygenation (eq. 2.1) and decarboxylation (eq. 2.2)

$$CH_3\text{-}(CH_2)_m\text{-}COOH \xrightarrow{H_2} CH_3\text{-}(CH_2)_m\text{-}CH_2OH + H_2O \xrightarrow{H_2} CH_3\text{-}(CH_2)_m\text{-}CH_3 + H_2O \quad (2.1)$$

$$CH_3\text{-}(CH_2)_m\text{-}COOH \xrightarrow{H_2} CH_3\text{-}(CH_2)_{m-1}\text{-}CH_3 + CO_2 \quad (2.2)$$

Generally, HDO reactions produce H_2O (Direct HDO), CO (decarbonylation) and CO_2 (decarboxylation) and desired hydrocarbon compounds as the products and the product distribution depends on the reaction route and catalyst type.

2.2 Feedstocks for HDO process

Vegetable oils are an ideal source as they have a chemical structure with long chain fatty acid groups with 16 to 24 carbon atoms in length. Normal plant oils can be used for the production of diesel fuel because they are primarily made up of triglycerides, diglycerides, monoglycerides and free fatty acids. Choice of feedstocks depends on crop growing pattern of local regions and proper choice of feedstock can aid in the reduction of tariffs and transportation costs. Soybean oil is a potential source in the United States due to its higher production rate (Sirvastava et al. 2000). Production of rapeseed oil, palm oil, and sunflower oil dominates in Canada, Asia and Europe respectively. Hence, they can be the potential feedstocks for biofuel production in European nations. Based on the locality, similar considerations should be made while choosing a potential

feedstock for HDO reactions. Usage of renewable bio-based feedstocks as fuel resource has many advantages pertaining to economic, social and environmental aspects: (i) Stable supply of raw materials. (ii) Reduction in carbon footprint from the usage of liquid fuels, and (iii) profitable agricultural economy.

Most of the researchers have used model compounds to investigate hydrodeoxygenation reactions. Phenol is one of the highly preferred model compounds as it is an oxygenated compound with a simple structure (Mori et al. 2007). Feeds such as guaiacol (Filley et al. 1999; Bykova et al. 2012; Ghampson et al. 2012; Bui et al. 2011; Olcese et al. 2012), methyl heptanoate (Senol et al. 2007), sorbitol (Kim et al. 2013), vanillin (Ramirez et al. 2013) and acetic acid (Joshi and Lawal. 2012) have been tried and few papers have reported on HDO of real feedstocks such as bio-crude (Yang et al. 2009) and vegetable oils (Kubicka et al. 2010; Templis et al. 2011).

Production of third generation fuels is mostly based on bio-oils and vegetable oil. Bio-oils have gained considerable importance as a potential feedstock for production of hydrocarbon fuels by the process of catalytic upgradation. Lignocellulosic biomass is a promising renewable energy source and can be used to produce bio-based fuel. From the results on characterization of different biomass, it was concluded that pinewood is the most reliable source owing to its high calorific value, cellulose and hemicellulose content. Biomass can be classified as carbohydrates, lignin and fats/oils. Carbohydrates consist of cellulosic and hemicellulosic materials. Fats comprises of triglycerides and fatty acids. Lignin can be hydroprocessed to form phenols and tar which can be further hydroprocessed to produce aromatics and naphthalenes (Ben et al. 2013). Similarly, sugars from carbohydrates of a biomass can be converted to sugar alcohols by hydrogenation and further hydroprocessed to yield gasoline products.

Due to abundant availability of canola oil (more than 3.3 million metric tons) and green seed oil in Saskatchewan, canola and green seed (non-edible) canola oil can be the potential feedstocks for HDO process in Canadian biofuels industry. Understanding the reaction mechanisms using real feedstocks can be challenging and HDO studies using model compounds is preferred to elucidate the reaction pathway before evaluating real feedstocks.

Oleic acid is the primary constituent of both canola and greenseed oil and the next two abundant fatty acids are linoleic acid and linolenic acid respectively. Oleic acid is a straight-chained carboxylic acid with eighteen carbon atoms and one carbon-carbon double bond. Linoleic and linolenic acid are also straight-chained carboxylic acids containing eighteen carbon atoms, but with two and three carbon-carbon double bonds respectively. Hydrodeoxygenation and hydrogenation of oleic, linoleic and linolenic acids will be the key steps in producing a diesel fuel product from canola or greenseed oil.

Greenseed (non-edible) canola oil has a high content of chlorophyll and due to its non-edible nature, it is considered as a "waste product" (Mungroo et al. 2011). The major pigments in canola and greenseed canola oil are chlorophylls and pheophytins. Due to the high content of chlorophyll in greenseed oil, it appears green and it is considered non-edible making it a potential source for HDO reaction to obtain bio-based diesel products. The high chlorophyll content of green seed canola oil is reported to inhibit the activity of hydrogenation catalyst. Moreover, the presence of pigments has been reported to have detrimental effects on the stability of oil and the biodiesel and bleaching of the oil are proven to remove the pigments (Mungroo et al. 2011). Cerny et al. (2013) carried out hydrodeoxygenation reaction using zeolite USY catalyst and different feedstocks such as canola oil, palm oil, oleic acid, stearic acid, cis-9-octaden-1-ol and octadecan-1-ol to study the influence of the nature of carbon-oxygen bond and the degree of

unsaturation present in the reactant. It was concluded that the usage of saturated alcohols resulted in the formation of the most desired products (iso-alkane). Using unsaturated feedstocks instead of the saturated ones resulted in the increased formation of aromatics (>10%).

2.3 Catalyst development for HDO process

Design of a catalyst can be stated as the systematic application of available information for the selection of a catalyst in a specific reaction. It is a challenging task because, accurate and specific methods for catalyst development and design for specific reaction system are generally scarce and in most cases, it works on trial and error method. Generally, a variety of catalysts can be predicted to perform well for a specific reaction and can be checked only by experiments. The number of catalysts to be tested can be reduced by proper application of catalyst design procedure.

Methods for designing a totally novel catalyst and altering an available catalyst for specific purpose differ slightly. Before designing a completely novel catalyst, technical, economic and environmental evaluations are mandatory. Catalysts developed should be technically feasible with no harm to the environment and should be cost-effective. However, if a catalyst needs to be designed for an already existing mechanism, the design could be carried out based on some chemical grounds. Fig. 2.2 illustrates the different support materials and active metals that are being employed for hydrodeoxygenation reaction. Zeolite materials are used quite extensively as they offer high acidity that enables cracking of C=O bond in feed oils and aids hydrogenation. Recently, mesoporous materials are gaining importance as they offer moderate acidity and also the required surface area and pore diameter for the reaction of real feedstocks that are relatively heavier molecules.

2.3.1 Different catalyst used for hydrodeoxygenation process

Many literatures have reported on hydrotreating reactions using conventional metal sulfide catalysts (Senol et al. 2005) and noble metal catalysts (Wawrzetz et al. 2010). However, noble metal catalysts are costlier than transitional metal sulfide catalysts and the cost factor limits the applicability of noble metals as catalysts for HDO reactions (Wildschut et al. 2010). Transition metallic sulfides of nickel, cobalt and molybdenum are proven to be efficient catalysts for hydrotreating reactions such as hydrodesulfurization (C-S) and hydrodenitrogenation (C-N). Hence, it can be assumed that the same active metals could work for hydrodeoxygenation (C-O) reactions. Sulfidation process is carried out at high temperature (280-350°C) using hydrogen sulfide (H_2S) or carbon disulfide (CS_2).

Senoi et al. 2007 reported that the usage of H_2S as sulfiding agent is more beneficial than CS_2 due to a decrease in hydrogen consumption and coke formation. High oxygen (>30 wt.%) and low sulfur content (<3 wt%) of the feed (vegetable oil) can cause oxidation of the active catalyst phase and thus deactivating the sulfide catalyst. The use of non-sulfided catalysts for hydrotreating of fossil fuels and model compounds have been studied and it was shown that non-sulfided catalysts can be successful in removing many impurities such as oxygen, sulphur, and nitrogen. Specifically, a review by Furimsky (2003) states that metallic carbide and nitride catalysts have a high affinity for removing the impurities (nitrogen, sulfur, and oxygen) by hydrotreating process. Li and Huber (2010) studied on aqueous-phase hydrodeoxygenation of sorbitol using $Pt/SiO_2–Al_2O_3$ catalyst and have concluded that dehydration reaction occurs on the bronsted acid sites of the Pt containing support. The severity of operating conditions depends on the nature of the feed. Especially, heavier feed requires high temperature and pressure for proper hydrogenation.

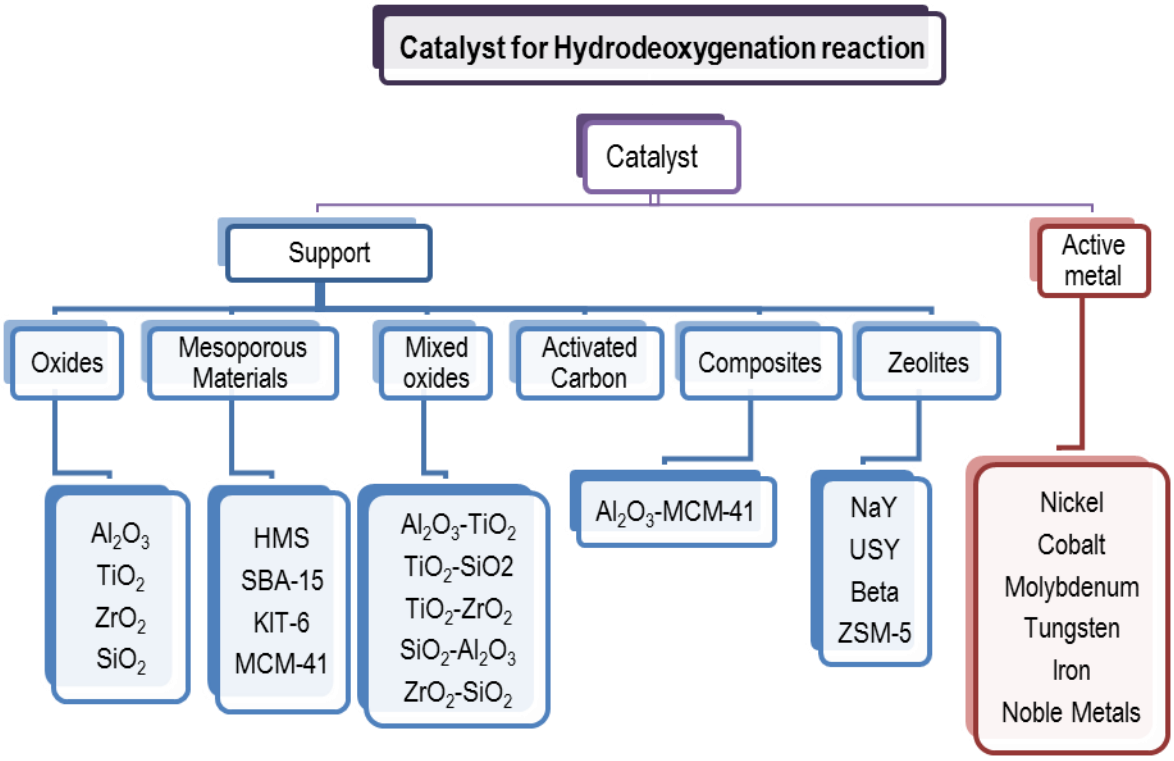

Fig. 2.2 Catalyst development for hydrodeoxygenation reaction

(Reproduced from Arun et al. (2015) with permission from Elsevier)

Zhao et al (2011) have performed hydrodeoxygenation of phenols to cycloalkanes using dual-functional catalyst system (Pd/C and H_3PO_4). They have studied the influence of catalyst support, pH value of an aqueous solution, metal sites, and temperature on the HDO activity. In HDO reactions of vegetable oils or bio-oils, it is always preferred to promote the hydrogenolysis of carboxylic groups or carbonyl groups over saturated C-C bonds as the latter can reduce the octane number of the produced fuels and can result in undesired hydrogen consumption (Huang et al. 2011). Bykova et al. 2012 have used nickel based sol-gel catalyst for the hydrodeoxygenation of guaiacol. Different loadings of nickel and copper on stabilizing components such as γ-Al_2O_3, CeO_2, ZrO_2, SiO_2, and La_2O_3 were employed to investigate the

HDO reaction. Nickel based sol-gel catalysts have been reported to outperform the conventional sulfide Ni(Mo), Co(Mo) and noble metal catalysts owing to factors such as higher stability towards coke formation, low cost, stability towards leaching of active components. Presence of copper aids in the reduction of nickel oxide at a lower temperature and hinders coke formation. Nickel supported on SiO_2 (without copper) gave better conversion of guaiacol (97.5%). However, degree of coking was high in comparison to other catalysts with copper loading. One specialty about this study is the use of pure guaiacol without any solvent.

Ardiyanti et al. 2012 used bimetallic Ni-Cu supported on δ-Al_2O_3 catalysts for the hydrodeoxygenation of fast-pyrolysis oil. δ-Al_2O_3 is thermally more stable and less acidic than γ-Al_2O_3 and this helps in reduced coke formation. The loadings of nickel and copper were changed and their effects on hydrodeoxygenation rate were monitored. Leaching levels and carbon deposition were lowest when the nickel loading was maximum (16 wt. %) indicating that usage of promoter's aid in increasing the resistance towards coking. Lee et al. 2013 studied the hydrogenation of model (oxygenated) compounds such as acetaldehyde, propanal, acetone, xylose, furfural and furfuryl alcohol using monometallic catalysts (Pd, Pt, Ru, Rh, Ni and Co) supported on Alumina. Moreover, they used the same catalysts to investigate the aqueous phase hydrogenolysis of tetrahydrofurfuryl alcohol (THFA) and xylitol. From their results, it was concluded that Rh seems to outperform all the other mono-metallic systems for hydrogenation reaction. Additionally, from their studies on hydrogenolysis of THFA and Xylitol, it was confirmed that Rh is a promising active metal for both hydrogenations of C=O and C=C bond and hydrogenolysis of C-C bond. However, Pt, Ni and Co are reported to be more suitable for hydrogenolysis of C-O-C bond. During the hydrogenolysis of THFA, 20wt% of Ni/Al_2O_3 is reported to give a conversion of 17.3% with 0% selectivity towards 1, 2-pentanediol and 59.2%

selectivity to 1, 5 pentanediol. However, 3wt% Pt/Al_2O_3 gave 9.3% conversion and 38.9% selectivity towards 1,2-pentanediol and 0% selectivity to 1, 5 pentanediol. Echeandia et al. 2010 studied on the synergetic effects of tungsten precursors (silicotungstic (HSiW), phosphotungstic (HPW), and tungstic (HW) acids) in the hydrodeoxygenation of phenol over Ni-W supported on active carbon. It was stated that tungsten from heteropolyacids (HPA) performed better and activated carbon gave better conversion than the conventional alumina support. Chances of methanation are high during HDO reactions. CO and CO_2 produced by HDO reactions through decarbonylation and decarboxylation can react with H_2 (water-gas shift and methanation reactions) to form methane. Methane is a worse green house gas than CO_2 and hence this reaction is highly undesirable. The catalyst for HDO reaction should be particularly designed so that these undesired side reactions are inhibited.

2.3.2 Choice of support

Choice of support is also a key factor in determining the hydrodeoxygenation activity of different catalysts. The most common and conventional support is γ-Al_2O_3 (Elliott, 2007). The γ-Al_2O_3 support has many beneficial properties such as high stability and moderate/slight acidity. However, catalyst deactivation due to coke formation is a major problem especially with the use of alumina support. Alternative materials such as SiO_2, active carbon, TiO_2, ZrO_2, Nb_2O_5, zeolites and various metal oxides were used in HDO reactions (Serrano-Ruiz et al. 2010). Hydrodeoxygenation reactions have been traditionally carried out using moderate-highly acidic support materials such as oxides of alumina, silica, zirconia and all these materials have high ionic potential. Support materials such as calcia and magnesia are basic materials with low ionic potential and usage of basic supports and thoria (acidic support) is scarce with respect to HDO reactions. One interesting fact about using activated carbon as support is that their activity

depends on the preparation method and hence, tailoring of their activity is a possibility. This unique property can make activated carbon a suitable choice as a support material for HDO reactions. Low-temperature carbons have acidic hydrophilic surface while high-temperature carbons tend to have basic and hydrophobic surfaces.

Chiappero et al. 2011 have reported the occurrence of both the desired and undesired pathways using PtSnK supported on silica. However, selectivity towards formation of α-olefin was reported to be higher (>50%) compared to olefin isomers. Bui et al. 2011 compared the support effects (Zirconia, titania and Al_2O_3) for CoMoS catalyst on the hydrodeoxygenation of guaiacol. Guaiacol is a model compound used to represent lignin**.** It was concluded that the performance of zirconia support was better than titania and γ-Al_2O_3 in terms of HDO conversion and product selectivity. NiMo supported on ZrO_2, TiO_2 and γ-Al_2O_3 were characterized using Raman spectroscopy to confirm the occurrence of desired metal-oxide species. Zirconia support offers both basic and acidic nature; basic nature of the support material helps to reduce coke formation and acidic nature helps to aid hydrogenation and subsequent $C_{(sp2)}$-O bond cleavage and deoxygenation reactions. Olcese et al. 2013 have compared the performance of Fe/SiO and Fe/Activated carbon for hydrodeoxygenation of guaiacol. For the same iron loading, the guaiacol conversion was higher with the usage of silica support than activated carbon. However, the selectivity towards desired product was higher with the usage of activated carbon support material.

Catalyst design for HDO reactions can be done by altering the host lattice (support) and seeing the influence on the guest metal ion on catalytic activity. When the host lattice changes, the interaction and the co-ordination environment of the guest ion changes. Alternatively, studies can be done by keeping the host lattice same and varying the concentration and/or nature of the guest

ion (change in the active metals). The primary advantage of using porous support is that the extent of availability of active metal for catalytic reactions can be controlled. Preparation methods can govern the diffusion limitations to obtain well-distributed metal catalysts.

Molybdenum forms polymolybdate species at any loading on silica support due to the similarity in isoelectric points of silica and MoO_3. Generally, active metals such as Ni or Co are used and Ni has better activity towards hydrogenation than Co. A lower activity towards HDO can be directly linked to lower acidity of the catalyst support materials. Nava et al. 2009 also stated that catalyst acidity and extent of coke formation have no correlation which seems to contradict to their statement where lower acidic strength of MCM-41 was related to the lower coke formation in comparison to zeolite which has considerable higher acidity.

Influence of sulfidation rate has lesser influence than the acidity of support. Hence, degree of carbidation or nitridation of exposed active metal species may not play a vital role in HDO activity in comparison to the acidity of the support. In comparing the supports SBA-15, SBA-16, MCM-41 and DMS-1, Nava et al. 2009 have stated that HDO selectivity towards desired products (paraffin's and olefins) was better in DMS-1 support material. Formation of Lewis acid sites is important for hydrogenolysis during HDO reactions and the formation is related to the local structure of silanol groups when silica-alumina is used as the support material. Incorporation of aluminum increases the catalyst acid strength. As aluminum is incorporated in the vicinity of a silanol group, the surface OH groups become a Bronsted acid site. It is widely accepted that activity of catalyst for hydrogenation can be increased by promoting the acidity of catalyst by introducing acidic solvents or acidic supports. Increase in acidity reduces the adsorption energy for hydrogen on catalyst. Kubicka et al. 2013 studied on the deoxygenation of rapeseed oil using support material such as SiO_2, TiO_2 and Al_2O_3 using nickel (3.3 wt%) and

molybdenum (15 wt%) as catalyst. HDO reactions were carried out at a temperature range of 260-300°C and hydrogen pressure of 3.45 MPa. It can be observed from their work that product selectivity depends on the nature of support material to a considerable extent. TiO_2 supported NiMo catalyst exhibited high selectivity towards hydrodeoxygenation product in comparison to other support materials. In the case of TiO_2 support, the active phase was not dispersed well and the active phase cluster size was high. However, SiO_2 exhibited better dispersion of active phase in comparison to Al_2O_3 and TiO_2 and this good dispersion is reported to be the main reason for the preferential decarboxylation over SiO_2. From this work, it is clearly observed that metal-support interaction and the support properties play a crucial role in the choice of reaction pathway and also the formation of desired products.

Yang et al. 2013 studied on the hydrodeoxygenation of anisole over nickel supported on materials such as carbon, γ-Al_2O_3, SBA-14, Al-SBA-15, CeO_2, TiO_2 in a fixed bed reactor system. Major products formed by the hydrodeoxygenation of anisole are hexane, cyclohexane, benzene and toluene. Conversion of anisole and selectivity towards products differed significantly depending on the different supports. In the case of Al-SBA-15 and SBA-15, the conversion of anisole showed less difference (<3%). However, the selectivity towards the products differed significantly (>5%). Conversion and selectivity were reported at two reaction temperatures (290°C; 310°C) and liquid hourly space velocity (LHSV) at 20.4 h^{-1} and 81.6 h^{-1}. It was reported that, at higher temperature (310°C), the selectivity towards hexane was high (LHSV-20.4 h^{-1}; Cat: Ni/SBA-15; S_{hexane}=40%). At a temperature of 290°C, the selectivity was 22% at the same process conditions.

Zhang et al. 2013 synthesized nickel (different loadings) supported on ZSM-5 and Al_2O_3. ZSM-5 represents a highly acidic support material, while Al_2O_3 represents moderately acidic support

material. Conversion of bio-oil using nickel supported on ZSM-5 and Al_2O_3 (10 wt%) was 91.8% and 20.9% respectively. However, characterization of the catalyst materials to analyze the metal-support interaction is essential to support the conclusions substantially. Information on active metallic surface area and metal dispersion are recommended to help find the justification for the significant difference in the conversion of bio-oil. Zhao et al. 2013 synthesized nickel supported on HZSM-5 and Al_2O_3-HZSM-5 and evaluated them for the hydrodeoxygenation of phenol. The purpose of this study was to understand the influence of Al_2O_3 binder on the Ni/HZSM-5 catalyzed hydrodeoxygenation of phenol. Catalyst samples were characterized using XRD, TEM, IR, TPR, EXAFS, and XANES and it was concluded that Ni/Al_2O_3-HZSM-5 had higher concentration of nickel atoms in comparison to Ni/HZSM-5. Moreover, usage of binder like Al_2O_3 resulted in strong and higher adsorption capacity of reactant molecules on Al_2O_3 leading to better product conversion. Catalyst deactivation due to sintering is also reduced by the use of binders. Nickel oxide forms a strong chemical bond with the binder (NiO- Al_2O_3) and this strong chemical interaction makes the reduction of NiO/ Al_2O_3-HZSM-5 tougher than NiO/HZSM-5 as confirmed from their TPR results.

Over the years, usage of basic support materials has not gained considerable attention. Acid-base interaction between the basic support and the metal solution can promote dispersion of active metal species on catalyst support. Secondly, coke formation can be inhibited by the basic nature of the support. The literature on hydrodeoxygenation reaction using MgO-supported catalysts is generally scarce. Yang et al. 2009 studied on hydrodeoxygenation of bio-crude using phenol as a model compound in supercritical hexane at 300-450°C and a hydrogen pressure of 4.99 MPa using sulfided CoMo/MgO and CoMoP/MgO catalyst. It was concluded that the basic support is active for hydrodeoxygenation reaction only at reaction temperature greater than

350°C. XPS analysis was performed on fresh and spent CoMo and CoMoP catalysts. It was found that the carbon deposition (coke formation) on the MgO supported catalyst was considerably less (< 20%). Since the bond energy of C=O is high in fatty acids, support materials with moderate to high acidity are generally preferred. However, cracking reactions renders products with less carbon number. One of the major roles of support is to adsorb reactant molecule near the active metal particles. During HDO, H_2 molecules adsorb on active metal and are supplied to the reacting molecule by spill–over mechanism. Adsorption of the reacting molecule can vary depending on the acid-base nature of the support material and this affects selectivity towards certain products. Velu et al. 2003 have stated that phenol (popular model compound for HDO reaction) adsorbs in non-planar fashion on basic supports and it adsorbs in co-planar fashion with respect to the surface on acidic supports. Support materials such as CeO_2 and ZrO_2 are gaining importance owing to their main advantages like higher thermal stability, better dispersion of metals, ability to store oxygen and redox properties.

Hydrodeoxygenation of bio-based feedstocks deals with bulkier molecules and hence support materials such as MCM-41 which has a high surface area in the range of 600-1000 m^2/g and homogenous pore diameters from 1.5 to 10 nm are highly recommended. The acidity of support material plays a crucial role in the degree of coke formation. Support materials such as zeolites are highly acidic and can lead to higher degree of coke formation. However, moderate acidity is essential for the breaking of the carboxylic acid group when vegetable oils are used as feedstock during hydrodeoxygenation. Using support material such as MCM-41 which has a lower strength of acidic OH groups produces a minimum amount of coke in comparison to strongly acidic support materials. SBA-15 can be an effective support for hydrotreating reactions. SBA-15 with hexagonal pores in a 2D array has thicker walls (3-9nm) than MCM-41 and this makes

them more thermally stable than MCM-41 (Nava et al. 2007). Belonging to the same series, SBA-16 was synthesized and scarcely used in hydrotreating reactions. SBA -16 is cubic (1m3m) cage-structured mesoporous silica material and it can be a promising support for hydrodeoxygenation of bio-based oils because it has a body-centered structure in which each mesopore is connected to eight neighboring mesopores and this allows easier diffusion of bulkier molecules into pores (Nava et al. 2009). Nava et al. 2009 published a significant article to report on usage of disordered mesoporous silica (DMS-1) having a surface area in range of 600-1000 m^2/g.

A wide range of acidic, neutral and basic supports have been used for hydrodeoxygenation reactions. Most of the studies have focused on using acidic (ZrO_2) or moderately acidic supports such as Al_2O_3 and SiO_2. Usage of neutral supports such as SBA-15, MCM-41, and KIT-6 are gaining importance. Overall, studies on the basic support are scarce and this is due to their lower activity at temperatures less than 350°C. On a commercial scale, carrying out reactions at reaction temperatures above 350°C may not be viable owing to the huge energy supply. Acidic supports have the potential to break the C=0 bond in fatty acids and can perform hydrodeoxygenation at temperatures less than 350°C. Cracking and coke formation are crucial parameters that need to be addressed.

Support material which offers intermediate metal-oxygen bond strength is considered to be the best support materials. Strong metal-oxygen bonding causes difficulty in the creation of oxygen vacant sites on the catalyst material to adsorb oxygen containing compounds. Weak metal-oxygen bonding makes the abstraction of oxygen from the feed challenging. Basic support offers higher resistance towards sintering and deactivation, but the conversion and hydrodeoxygenation rate are reported to be less in comparison to acidic support materials. Though acidic support

materials offer higher conversions, they suffer from deactivation significantly. Conclusively, moderate to slightly acidic supports such as TiO_2, ZrO_2 and Al_2O_3 have gained great importance and their usage is highly recommended for hydrodeoxygenation systems.

2.3.3 Promoters and their role

Over the years, cobalt, tungsten, and nickel have been used as promoters for hydrotreating reactions (Ferrari et al. 2002; Senol et al. 2005). Usage of bimetallic or multi-metallic catalysts are gaining considerable importance as they show two distinct effects: i) '*Ensemble effect*" caused by the influence of geometry and ii.) '*Ligand effect*' due to the influence of electronic interaction (Trimm, 1980). Usage of bimetallic catalysts are reported to show better catalytic activity than single metal catalysts. Amount of promoter used is a crucial parameter and as reported by Ferdous et al. (2004), excess usage of Ni (promoter) can possibly result in the formation of Ni-γ-Al_2O_3 (Promoter-support interaction) and thus lessening the availability of active sites (Ni-Mo-S) for catalytic reactions. Excess promoters can accumulate on the desired MoS_2 phase and make the catalyst inactive. In hydrotreating reactions using molybdenum sulfide catalysts, promoters increase the catalytic activity of the active metal used by donating electrons to the metal, thus weakening the metal-S bond. A similar trend can be assumed for the metallic carbide and nitride catalysts.

Use of promoters such as boron, leads to the formation of new Lewis and Bronsted acid sites, increasing the overall acidity of the catalyst material. Addition of phosphorous also has a similar effect as boron (Lewandowski and Sarbak 2010). Presence of boron alters the oxide structure of molybdenum. It helps in increasing the density of octahedral molybdate species in comparison to tetrahedral MoO_4^{2-} species and thus promoting the activity of the catalyst. Moreover, promoters alter the catalyst geometry by increasing the number of stacks. Usage of promoters such as cobalt

(Co) and lanthanum (La) was reported to increase the selectivity of catalyst (> 90%) towards oxygen free products (Wang et al. 2011).

Romero et al. (2010) studied on the hydrodeoxygenation of 2-ethylphenol using unpromoted Mo/Al_2O_3, $CoMo/Al_2O_3$, and $NiMo/Al_2O_3$ catalysts. It was concluded that using promoters increased the deoxygenation rate. Moreover, nickel was reported to promote only hydrogenation, but cobalt promoted both hydrogenation and direct deoxygenation reaction. From their results, it could be seen that the incorporation of active metal and the promoter seems to increase the BET surface area of the support material. Generally, clogging of pores occurs while loading and the increase in the BET area seem to be quite contradicting. Villarroel et al. (2008) studied on the promotional effects of promoters like Mn, Fe, Co, Ni, Cu and Zn through spillover hydrogen for hydrodesulphurization reaction. The promoters are reported to favor the migration of hydrogen spillover. One of the major factors that need to be considered during the choice of promoter is promoter-support interaction. Based on the catalyst activation conditions and the oxidation state of the metal, some promoters (eg. Nickel) form a strong chemical bond with support and this reduces the activity of the catalyst.

2.3.4 Metal carbide and nitride catalysts

Many aspects of the hydrotreating reactions over conventional catalysts have been reported in scientific literature. Metallic carbides and nitrides of transition metals such as molybdenum and nickel have been proven to be beneficial for hydrogenation and deoxygenation reactions. Hydrodeoxygenation activity of metallic carbide or nitride catalyst will depend on factors like anionic vacancies produced by reduction and the bronsted acidity of the metal. Noble catalysts are generally expensive and this causes limitations in their usage for hydrodeoxygenation

reactions. Surface structure and chemical composition of catalysts determine the catalytic activity. Hence, preparation method for catalysts plays a crucial role.

Temperature programmed reduction (TPR) method developed by Lee et al. (1987) is the most prominent and used method for synthesizing reduced catalyst. The oxide precursors are converted to the active form (sulfide, carbide, phosphide or nitride) before being used in hydrodeoxygenation of biobased liquid feedstocks (Peterson et al. 2008; Yang et al. 2012). Catalyst obtained from in-situ decomposition showed better hydrogenation activity than catalysts obtained by ex-situ decomposition for the hydrodesulfurization of dibenzothiophene. In hydrotreating reactions, well dispersed catalysts can perform better than crystalline catalysts. The degree of stacking has a crucial effect on the catalytic performance and Yang et al. (2008) have reported that selectivity between hydrogenolysis and hydrogenation can be affected by the extent of stacking.

Heating rate, temperature, and duration of carburization and/or nitridation, the ratio of hydrocarbon/H_2, the source of carbon and metals are the important parameters to be considered during development of novel catalysts. Preparation of metal carbides is more difficult than metal nitrides since surface carbon deposition is a major problem during the preparation of carbide catalysts if proper temperature and carburization composition are not chosen. Metal carbides and nitrides have to be passivated in a mixture containing 1% or less of O_2 as they are pyrophoric. In the past, metal nitride catalysts have attracted a lot of attention. During the catalyst activation, pure NH_3 or a mixture of ammonia and helium is used. H_2/methane or H_2/ethane was used as the reduction/carburization mixtures.

Carbidation or nitridation of metal-oxygen species will produce water similar to the production of ambient water during sulfidation of metal-oxygen species. Presence of water weakens the

metal-oxygen bond and decreases the activation energy for carbidation or nitridation and it also provides more surface protons resulting in lower activation energy for Bronsted site assisted sulfidation. By carburization or nitridation, the early transition metals can exhibit the noble metals-like behavior. Since group VI metal carbides and nitrides resemble noble metals, they are generally more resistant to recarburization than the Group V metal carbides and nitrides.

Ni-S interaction has a detrimental effect on the reactivity of nickel and hence, a similar trend can be assumed for hydrodeoxygenation systems wherein Ni-O interactions should be minimized. The C-C bond cleavage occurs on active metal sites while C-O bond cleavage occurs on acid sites by dehydration reactions (Ryymin et al. 2010). Frauwallner et al. (2011) synthesized molybdenum carbide catalyst using toluene as the carbon source. Raman spectroscopic analysis of Molybdenum oxides (MoO_3 and MoO_2) shows sharp nature of the peak indicating that the catalyst had a highly ordered structure. During the reduction of precursor material (MoO_3), the removal of oxygen results in the generation of oxygen vacancies (anionic vacancies). Mo_2C and MoO_3 were compared based on Raman shift in the 600-1100 cm^{-1} region of Raman spectroscopy. Broadening of peaks was observed in the case of metallic carbide catalysts indicating that there is decrease in crystallinity as the concentration of oxygen vacancies is increased.

Collapsing of ordered mesoporous structure during high-temperature calcination is a common phenomenon. It should be noted that catalytic performance of transition or noble metals are better with high surface area mesoporous oxide support than commercial low surface area support and the former can offer a higher degree of dispersion with increased stability of metal particles upon calcination and reduction. The term high-low surface area seems to be relative and clear and specific range of surface area for enhanced HDO activity is yet to be documented.

Depending on the catalyst loading and calcination temperature, the catalyst precursor exists in different forms: (i). isolated tetrahedral species, (ii). polymolybdates or (iii). MoO_3 when molybdenum is used as active metal. HDS activity of a sulphided catalyst is highly dependent on the surface concentration of S^{2-}. Hence, similar correlation can be observed in case of metallic nitrides (N^{3-}) and carbide catalysts.

Understanding the reaction mechanism using model compounds such as oleic acid and stearic acid will help us to develop efficient catalysts for real feedstocks. HDO of carboxylic acid proceeds by three routes: Route 1 involves ketonization by the cleavage of C-O bond forming ketones which undergoes further hydrogenation to produce alcohols. Alcohols undergo further deoxygenation (dehydration and hydrogenation) to produce paraffin. Route 2 involves the formation of aldehyde through hydrogenolysis by the C-O bond cleavage forming alcohols. Alcohols can undergo dehydration and hydrogenation to yield alkanes or they can react with the feed (carboxylic acids) forming esters. Route 3 involves the breaking of C-C bond forming alkanes. CO_2 and CO are formed as byproducts through decarboxylation and decarbonylation reactions respectively (Fig. 2.3).

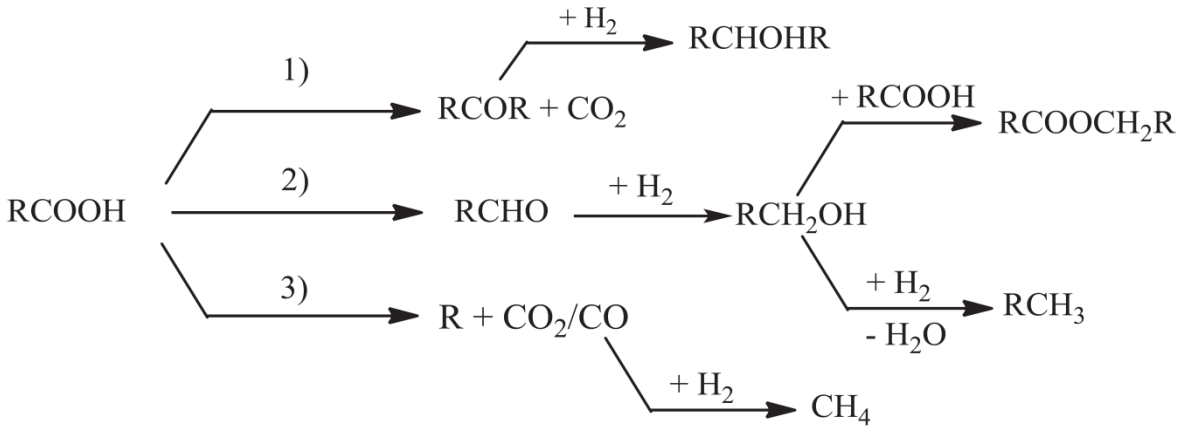

Fig. 2.3 Main reaction pathways for HDO of carboxylic acids, R represents alkyl groups

(Chiappero et al., 2011)

Increase in acidity aids hydrogenolysis reaction which is very crucial for breaking the C-O bond in bio-based oils/feedstocks during hydrodeoxygenation. As stated by Ferdous et al. (2004), HDS, HDN or HDO activity depends on the extent of dispersion of active metal on the support material and on the state of the active metal phase. Energies involved in the bonding of C-O, C-N, and C-S is essential to design the catalyst. The C=O bond is stronger (745 kJ/mole) than C=N (615 kJ/mole) and C-S bonds (477 kJ/mol). In case of single bonds, the energy of the bonds are as follows: C-O: 351 kJ/mole; C-N: 276 kJ/mole; C-S: 255 kJ/mole.

All these values indicate that the order of difficulty in hydrotreating can be arranged as follows: HDO>HDN>HDS. Little information is available on the difficulty level of hydrodemetallization reactions.

2.3.5 Catalyst activation and deactivation.

The rate of hydroprocessing reaction depends on the availability of active surface hydrogen on the catalyst surface. Catalytically active surface must be capable of adsorbing gaseous H_2, activating the adsorbed hydrogen and transferring it to the reactant molecules. Hydrogen activation happens at the metallic sites and dual sites. The activation process can be hindered if the adsorption and activation of hydrogen are slower than the adsorption of reactant molecules and product must desorb rapidly so that another adsorption–activation–transfer–desorption cycle occurs. Information available on metal carbides is less than metal nitrides and this may be due to the complex procedure involved with the preparation of metal carbides.

Stability of catalyst is a critical parameter to be considered while designing a catalyst. Most catalyst shows a decrease in activity with time and this can be attributed to the partial blocking of active edges of MoS_2, Mo_2C and Mo_2N catalysts or formation of carbonaceous deposits on the

catalyst surface leading to fouling. Generally, deactivation rate is higher for the catalyst with higher acidity. Blockage of pores by deposits also hinders the activity. Almost in all the works on hydrodeoxygenation of bio-based feedstocks, tremendous loss of active surface area and pore volume have been reported for spent catalyst in comparison to fresh catalyst.

Catalyst deactivation during hydrodeoxygenation can pose a serious problem on the reusability of the catalyst. Deactivation could be temporary or permanent and permanent deactivation requires the replacement of catalyst. It could be caused by catalytic poisoning or by the loss of surface area (sintering). Temporary deactivation is generally caused by deposition of carbon or sulfur and the catalyst can be restored by gasification using air/stream mixtures. Properly designed catalyst will represent minimum deactivation. All catalyst undergoes deactivation (reversible/irreversible) at the hydrodeoxygenation reaction conditions. However, the deactivation rate changes with the catalyst. In comparison to carbide and nitride catalysts, the rate of catalyst deactivation due to coke formation is higher in the case of sulphided catalysts (Xiong et al. 2011). Using H_2S instead of CS_2 as the sulfur source in preparing sulphided catalysts shifted the selectivity from C_7 to C_6 hydrocarbons. Additionally, the degree of coke formation on catalyst depends on temperature and pressure of reaction. Higher reaction pressure can help in reduced coke formation. At any reaction temperature between 350°C to 375°C, the degree of coke formation is minimized. At lower temperatures, preference for hydrodeoxygenation reaction can be subdued in comparison to other polymerization reactions if aromatic compounds are used as feedstocks.

2.3.6 Salient features of different characterization techniques

Spectroscopic characterization techniques can be performed in different levels: Macroscopic, mesoscopic and microscopic. Most of the characterization techniques are in mesoscopic level

dealing with the activity of catalyst per unit surface area and elucidating the relationship between the catalyst structure/composition and catalytic behavior.

Spectroscopic characterization is performed by excitation of the catalyst/sample using excitation sources such as heat, ions, photons and electromagnetic field. In the case of TPD/TPR, heat is used as the source to characterize samples. Techniques such as XPS are surface sensitive and can help elucidate surface-specific information, and the photoelectric effect is used to evaluate samples.

In the case of Raman/IR spectroscopy, change in polarizability indicates that the vibrations are Raman active. Permanent dipole moment for the molecule is not necessary in the case of Raman spectroscopy. X-rays are used as the source in XRD to excite the sample and study diffraction patterns. XRD is primarily used to identify the phase of a crystalline material and average bulk composition can be determined by this technique (Lamberti et al. 2016). Using Rietveld refinement, it can be used to determine the crystal structure and unit cell dimensions. The main strength of this technique in comparison to X-ray Absorption Spectroscopy (XAS) is the minimal sample preparation and data interpretation is easier in comparison to XAS. Limitations of this technique are: sensitivity to the crystallinity of the sample, access to the standard file is necessary for d-spacing calculations and occurrence of peak overlay.

Based on spectral regions XAS is divided into XANES (X-ray Absorption Near Edge Spectroscopy) or NEXAFS (Near-Edge X-ray Absorption Fine Structure) and Extended X-ray Absorption Fine Structure (EXAFS). XANES or NEXAFS focuses on the multiple scattering contributions. EXAFS focuses mainly on single scattering contributions. From the pre-edge and XANES, information about covalency, electronic structure, oxidation state and site symmetry can be obtained. EXAFS provides information about types of ligands, atomic distances and

coordination number (Lamberti et al. 2016). All of these techniques provide valuable information under vacuum conditions for single crystals. However, it is essential to design experiments for in-situ characterization of real catalysts in experimental conditions to understand the morphological changes in the catalyst as the reactions are performed.

2.4 Life-cycle analysis of HDO process

Presently, commercial usage of generic biomass and non-edible oils to produce bio-oils that can be further hydrotreated to produce jet fuels and synthetic fuels are in progress. Biomass for biofuel production can be broadly classified as herbaceous, woody and green-wastes. It is very important to find commercial values for co-products formed during biofuels production and this is the only means to make the green fuels ‘eco-friendly' on a commercial scale. Before justifying the commercialization of alternative fuels to meet present energy demands, justifications based on their environmental impacts are essential and hence, life cycle assessment (LCA) is very crucial. As shown in Fig. 2.4, the environmental load of a process and its products can be evaluated and assessed using LCA from its cradle to grave (Cherubini and Strømman. 2011; Gnansounou et al. 2009; Kim and Dale. 2009).

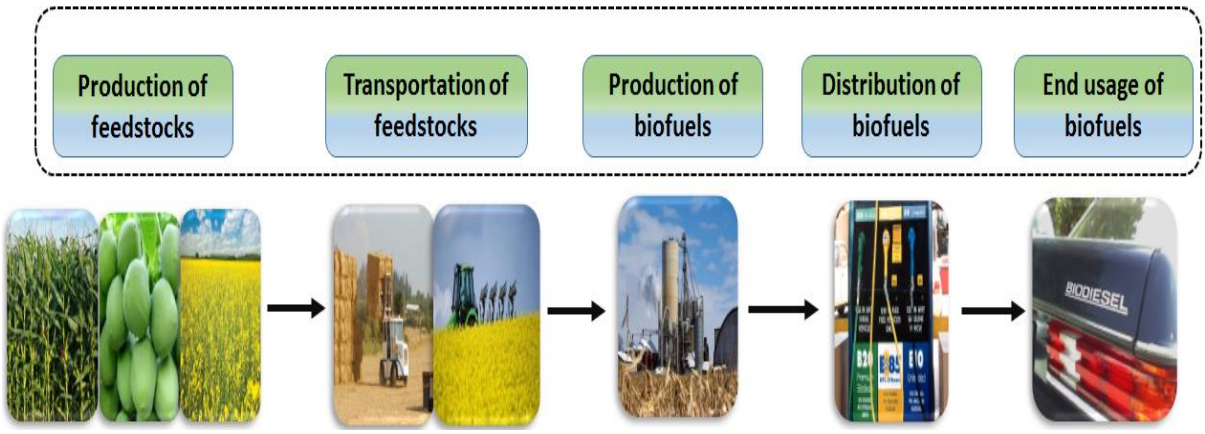

Fig. 2.4. Cradle to grave analysis of biofuels production process

Various environmental aspects such as land usage, ozone layer depletion, acidification, eutrophication and endemic air pollution are included in the LCA and it is a method of comparing biofuels and fossil fuels on the basis of their energy efficiency, impact on the environment and economic parameters. LCA of biofuel industries are generally data intensive and various LCA models have been applied to study the biofuel sector (Wang et al. 2011). Most often, LCA analyses are performed based on the standard norms provided by ISO 14040-43. Sobrino et al. 2009, 2010 developed an LCA model for the comparison of biofuels and fossil fuels production processes and they provided model tools for management and optimization of production resources. For the growth of biomass, usage of fertilizers and other equipment are essential. Hence, the growth of biomass may contribute to GHG emissions and energy spent for the growth of biomass is being questioned by the scientific community worldwide (McKone et al. 2011).

Lignocellulosic biomass such as pine wood or switch grass are being cultivated specifically for the production of biofuels and in such cases, the biomass treatment plants are usually located in close proximity to the biomass cultivation lands. Usually, pyrolysis of biomass is carried out to produce biooil. Fast and slow pyrolysis of biomass to yield biooil requires high reaction temperature (>300°C) and can contribute considerably to the emission of greenhouse gases. Moreover, hydrotreatment of biooil to produce biofuels requires the use of hydrogen. The by-products (water, CO_2, and CO) may contribute to GHG emissions if not used efficiently. Biofuels produced from the plants are usually transported to the end stations for final disposal to customers. Transportation of biofuels through locomotives such as trucks and railways, directly and indirectly, contribute to considerable GHG emissions.

2.4.1 LCA methodology

LCA calculations are based on "well-to-wheels" approach incorporating all the emissions from the procurement of feedstocks to the end usage of biofuels. Life cycle assessment quantitatively predicts the influence of a process on the environment under different factors (global warming, the rate of acidification and eutrophication). Major activities involved during LCA are 1. Definition of the goal and identification of the scope of the assessment; (2) collection of inventory data on materials and energy flows, emissions and release of waste in the process; (3) evaluation of performance of life-cycle assessment and (4) interpretation of the analyzed data and development of decisions based on the life-cycle, sensitivity and uncertainty analysis. Common factors that are analyzed during LCA are: impact on climate, emission of pollutants and their impact on the environment, impact on water resources, land usage, human health, and ecology.

Over the years, LCA has gained importance as a powerful assessment technique to analyze the environmental burdens caused by different operations in biofuel production industries (Kauffman et al. 2011; Hsu 2012). Understanding the sustainability of a newly developed process is of great concern for commercialization of novel lab scale processes (Fig. 2.5).

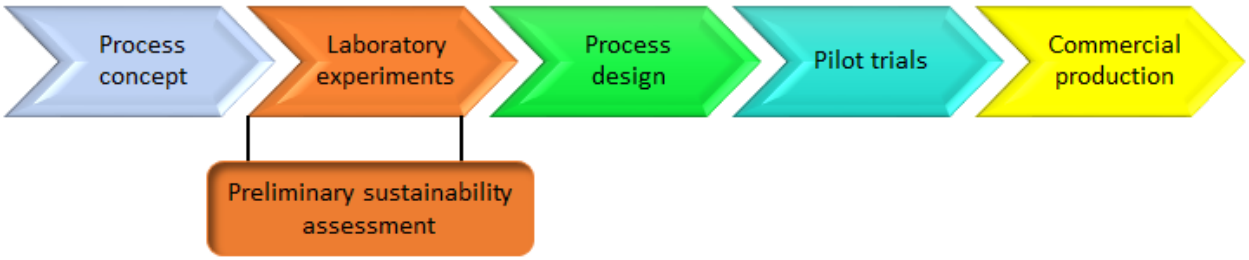

Fig. 2.5. Development of process and methodology application (Reproduced from Patel et al. (2012) with permission of The Royal Society of Chemistry, http://dx.doi.org/10.1039/C2EE21581K)

Sustainability studies deal with the assessment of economic feasibility, environmental impact, potential risks and the advantages of the green chemistry process. For qualitative and quantitative life-cycle assessment, many packages such as e-factor2, Ecoscale4, GME3, ProSuite5, BASF eco-efficiency6, and sustainability consortium Open IO7 exist. Most of these packages require a considerable amount of input data for accurate analysis and directly affect time, resource management and investment.

Major tasks and challenges for life-cycle assessment of biofuels are (McKone et al. 2011):

- Updated information on farming of feedstock by farmers, availability of different feedstocks and land usage
- Prediction of practices and technologies involved in biofuel production
- Characterization of tailpipe emissions and understanding their health consequences
- Life cycle assessment involving time as an independent and significant factor
- Assessment of transitions and end states in the process
- Accounting uncertainty and variability during analysis.

Defining a system boundary in LCA is crucial for defining the objective of life cycle assessment and assessments are performed by attributional or consequential methodology (Kauffman et al. 2011). In attributional methodology, supply-chain interactions are used to correlate the production rate of a particular product and the GHG emissions associated with the process. Consequential approach illustrates the change in GHG emissions with respect to the change in demand for a particular product and it indicates the direct and indirect effects within a particular system boundary. During LCA, optimization of production factors and maximization of profit and availability of resources are important. Production factors include goods related to land,

labor and capital that are used for production. Labour includes man power, number of people available as labors in a particular province or country. Capital includes constructions, trucks, machinery, and equipment for the process (Assen et al. 2014; Uchida et al. 2012). Study by Searchinger et al. (2008) indicates that the promotion of first generation fuel such as corn to ethanol can cause increase in the greenhouse emission by two folds in a span of 30 years rather than reducing them if the land is used for the cultivation of corn plants after the clearance of forests and grasslands.

Clearance of grasslands for the growth of these agricultural crops causes the shift in carbon balance and in fact increases carbon emissions. Liang et al. (2013) studied the economic and environmental impact of biofuel production process using different feedstocks such as soybean, jatropha, castor, oil from vegetables, algae, waste extraction and waste cooking oil. However, regional preference towards a particular feedstock is an important parameter for successful development and commercialization of biomass based bioenergy production process.

In North America, most promising feedstocks are corn, soybean and canola oil. However, the debate over food versus fuel on the choice of feedstocks is well known. In Canada, green seed canola oil, the non-edible form of canola oil is gaining attention as a promising feedstock for biofuel production. Fig. 2.6 illustrates the choice of biomass raw materials for bioenergy production. As illustrated in Fig. 2.6, attention towards palm oil, sugar cane and jatropha are comparatively less and this could be attributed to the regional preference towards particular feedstock based on its commercial value and availability. Brazil and other South American countries primarily focus on the usage of sugar cane for biofuels (especially bioethanol) production. However, Asian countries such as Malaysia and India are presently focussing on palm oil and karanja oil respectively.

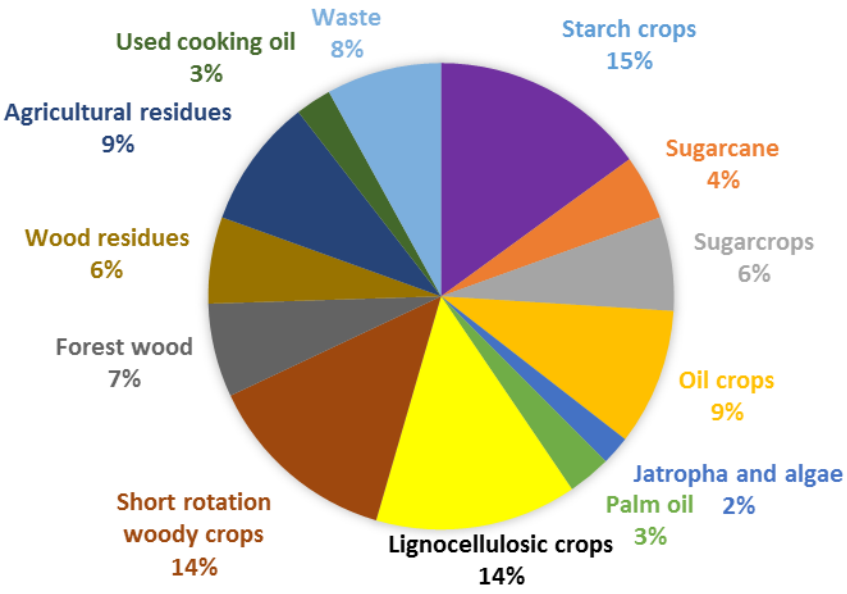

Fig. 2.6 Choice of biomass raw materials for LCA (Cherubini and Strømman. 2011)

During life cycle assessment, it is very important to find a commercial value for all the by-products formed during the process. In the case of transesterification of plant-based oils to produce biofuels, glycerol and seed cake after oil extraction are obtained as by-products. Usually, seed cake is used as organic fertilizer and glycerol is used to produce cosmetics and bio-lubricants. Table 2.1 compares the chemical properties of the biofuels to commercial fossil fuels. As seen in Table 2.1, the sulfur levels of biofuels are less (<0.09 %) in comparison to fossil fuels (>0.15%). Flash point of biofuels is greater than those of fossil fuels making its storage economical and safe. However, the major drawback is the high water content (>0.04%) in biofuels. Recently, hydrotreatment of vegetable oils has gained attention. During hydrotreatment, the oxygen content in the fuel can be completely removed yielding straight chain paraffin, alkenes, and isomerized products. Review published by Cherubini and Stromman. (2011) provides comprehensive information about the global approach towards life cycle assessment of bioenergy systems. Souza et al. (2012) compared between traditional sugarcane ethanol production system (TSES) and joint production system (JSEB) using ISO 14040:2006 and ISO

14044:2006. In South America, sugarcane (Saccharum spp.) is established significantly as a potential feedstock for ethanol production due to its high yield (7.6 m^3 ha^{-1} y^{-1}). It was concluded that the emission levels for JSEB were 23% lesser than the emission levels for TSES. Fundamentally, they have deleterious effects on the environmental credibility of biofuels and there are certain ways to increase the credibility. Genetic modification of crops to produce seeds with a higher yield of fatty acids or increasing the photosynthetic ability and nitrogen absorbing potential of plants to increase the overall yield of seeds are some techniques that can be of interest to the present generation researchers. It is highly recommended to promote the production of biofuels from waste biomass and crops grown on croplands that are considered waste or non-productive in terms of soil nutrients and mineral contents. In this way, it is easier to minimize the carbon debt (Fargione et al. 2008). Figure 2.7 indicates the stages involved during cradle to grave LCA of canola oil based biofuel production process. During the production of feedstock (canola oil), major factors that impact environment are the usage of fertilizers and transportation of canola oil.

Usage of fertilizers affects the acidification and human toxicity. Transportation of canola oil and canola crushing unit contribute to GHG emissions. Canola oil can be used to produce biodiesel through transesterification process or it can be used to produce green diesel using catalytic hydrotreatment process. During transesterification process, methanol is employed as a reactant with acid/base catalyst. Usage of these chemicals will contribute to human toxicity and acidification. During hydrotreatment process, hydrogen is employed and mostly, CO_2 and CO are obtained as by products. Severe operating conditions can contribute to release of energy and to overall GHG emissions.

Table 2.1. Comparison of fuel properties (Reproduced from Taufiqurrahmi and Bhatia. (2011) with permission of The Royal Society of Chemistry, http://dx.doi.org/10.1039/C0EE00460J)

Fuel property	Waste cooking oil	Biodiesel from waste cooking oil	Commercial diesel fuel	Commercial gasoline
Kinematic viscosity ($mm^2 s^{-1}$, at 313 K)	36.4	5.3	1.9-4.1	-
Density (kg L^{-1}, at 288 K)	0.924	0.897	0.075-0.840	0.718-0.778
Flash point (K)	485	469	340-358	265.8
Pour point (K)	284	262	254-260	
Cetane number	49	54	40-46	(Octane) 86-92
Ash content (%)	0.006	0.004	0.008-0.010	-
Sulfur content (%)	0.09	0.06	0.35-0.55	0.15 (max)
Carbon residue (%)	0.46	0.33	0.35-0.40	-
Water content (%)	0.42	0.04	0.02-0.05	0.01 (max)
Higher heating value (MJ kg^{-1})	41.4	42.65	45.62-46.48	47.8
Free fatty acid (mg KOH/g oil)	1.32	0.1	-	-
Saponification value	188.2	-	-	-
Iodine value	141.5	-	-	-

Till date, the biomass is being transported using railways and trucks which predominantly depend on fossil fuel resources. Research on the development of commercial scale mobile biomass processing unit can aid in increasing the overall environmental credibility of the process. Co-processing or altering the present hydrotreating unit to accommodate biomass feedstocks will contribute positively to the overall environmental impact of these futuristic biofuels productions processes. Being an edible feedstock, usage of corn is not recommended as it is more important to meet the dietary needs of the people than to fuel the energy needs of future. Moreover, blending bioethanol in excess with gasoline (>15% by volume) can cause severe engine damage (Lin et al. 2013).

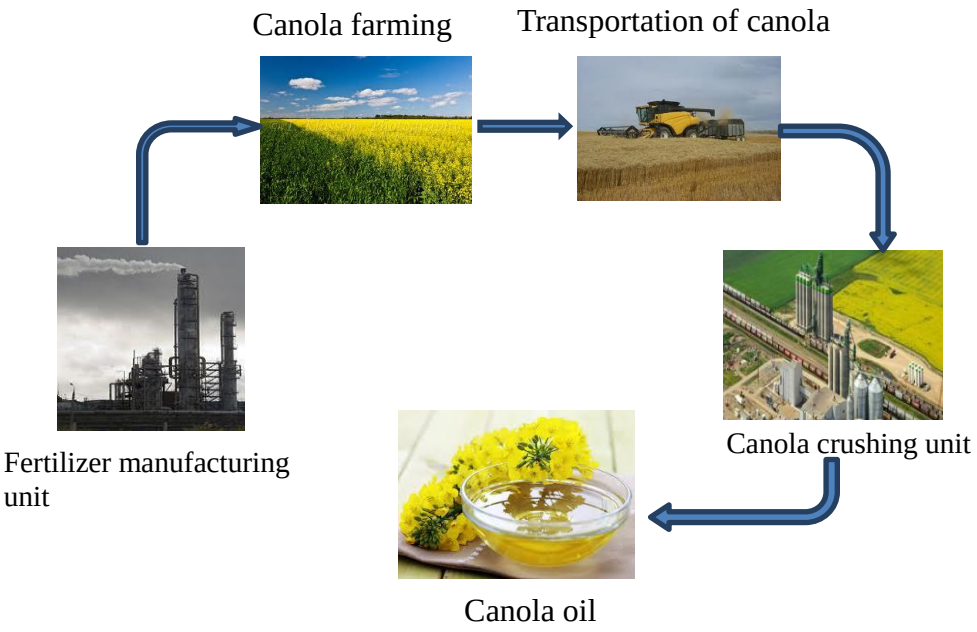

Fig. 2.7 LCA of canola oil production

Challenges involved in facing the food vs fuel problem associated with most of the agricultural crops have resulted in search of feedstocks such as lignocellulosic biomass and micro algae as feedstocks for alternate fuels production (Alvarado-Morales et al. 2013). Terrestrial or aquatic biomass such as wood chips, agricultural crops, aquatic plants and their waste have gained attention as the potential renewable energy sources for biofuels production. By and large, life cycle assessment is the only means to justify the fact that alternate fuels from bio based resources are comparatively efficient than fossil fuels in terms of energy usage and cost. US Environmental Protection Agency (EPA) carried out life cycle assessment of biofuels production pathway to find the methodology that can satisfy the GHG emission conditions put forth by RFS2 and it released a final rule that was effective from July 2010. To conduct LCA, EPA mandates the measurement of generation of carbon dioxide equivalent (CO_2e) per mega joule (MJ) of biofuels.

Usually, calculations are based on both direct and indirect emissions. However, this approach has a major pitfall, as it doesn't provide an allowance for emission measurements in biofuels

production pathway from a single feedstock. This case is particularly important if there is a scarce agricultural land source. As explained in Kauffman et al. (2011), a case study can be considered where a hectare of land is used for cultivating corn and another hectare used for the cultivation of switch grass. Hectare of land with corn yields corn seeds and the Stover. Corn seeds can be used as a source for producing oil that acts as a feedstock for human consumption and for production of alternate fuels. Non-edible corn stover can be used as a feedstock for the production of bio oil and biochar.

Neupane et al. (2011) carried out LCA of bioethanol production from woodchips. During the cradle-to-grave analysis of this process, it was concluded that the environmental emissions were higher during harvesting, processing of woodchips and during their transportation to the facility for biofuel production. Moreover, second generation fuels pose concerns related to feedstock collection networks and technology commercialization. Melamu and Blottnitz (2011) analyzed the carbon debt and the energy efficiency of a South African industry that produced bagasse. They considered seven scenarios related to the production and usage of bagasse. In one scenario, the manufacture of bagasse was carried out without any diversion with another scenario involving 100% diversions. Factors such as global warming potential (GWP), usage of non-renewable energy sources (coal for heat and natural gas), eutrophication of aquatic systems and acidification of land and terrestrial components were considered during LCA. It was concluded that the scenario which involved 100% diversion of bagasse to bioethanol proved to be worst in terms of energy consumption and expenditures. The base scenario involving no diversion of bagasse was concluded to outperform the other scenarios with respect to the various environmental factors. Garcia et al. 2011 analyzed on one current and four possible future

modalities for the production of sugarcane ethanol fuel in Mexico. GHG emissions and the energy balance for the five modalities were estimated.

Usually, CO_2 release from biofuel combustion is given less importance as CO_2 is sequestered by plants during their growth and respiration and this concern is still in debate. The global warming potential due to CO_2 from biofuels is taken as zero. In Mexico, sugar cane is widely used as feedstock for ethanol production in Brazil. To avoid food versus fuel conflict, certain assumption were accounted for the life cycle assessment. Some of the important assumptions are (1) sufficient rainfall ranges; (2) long frost-free period; (3) considerable potential yields and (4) usage of present lands. Guinee et al. (2011) predicted the trend in growth of LCA of biofuel production systems. Future LCA studies will involve sustainability analysis (SA) deepening the scope of LCA and promoting its interdisciplinary relationship.

As stated earlier, traditional LCA (based on ISO 14040 framework) involves the definition of scope and goals, inventory analysis, impact assessment followed by interpretation. Results from the LCA usually have an impact on strategic planning, drafting of public policy, marketing, product development and improvement. Production of biodiesel from various feedstocks has been studied extensively over the last decade. Recently, life cycle assessment of biodiesel production process has become the limelight in the bioenergy sector. Biodiesel production from waste extraction oil and algae are presently gaining attention and globally, focus on commercialization of algae and waste oil based biofuels are rising. One major challenge or drawback is that biodiesel has less oxidative stability and poor cold flow properties. Considering these challenges, production of hydrotreated renewable diesel can be hypothesized to be a better route in terms of economic and environmental compatibility. Most desired reaction route will be the direct deoxygenation of feedstock resulting in a product with same carbon number and water

as a by-product. It should be noted that the reaction mechanism is shown in Fig. 2.8 is generalized and there will be several intermediate reactions involved in this process. Biooil obtained through pyrolysis of lignocellulosic biomass has a considerable proportion of solid mass. Physical and chemical treatments are employed for the removal of the solid mass and other impurities. Purified biooil is hydrotreated in the presence of excess hydrogen to produce renewable gasoline, LPG and diesel fuel as products and water are obtained as a byproduct during direct hydrodeoxygenation.

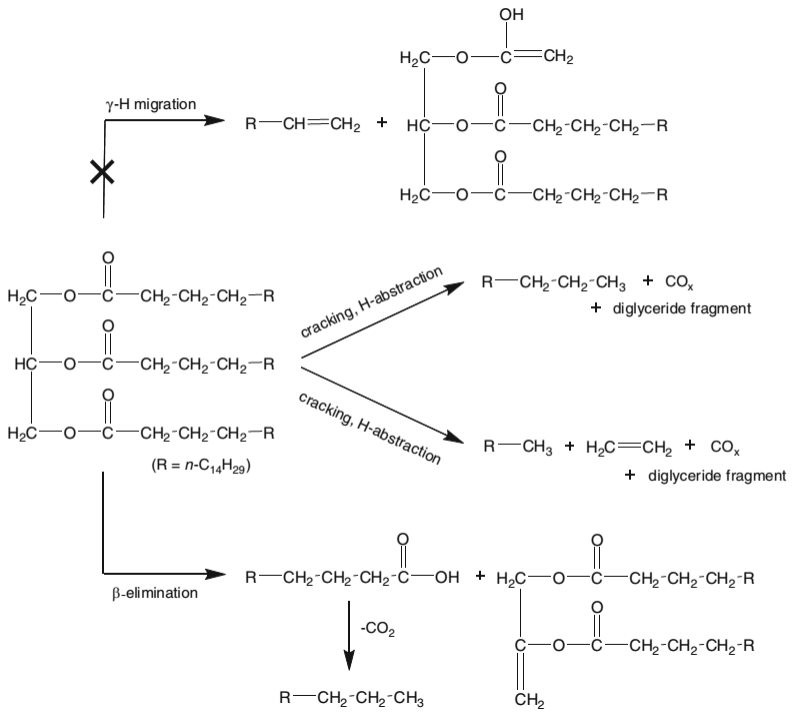

Fig. 2.8 Simplified reaction scheme for tristearin deoxygenation (Reproduced from Morgan et al. (2010) with permission from Springer, http://dx.doi.org/10.1007/s11244-010-9456-1)

As stated earlier, hydrotreatment is an energy intensive process and globally, researchers are working on the development of a novel catalyst that can carry out hydrotreatment reactions in less severe conditions on a commercial scale making the process energy efficient and environmentally friendly. Lin et al. (2013) have performed sensitivity analysis for the production of bio-based fuels from corn seeds and corn stover. Biomass (corn stover) was employed for the

production of bio-oil which can be further hydrotreated to produce diesel fuel substitutes such as higher carbon paraffin and olefins. Requena et al. (2011) compared the environmental impact of three different processes that employ rapeseed oil, sunflower oil, and soybean oil as feedstock for alternative fuels production. For assessing the sustainability of biofuels, life cycle assessment is the most standard framework and it was concluded that the production of sunflower seeds has an environmental impact than the rapeseed or soybean seed production. This is attributed to the large occupation of land by sunflower in comparison to the rapeseed and soybean plants. Larger land occupation results in increased usage of insecticides and pesticides.

Wang et al. (2011) employed Greet 1.8c to analyze the biofuel production from soybeans and the pathway was evaluated on parameters such as energy usage, GHG emissions within the U.S energy scenario. Renewable diesel is produced by the hydrotreatment of vegetable oil producing diesel fuel substitutes. In soybean to biodiesel conversion, soy meal and glycerine are obtained as co-products. During the hydrotreatment pathway, soy meal, fuel gas, and heavy oils are obtained as co-products. From well to wheel stage, biodiesel and renewable diesel pathways were compared for their total energy usage. It was concluded that the choice of method for analysis plays a crucial role in the determination of WTW (well-to-wheel) results. Moreover, maintaining the transparency of the selected method plays a vital role in the accuracy of the life cycle assessment (Table 2.2 and 2.3). Review by Yan et al. (2010) focusses on the well-to-wheel analysis on energy usage and greenhouse gas emissions from biofuels in US and China. It is very evident that U.S and China are the largest consumers of energy in terms of usage of fossil fuels and hence they seem to be the largest emitters of greenhouse gases. Till date, comparative LCA coupled with sustainability analysis on all these processes is not available in literature and it can be a potential area to focus on.

Table 2.2. Comparison of fossil fuel and biofuels in terms of heating value and CO_2 emissions (Reproduced from Yan et al. (2010) with permission of The Royal Society of Chemistry, http://dx.doi.org/10.1039/B915801D)

Fossil/Renewable fuel	Lower heating value		Tank-to-Wheel (TtW) CO_2 emissions	
	MJ kg^{-1}	MJ l^{-1}	g MJ^{-1}	g l^{-1}
Gasoline	44.8	33.15	69	2295
Diesel	43.4	37.76	73	2759
Ethanol	26.8	21.18	71	1513
Biodiesel	38.0	33.44	75	2494
FT diesel	43.6	34.01	71	2431

Table 2.3 TtW fuel economy for passenger cars using different fuels (MJ km^{-1})[a] (Reproduced from Yan et al. (2010) with permission of The Royal Society of Chemistry, http://dx.doi.org/10.1039/B915801D)

Gasoline	Diesel	Ethanol blend (E10)	Ethanol blend (E85)	Biodiesel blend (B20)	Fischer Tropsch Diesel (FTD)
2.600	2.166	2.544	2.455	2.148	2.166

[a] Note: average fuel economy for new gasoline passenger cars sold in the US and China were found to be nearly the same—2.6 MJ km^{-1} ; diesel cars are assumed to be 'functional-equivalent' with gasoline cars; fuel economy for cars fuelled with E10,5 E856 and B205 is based on relative changes to their gasoline or diesel counterparts; fuel economy for cars fuelled with FTD is assumed to be the same with diesel.

Presently, it is tough to avoid usage of fossil fuels for generation of biomass and their transportation. Hence, it is advised to focus on alternate ways to neutralize the overall GHG emissions from bioenergy process.

2.4.2 Discussion on life-cycle assessment

As the source for biodiesel shifts from first to the third generation, it indicates that the characteristics of the processes also differ. Environmentally benign biofuel production processes are expected to possess low energy inputs in all steps from crop cultivation, processing, and production of biofuels. Moreover, it should possess better energy balance, enhanced engine

performance and lower greenhouse gas (GHG) emissions and these characteristics of biofuels can be quantitatively analyzed using life-cycle assessment.

Three major energy related concerns influencing the society are growth in population, increase in global emissions and depletion in fossil fuel resources. The increase in the population indicates that use of land for cultivation, timber production and other agricultural activities will increase. The Renewable Transport Fuel Obligation (RTFO) policy defined "meta-standard" that includes 5 environmental and 2 socio-economic principles for analysis. Currently, Renewable Fuels Agency (RFA) administers RFTO and it monitors the report on carbon balance and sustainability from different parties.

In U.S., the current rate of ethanol production from corn is adequate to commercialize E10 blend (max. blend of 10% of ethanol in gasoline) throughout the country. In such a scenario, it is challenging to convince farmers to cultivate crops such as switchgrass, miscanthus or other feedstocks for biomass production without providing financial security. Globally, most of the arable lands are being employed to produce food crops. Usage of marginal or degraded lands for biomass production can be promising to deal with concerns related to indirect land-use change (ILUC). The scale of operation of biofuels production industry will be of major concern as biofuels production directly depends on factors such as biomass growth and its production rate, choice of processing technology and logistics related issues. By 2050, the global aviation industry planned to reduce its emissions by 50% through improvement in air traffic management, improved design of aircraft and promoting the commercial use of biomass based fuels (Mu et al. 2014). Renewable jet fuel production (farnesene) from sugar cane base had a life cycle emission of 21 g CO_2 eq/MJ (approx.) while its fossil fuel counterpart gave an emission of 80-95 g CO_2 eq/MJ range (Moreira et al. 2014). Presently, it can be stated that biogas production is more

energy favorable in comparison to the process which involves the combination of biogas and bioethanol production. Sensitivity analysis is crucial to test the robustness of the results obtained using life cycle assessment. Land use change (LUC) defines the release of sequestrated carbon into the atmosphere when carbon rich land such as forest lands are converted to low carbon content lands such as agricultural areas for the growth of oilseed crops and this release of carbon creates carbon debt and increases the annual energy usage in a biofuel industry. It is evident that development of biofuels from biomass is still in rudimentary stages and considerable research work is essential for the optimization of biofuel production cost and energy utilization.

LCA studies are usually limited to analysis of balance in greenhouse gases and energy transfer between the system and its surrounding. Choice of feedstock for biofuels production is highly dependent on the agricultural subsidiaries available for the growth of crops for biofuels production. Countries with multiple feed sources such as corn, canola, rapeseed, and soybeans should concentrate on the minimization of arable land usage for the cultivation of bioenergy crops. The Economic and environmental credibility of co-products is essential to completely justify that investments in biofuels sector are profitable and it will meet the present energy demands and also curb greenhouse emissions. Most of the LCA incorporates the quantity of energy into an analysis. However, quality of energy (exergy) is an important concept and is proven to be a powerful technique to assess the sustainability of bioenergy technology. Production of biofuels from algae needs considerable attention from the research community before it can be commercialized.

2.5 Summary of Literature review

Overall, studies on hydrodeoxygenation of bio-based feedstocks to produce green diesel (paraffin and olefins) are gaining attention in this decade. The synthesized catalyst should have minimum

promoter–support interaction to ensure that the formation of active sites is not hindered. For hydrodeoxygenation reactions, it is recommended that metallic carbides and nitride catalyst should be preferred over sulfide catalysts as the sulfur content in the obtained products is of great environmental concern. Hydrodeoxygenation reaction is a process of great commercial significance and research work should continue until the process is commercially viable worldwide. Studies on engine tests using green diesel synthesized through HDO route, emission studies, and process economics can complement the research and development activities related to the upgradation of bio-oils and bio-based feedstocks. The literature review proved that techno-economic and well-to-wheel analysis of biofuel production process especially hydrotreatment and micro algae biofuel processes are very crucial for the commercialization of futuristic fuel processes. The shift from the first generation to third generation feedstock looks positive but exergy analysis is very crucial to justify the fact that biofuels are actually beneficial.

It is evident that commercialization of a new era of bioenergy processes are challenging and it possesses considerable levels of risk. For instance, use of biofuels may require engine alteration, increased usage of additives during processes and also pose challenges in finding alternate uses for the by-products. In most of the cases, production of third generation biofuels from agricultural and forest based feedstocks is a complex process and hence, a holistic approach towards life cycle assessment is mandatory to analyze their environmental benefits and capital costs. Production of biofuels from algal biomass is gaining importance in this decade and hence it is too early to comment on the optimized production route for the synthesis of biofuels from algal biomass in a commercial scale.

CHAPTER 3

EVALUATION OF NiMo CATALYSTS SUPPORTED ON DIFFERENT SUPPORT MATERIALS (γ-Al_2O_3, SBA-15, AND HMS) FOR THE HYDRODEOXYGENATION (HDO) OF OLEIC ACID

The outcome (manuscripts/conference presentations) from this phase of work is listed below:

1. N. Arun, Y. Hu, A. K. Dalai. Comparison of nitride and carbide phase of NiMo catalyst for the hydrodeoxygenation of oleic acid and canola oil. *64th Canadian Chemical Engineering Conference*, Niagara Falls, Canada, October 19-22, 2014.
2. N. Arun, A. K. Dalai. Evaluation of transition metallic nitride catalysts for the hydrodeoxygenation of oleic acid. *Advance Biofuels Symposium*, Ottawa, Canada, May 27-29, 2014.
3. N. Arun, X. Cui, Y. HuA. K. Dalai (Contributed talk and Poster). Characterization of transition metallic catalysts by XPS: Application to green fuels synthesis. *Canadian Light Source, 16th Annual Users Meeting and Associated Workshops*, University of Saskatchewan, Canada, May 2-3, 2013.
4. N. Arun, A. K. Dalai. Hydrodeoxygenation of oleic acid over mesoporous supported metal nitride catalysts. *245th ACS National Meeting and Exposition*, New Orleans, USA, April 7-11, 2013.

Contribution of the Ph.D. candidate and collaborators

All the experimental and characterization work were conducted by Naveenji Arun. Manuscript writing and revision work were done by Naveenji Arun based on the suggestions from Dr. Ajay K. Dalai and Dr. Yongfeng Hu. Dr. R. V. Sharma proofread the manuscript before submission. Dr. X. Cui helped in XPS analysis of catalyst samples.

The contribution of this chapter to the overall Ph. D. work

This chapter focuses on the evaluation of reduced NiMo catalysts supported on different materials for the hydrodeoxygenation of oleic acid.

Abstract

Hydrodeoxygenation of oleic acid was performed using Ni-Mo supported on γ-Al_2O_3, SBA-15 and HMS in a batch reaction system over a reaction temperature range of 350-410°C and hydrogen pressure maintained at 6.55 MPa. The catalysts were synthesized using incipient wetness impregnation method (12 wt% Mo and 4 wt% Ni). Using techniques such as NH_3-TPD, XRD, TEM, BET and XPS, the catalysts were characterized to understand their physico-chemical characteristics. XPS analysis indicated that nitriding the catalyst leads to increased availability of promoter species on the surface of the catalyst. During hydrodeoxygenation reaction, the acidity of support material is a significant factor and from the NH_3-TPD analysis, it was found that acidity of γ-Al_2O_3 is higher than SBA-15 and HMS. Moreover, during HDO reactions, γ-Al_2O_3 showed better catalytic activity in comparison to SBA-15 and HMS support materials. At hydrotreating conditions (T=390°C, P_{H2}=6.89 MPa), NiMo supported on γ-Al_2O_3 showed better oxygen removal (77%) and selectivity of 42% towards C_{16}-C_{18} alkanes during 8 h batch reaction. A kinetic model was developed empirically for the HDO of oleic acid to form n-octadecane, and the activation energy required for this hydrodeoxygenation reaction was found to be 37 kJ/mol.

Keywords: Oleic acid, hydrodeoxygenation, mesoporous materials.

3.1 Introduction

Industrialization and urbanization are the major factors currently shaping our modern energy economy and these factors result in an increase in energy consumption and demand for clean

energy. Production of third generation fuels is mostly based on lignocellulosic biomass, bio-oils and vegetable oils. Since many of the vegetable oils are edible, their usage leads to food vs. fuel problem. In this regard, waste cooking oil has gained great importance as a feedstock to produce alternate fuels (Arun et al. 2015). To improve the social and economic feasibility of bio-based fuels, the use of affordable and low-quality feedstocks are recommended (Yang et al. 2012). Transesterification of vegetable oils is a prominent method to produce bio-based fuel. Hydrodeoxygenation can be a promising process to remove the O_2 content of the oils thus aiding in the production of high cetane bio-based diesel fuel. Hydrodeoxygenation is a process of removal of oxygenated compounds from a molecule usually in the form of water using a catalyst such as nickel-molybdenum supported on alumina and zeolite materials (Arun et al. 2015).

Mesoporous support materials are generally preferred for the hydrodeoxygenation reaction as they offer the pore diameter required for the diffusion of fatty acid molecules (Zarchin et al. 2015). The acidity of the support material influences the extent of cracking reactions. The higher the acidity of the support material, the greater is the extent of cracking reaction. In the present work, mesoporous materials supported transition metallic (Ni-Mo) nitride catalysts are evaluated for the hydrodeoxygenation of oleic acid (model compound). Since waste cooking oil such as canola oil contains >50 wt% of oleic acid (FFA), oleic acid was used as a model compound to study the hydrodeoxygenation reaction. Supports such as γ-Al_2O_3, SBA-15 and HMS were employed for synthesis of NiMo catalyst and their catalytic performances were investigated for hydrodeoxygenation of oleic acid and furthermore, catalyst activity was correlated with the physico-chemical characterization of prepared catalysts. Traditionally, NiMo supported on γ-Al_2O_3 is employed for the hydrodenitrogenation and hydrodesulfurization reactions. It is anticipated that NiMo catalyst system will also work for hydrodeoxygenation reactions.

Moreover, in this chapter, an attempt was made to study the influence of acidity of the support material on the hydrodeoxygenation reaction.

3.2 Experimental Section

3.2.1 Chemicals and reagents

Technical grade hydrogen (95%) was purchased from Praxair, Saskatoon, Canada. Alumina support material was purchased from Alfa-Aesar, MA, USA. Nickel nitrate (99.9% purity), Ammonium heptamolybdate (99.9% purity) and tetraethylorthosilicate (99.9% purity) were purchased from Sigma-Aldrich, Ontario, Canada.

3.2.2 Catalyst synthesis

Commercial γ-Al_2O_3 (Alfa Aesar, Canada) was used along with the synthesized support materials. Nickel nitrate ($Ni(NO_3)_2$) and ammonium heptamolybdate ($(NH_4)_6Mo_7O_{24}$) were used as the precursors for nickel and molybdenum respectively. An aqueous solution of nickel (4 wt.%) and molybdenum (12 wt.%) salts were added to the support materials using incipient wetness impregnation method (Fig.3.1).

Temperature programmed nitridation was carried out in the presence of NH_3 (100%) to obtain the NiMo nitride catalyst and the catalysts were designated as NiMoN/γ-Al_2O_3, NiMoN/SBA-15, and NiMoN/HMS. As the nitrided catalyst can be pyrophoric, they were passivated with a mixture of 1% O_2 and 99% He for 2 h at 300°C prior to storage. Before each reaction, the catalysts were activated in the reactor using hydrogen.

3.2.3 Catalyst characterization

Micromeritics adsorption (Model ASAP 2000) was employed at 78 K using liquid N_2 to measure surface area and pore size of the catalyst. The catalyst samples were evacuated to less than 6.6

$\times 10^{-4}$ Pa, at the temperature of 200°C. Cross-sectional area for the nitrogen molecule that is physically adsorbed was taken to be 0.1620 nm^2.

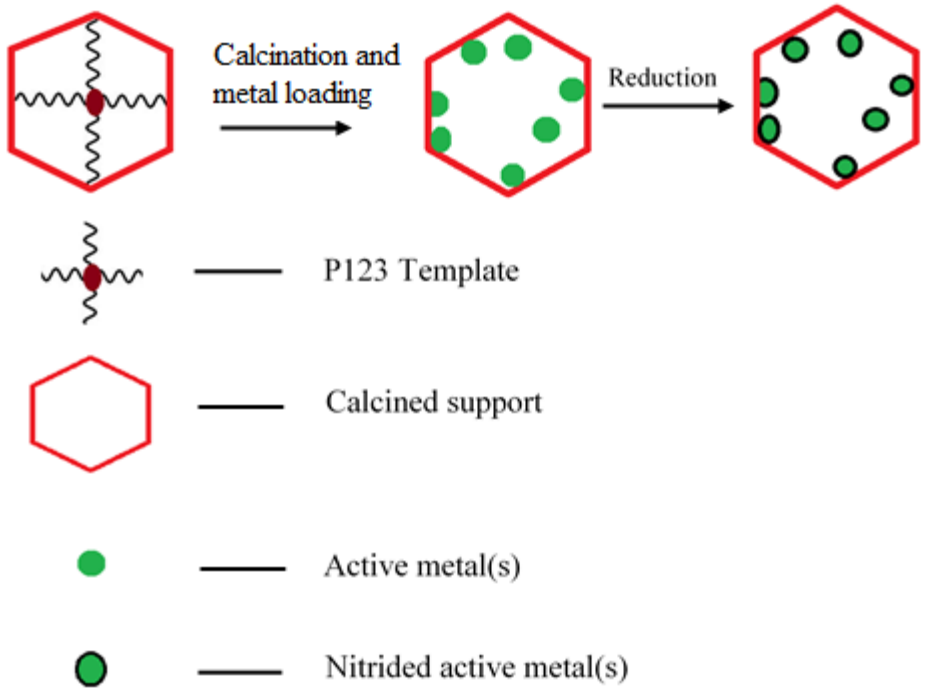

Fig. 3.1. Synthesis of transition metallic nitride catalysts using incipient wetness impregnation method

Powder X-ray diffraction (XRD) was employed to evaluate the different phases present in the synthesized catalysts. Diffraction patterns were detected using Bruker Smart 6000 CCD detector and recorded on a D8 diffractometer using Cu Kα radiation (40 kV and 30 mA) with a step size of 0.02 in 2θ values. TPD/TPR Quantachrome (USA) instrument was employed to perform the ammonia-TPD to understand the extent of acidity of catalysts. Initially, 100 mg of the catalyst was placed in a tube made of quartz tube and helium was purged on catalyst material at 550°C for 1 h. After purging, catalyst was cooled to 40 °C. Then, 3 wt% NH_3 in nitrogen flowing at 30 mL/min was used for the saturation of the catalyst for a duration of 120 min. Ammonia that was physically adsorbed on the catalyst was removed using helium at temperature of 100°C for a

duration of 1 h. The temperature of the samples was increased from 100 to 600°C at constant ramping of 10 °C/min. TPD signals were recorded using thermal conductivity detector (TCD). X-ray photoelectron spectroscopy (XPS) study was carried out using X-rays from the VLS-PGM Beamline at the Canadian Light Source (CLS). The energy range employed in this study was 5.5-250 eV and the spectra were collected using a Scienta SES-100 analyzer (Scienta Omicron GmbH, Germany) in the photoemission mode. Philips CM10 (1990) was employed to obtain the transmission electron microscope (TEM) images to study the morphological characteristics of the synthesized catalysts. Before obtaining electron micrograph images, the catalyst samples were ground and solvent (ethanol) was used to disperse the metals and the samples were rigorously mixed using ultrasonic bath (Zhang et al. 2013).

CO chemisorption was measured using Micromeritics ASAP 2020 chemisorption system. About 0.02 g of catalyst was evacuated under vacuum and after evacuation at 110°C for 1h, catalyst samples were heated to 350°C in hydrogen atmosphere at constant ramp rate (10 °C/min). Coke deposition on the catalysts after each catalytic run was measured using C, H, N and S analyzer (Vario EL instrument). Inductive Coupled Plasma-Mass Spectroscopy (ICP-MS) was used to obtain elemental composition of fresh and regenerated catalysts (Sharma et al. 2013). Concentrated hydrofluoric acid (50% v/v) was used to dissolve fresh and the regenerated catalysts (~0.1 g) and during dissolution the temperature was maintained in the range of 100-150°C. Using 0.2 N HNO_3, final sample was prepared and analyzed using mass spectrometer.

3.2.4 Experimental setup and reaction procedure

Hydrodeoxygenation reactions were carried out in batch setup using Parr reactor (300 ml, Parr Instruments). The reactor consists of a four bladed impeller for agitation. For each catalytic run, 20g of oleic acid and 30g of solvent (dodecane) were used along with 2 wt% (of total feed)

loading of the nitride catalyst. After loading the calculated quantities of the feedstock (oleic acid) and the solvent (dodecane), the autoclave was flushed with nitrogen and then pressurized using hydrogen to obtain the desired reaction pressure. A constant agitation speed of 700 rpm and hydrogen pressure of 6.89 MPa were maintained for 8 h. Reactions were performed at 350°C, 370°C, 390°C and 410°C to study the influence of reaction temperature on the extent of hydrodeoxygenation reaction. During the reaction, constant hydrogen pressure was maintained and samples were analyzed by gas chromatography system (Agilent 7890A) with flame ionization detector (FID) and a 30m long DB-23 column. Spectrum GX (PerkinElmer, USA) was employed to record the Fourier transform infrared (FT-IR) spectrum to analyze the functional groups present in the feedstock and the product. On an average, 16 scans were taken from each sample in the wavenumber range of 375–4000 cm^{-1} and the resolution was maintained at 4 cm^{-1}.

3.3 Results and Discussion

3.3.1 Characterization of catalysts

Physio-chemical properties of catalysts (surface area and pore volume) and metallic surface area (measured through CO chemisorption) of the catalysts are presented in Table 3.1**.** It could be seen that the NiMo/SBA-15 has higher surface area (484 m^2/g) in comparison to other catalysts. Catalyst with high pore diameter (>10nm) helps in the movement of bulky molecules such as oleic acid through the pores which offer more active sites for the adsorption of the reactants and hence increased reaction sites. Hence, it was anticipated that γ-Al_2O_3 support should offer the better catalytic activity for hydrodeoxygenation of oleic acid. TEM images and histogram analysis of NiMoN supported on γ-Al_2O_3 and SBA-15 were performed to analyze surface characteristics of catalyst materials and obtain the particle size distribution based on TEM images (Fig.3.2 & 3.3).

Table 3.1. Physio-chemical properties of the transition metallic catalysts

Catalyst	BET surface area (m^2/g)	BET pore volume (cm^3/g)	Metallic surface area (m^2/g)	Pore diameter (nm)
γ-Al_2O_3	245	0.69	-	13.1
SBA-15	502	0.58	-	12.6
HMS	491	0.61	-	12.1
NiMoN/ γ-Al_2O_3	205	0.48	7.9	10.2
NiMoN/SBA-15	484	0.45	7.4	9.4
NiMoN/HMS	472	0.47	7.6	9.2

Layered structures corresponding to Mo_2N are observed (Fig.3.2a) in the case of NiMoN supported on γ-Al_2O_3. These layered Mo_2N slabs are responsible for higher catalytic activity of the catalyst. However, the presence of Mo_2N slabs on SBA-15 support material is not distinct in comparison to the occurrence on γ-Al_2O_3 (Fig. 2b). Therefore, it can be concluded that the higher activity of NiMoN/γ-Al_2O_3 for oleic acid hydrodeoxygenation is due the formation of layered Mo2N slabs in nitride phase of the catalyst. Fig.3.4 indicates the XRD peaks for fresh and spent NiMo catalysts loaded on γ-Al_2O_3 and HMS. NiMo/γ-Al_2O_3 exhibited a strong peak at 43° and 63°. These peaks are attributed to the formation of crystalline NiO species.

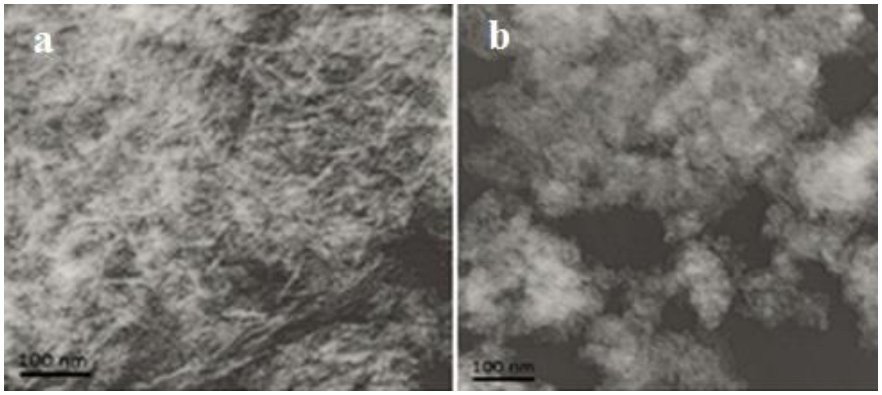

Fig. 3.2. TEM images of NiMoN supported on (a) γ-Al_2O_3 and (b) SBA-15

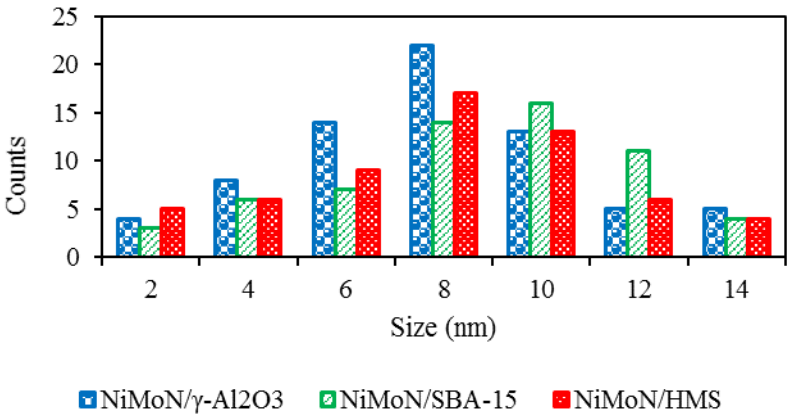

Fig. 3.3. Histograms indicating particle size distribution of Mo on (a) NiMoN/γ-Al_2O_3, (b) NiMoN/SBA-15 and (c) NiMoN/HMS

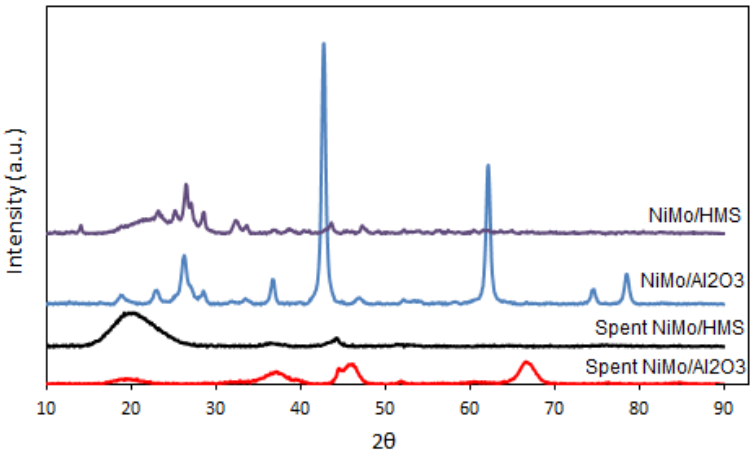

Fig. 3.4. XRD patterns of the fresh and spent NiMoN/γ-Al_2O_3 and NiMoN/HMS

Ultra-violet photoelectron spectroscopy (UPS) and X-ray Photoelectron Spectroscopic (XPS) studies were carried out to examine the oxidation states of the nickel and molybdenum species and elucidate the metal-support interactions. From these spectra, it was concluded that nitriding the catalyst resulted in the increase in availability of surface nickel species (Fig. 3.5). In comparison to the Al (2p) peak for oxide and nitride samples, it can be observed that, in nitride phase of catalyst, the Al (2p) peak shifted to lower energy (73 eV) in comparison to oxide phase (78 eV).

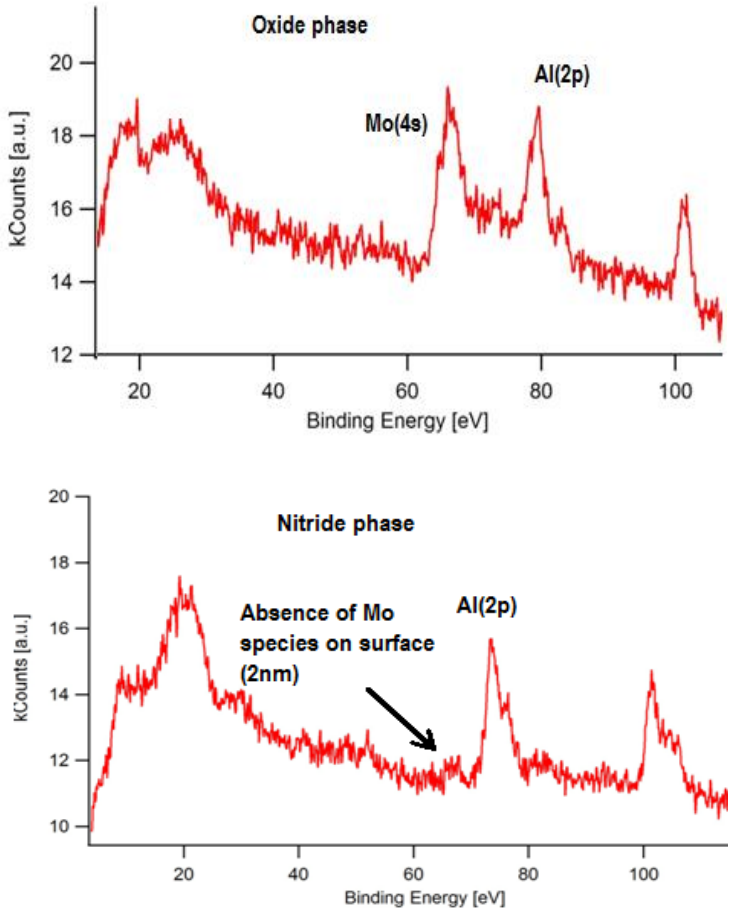

Fig. 3.5. XPS spectra for the NiMoO and NiMoN supported on γ-Al_2O_3

Additionally, the highly intense Mo (4s) peak of molybdenum is not evident for nitride phase of catalyst. The absence of Mo (4s) peak on the catalyst surface indicates that molybdenum atoms form strong chemical bonds with the support material and nickel subsequently bonds with molybdenum forming the desired NiMoN species. Based on the studies by Hada et al. 2000, it was proven that 100% reduction of molybdenum oxide to nitride is impossible under 973 K, and mostly Mo^{3+} and Mo^{4+} ions were observed during the nitridation of 4.8-18.7 wt.% Mo/γ-Al_2O_3. From the ammonia TPD results (Fig. 3.6), it can be seen that the alumina support has higher acidity than SBA-15 and HMS support materials. The moderate acidity of the alumina support

material is expected to be beneficial for the hydrodeoxygenation reaction as it aids the cracking reaction.

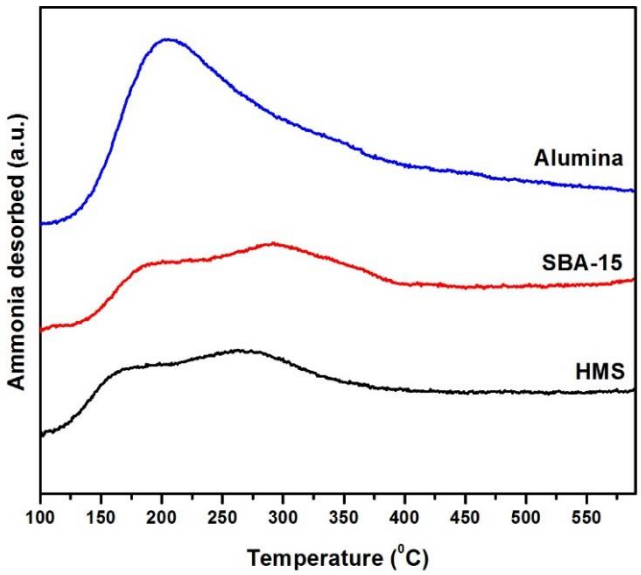

Fig. 3.6 NH_3-TPD profiles of NiMo supported on γ-Al_2O_3, SBA-15 and HMS

3.3.2 Effects of process parameters on the hydrodeoxygenation reaction

Products were collected after hydrodeoxygenation reaction for 8 h at 390°C and hydrogen pressure of 6.89 MPa using NiMoN/γ-Al_2O_3 catalyst were analyzed using GC and FTIR spectroscopy to determine the presence of functional groups in feedstock and product sample. The band at 1712 cm^{-1} is characteristic of stretching vibration of C=O (carbonyl group) in oleic acid and band at 1466 cm^{-1} is attributed to the asymmetric (=COO^-) stretching. Both these bands are almost absent in the product indicating that the catalyst was efficient to cause hydrogenolysis of the C=O bond followed by the deoxygenation. No stretching at 1286 cm^{-1} was observed indicating the absence of C-O stretch due to aldehydes and ketones. In the range of 3500 to 2500 cm^{-1}, the broad stretching is due to the stretching band of O-H which exists in dimeric form due to the hydrogen bonding (Zhao et al. 2013). The intense peak at 1384 cm^{-1} is attributed to the C-

O stretching vibrations involved with COOH groups (Kim et al. 2005). Symmetric and asymmetric stretching vibrations of the CH_2 and CH_3 groups are detected between 2800 to 2950 cm^{-1} (Fig. 3.7).

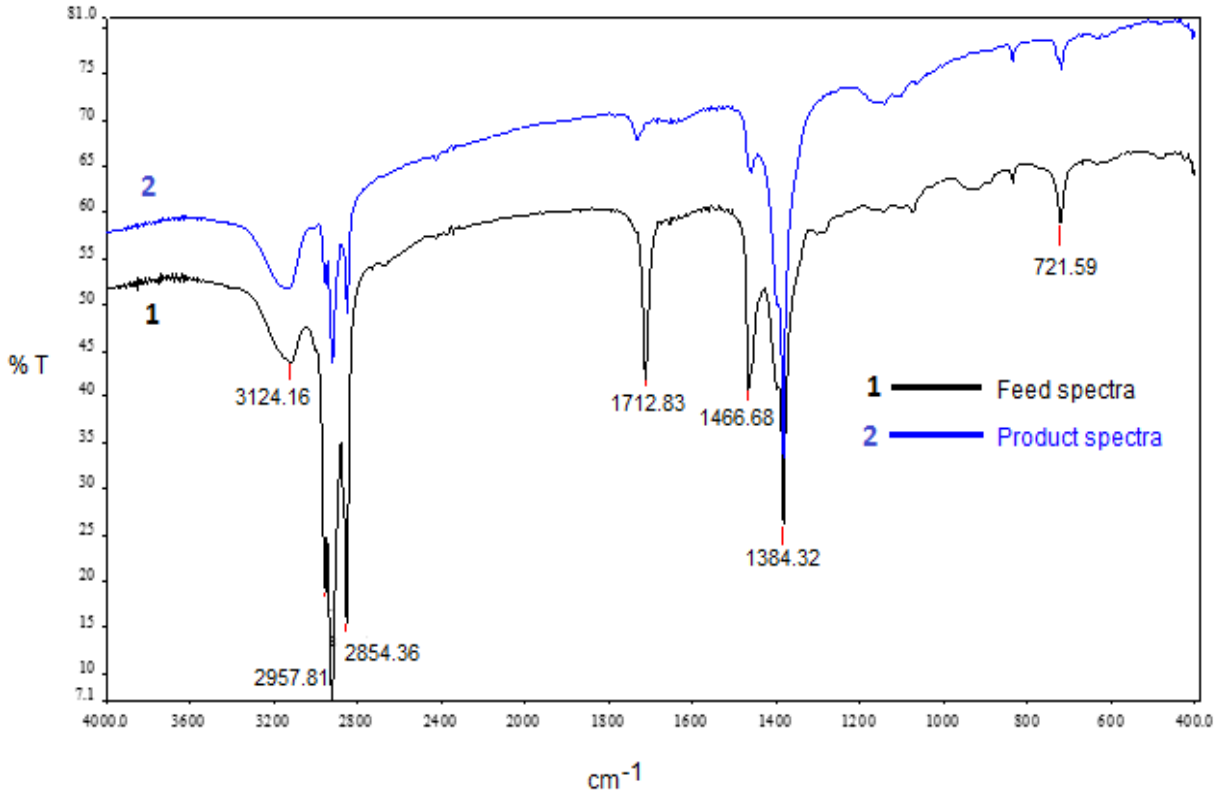

Fig. 3.7. FTIR spectra of the feed (oleic acid) and the hydrodeoxygenated oleic acid (product) Conditions: Oleic acid = 20 g, n-dodecane = 30g, catalyst loading = 2 (w/w) %, temperature = 390 K, speed of agitation =700 rpm and initial hydrogen pressure = 6.89 MPa

To understand the influence of acidity of support on the hydrodeoxygenation reaction, catalytic runs were carried out using different supports (γ-Al_2O_3, SBA-15 and HMS). Commercial γ-Al_2O_3 has higher acidity than SBA-15 and HMS as confirmed by the ammonia TPD measurements. Figure 3.8 indicates the influence of the supports on the hydrodeoxygenation of oleic acid. Hydrodeoxygenation reaction was performed at 390°C and hydrogen pressure of 6.89 MPa and at 800 rpm. Over the reaction time of 8 h, γ-Al_2O_3 support material gave a better

conversion (~45%) in comparison to the other support materials (35-40%). It is evident that the support acidity has a substantial influence on the hydrodeoxygenation reaction.

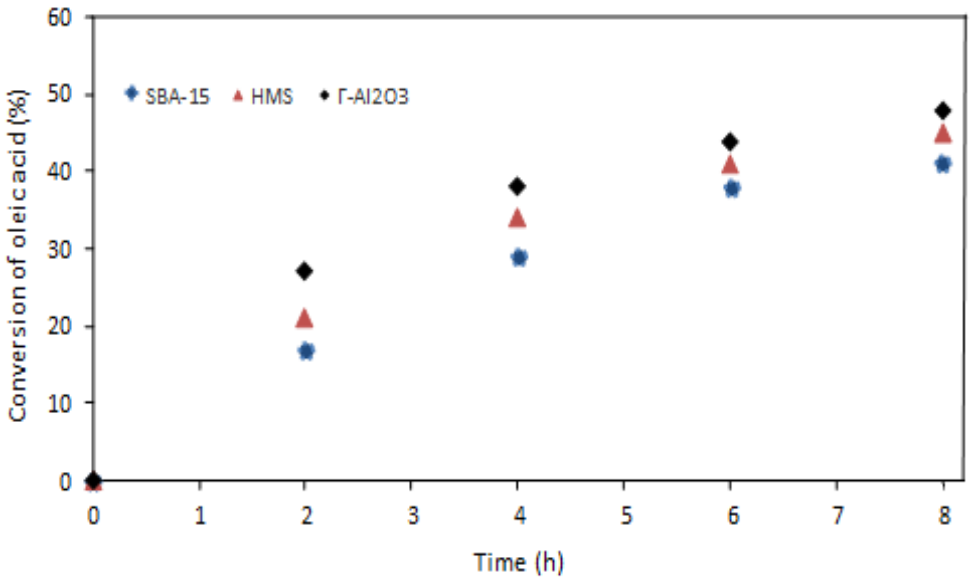

Fig. 3.8. Influence of support on the conversion of oleic acid.
Conditions: Oleic acid = 20 g, n-dodecane = 30g, catalyst loading = 2 (w/w) %, speed of agitation =700 rpm and initial hydrogen pressure = 6.89 MPa

Table 3.2 indicates the influence of agitation speed on extent of hydrodeoxygenation using NiMoN/γ-Al_2O_3 catalyst. It could be concluded that the speed of agitation does not have major influence on the hydrodeoxygenation reaction. Since no major difference in conversion was observed as the agitation speed increased from 500 to 1100 rpm, the reaction was carried out at 700 rpm. Figure 3.9 indicates the influence of temperature on hydrodeoxygenation reaction using NiMoN/γ-Al_2O_3. Over the different temperatures studied, the temperature has a significant effect and at 8 h, the conversion increased from 65 to 78% with increase in temperature from 350 to 410°C. During the reaction time of 8 h, the conversion reached a maximum of 80% on mole basis and then no notable change in conversion was observed over longer reaction time (>8 h).

Table 3.2. Effect of speed of agitation on % conversion and product selectivity during hydrodeoxygenation of oleic acid to form n-octadecane using NiMoN/γ-Al_2O_3.

Sr. No.	Speed of agitation (rpm)	Conversion, mole% (Oleic acid)	Selectivity,% (n-octadecane)
1	500	77±2	41±2
2	700	78±1	42±1
3	900	79±2	42±2
4	1100	81±1	42±1

Reaction condition: Oleic acid = 20 g, n-dodecane = 30g, catalyst loading = 2 (w/w)%, initial hydrogen pressure = 6.89 MPa, reaction time = 8 h

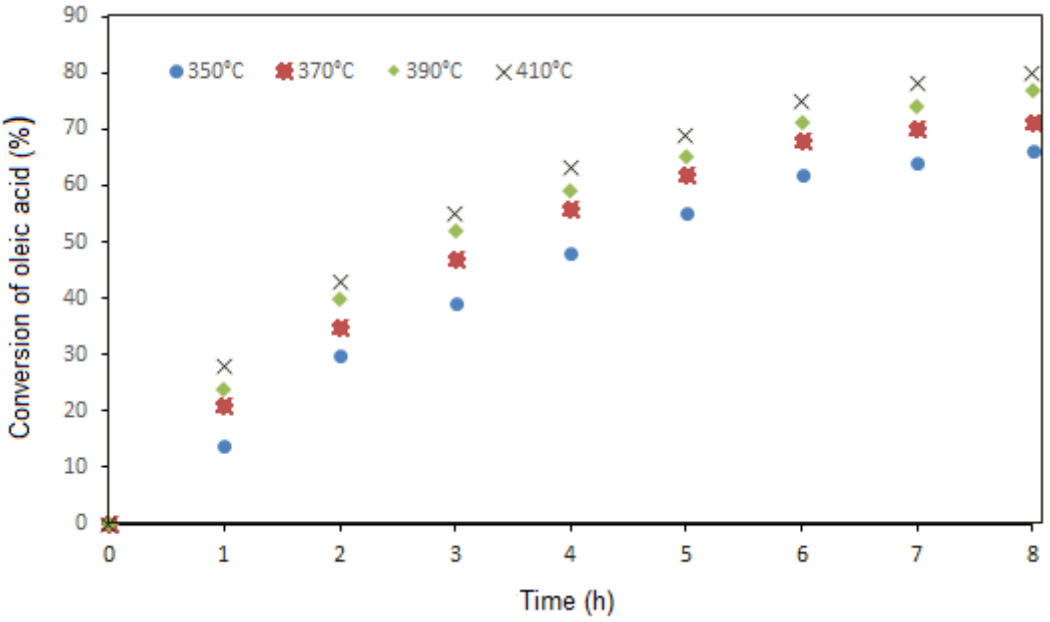

Fig. 3.9. Effects of temperature on conversion of oleic acid.
Conditions: Oleic acid = 20 g, n-dodecane = 30g, catalyst loading = 2 (w/w)%, speed of agitation =700 rpm and initial hydrogen pressure = 6.89 MPa

All the experimental runs were carried out thrice to confirm the reproducibility of the data. Regeneration of the catalyst was performed by washing the spent catalyst using methanol and

drying the catalyst at 110°C for 24 h and then calcining the catalyst at 550°C for 6 h. Elemental composition analysis using ICP-MS indicates a substantial difference in the active metal content of fresh and regenerated catalysts (Table 3.3).

Table 3.3. Elemental analysis of NiMoN/ γ-Al_2O_3 by ICP-MS

Elements	Elemental composition (wt%)	
	Ni	Mo
NiMoN/γ-Al_2O_3 (Fresh)	3.9	11.9
NiMoN/γ-Al_2O_3 (Regenerated)	3.2	10.3

3.3.3 Kinetics of hydrodeoxygenation of oleic acid

For the development of accurate reaction kinetics, elimination of external mass transfer resistance and internal diffusional resistance is important**.** As stated earlier, the agitation speed had a negligible influence on the oleic acid conversion. Therefore, the reaction was assumed to be free from external mass transfer resistance. During the development of the model, the concentration of hydrogen was not included as hydrogen was used in excess and the reaction was assumed to be first order. The energy of activation and pre-exponential factor were obtained from Arrhenius plot (plot of ln(k) versus 1/T). Fig. 3.10 indicates the kinetic plot to get the rate constant values for the reaction. The rate constant (k) values were used to obtain the activation energy. From Fig. 3.11, it was found that the activation energy during the hydrodeoxygenation of oleic acid was 37 kJ/mol.

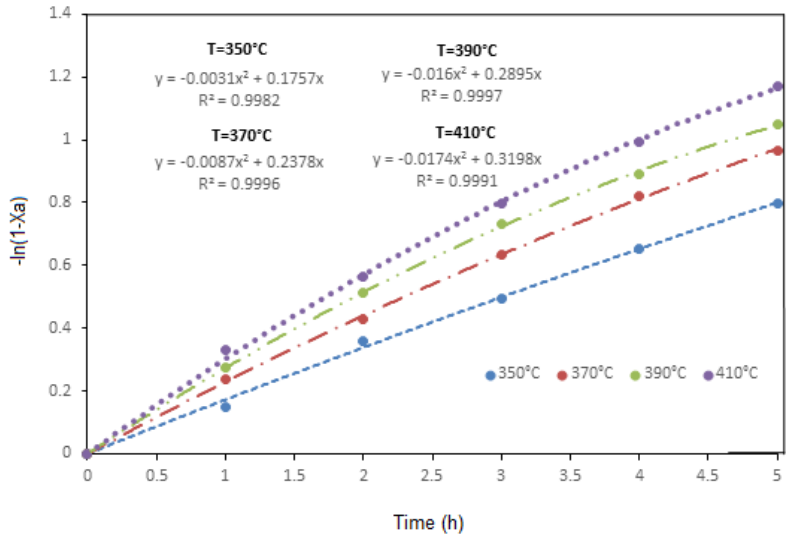

Fig. 3.10. Plot of $-\ln(1-X_A)$ vs time (min) to calculate the rate constant

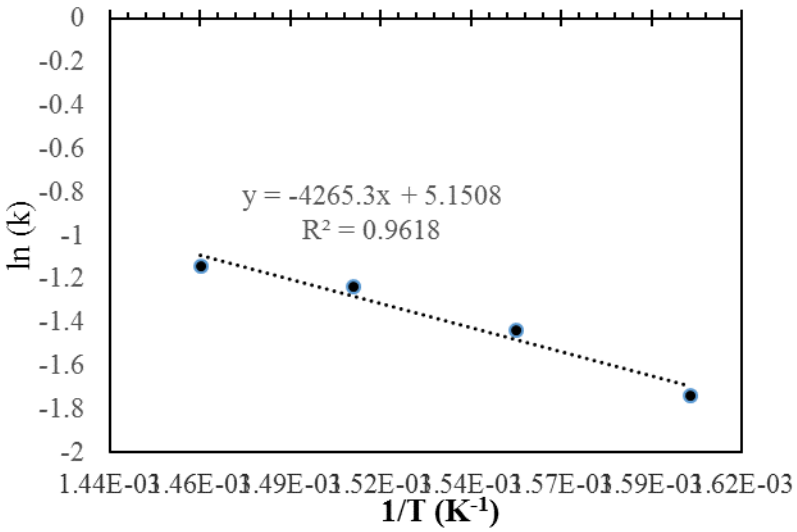

Fig. 3.11. Arrhenius plot for the conversion of oleic acid to n-octadecane using NiMoN/γ-Al_2O_3. Reaction conditions: Oleic acid = 20 g, n-dodecane = 30 g, catalyst loading = 2 (w/w)%, initial hydrogen pressure = 6.89 MPa; temperature (350-410°C) and speed of agitation (700 rpm)

3.4 Conclusions

NiMoN/Al_2O_3 catalyst had higher pore diameter (10.2 nm) in comparison to other catalysts that were evaluated. Evaluation results indicated that γ-Al_2O_3 support material performed well in terms of selectivity towards C_{18} paraffin (approx. 40%). Higher temperature (T> 390°C) favored

cracking reactions causing a decrease in selectivity towards C-18 paraffin. Order of performance based on HDO conversion and selectivity towards C-18 paraffin: γ-Al_2O_3 > SBA-15> HMS. It can be stated that, higher the acidity, higher the activity of the catalyst towards hydrodeoxygenation reaction. XRD results indicate that the promoter material was well dispersed on the support materials such as γ-Al_2O_3, SBA-15 and HMS. From the pseudo-first order kinetic analysis, the apparent activation energy was found to be 37 kJ/mol.

CHAPTER 4

NiMo NITRIDE SUPPORTED ON γ-Al_2O_3 FOR HDO OF OLEIC ACID: CHARACTERIZATION AND ACTIVITY STUDY

The outcome (manuscripts/conference presentations) from this phase of work are listed below:

1. Arun, N., Maley, J., Chen, N., Sammynaiken, R., Hu, Y., Dalai, A.K. NiMo nitride supported on γ-Al_2O_3 for hydrodeoxygenation of oleic acid: Novel characterization and activity study (2017) Catalysis Today, 291, pp. 153-159.
2. N. Arun, J. Maley, R. Sammynaiken, Y. Hu, A. K. Dalai. Understanding the Morphology of NiMo Catalyst Using Raman Mapping and X-Ray Absorption Spectroscopy (XAS). *24th North American Catalysis Society Meeting (NAM 24),* Pittsburgh, USA, June 14-19, 2015
3. N. Arun, R. V. Sharma and A.K. Dalai "Aviation biofuels from waste vegetable and non-edible oils: Overview, key issues and challenges", CURIOSITY, Graduate Research Conference 2014, University of Saskatchewan, March 6-8, 2014

Contribution of the Ph.D. candidate

All the experimental and characterization work was conducted by Naveenji Arun. Manuscript writing and revision work were done by Naveenji Arun based on the suggestions from Dr. Ajay K. Dalai and Dr. Yongfeng Hu. Dr. J. Maley helped in Raman mapping of catalyst samples. Dr. N. Chen provided with beam time to obtain EXAFS data from CLS. Dr. R. Sammynaiken supervised the EXAFS analysis of catalyst samples. Dr. R. V. Sharma provided key suggestions for the conference presentation.

The contribution of this chapter to the overall Ph. D. work

This research work was focused on analysis on structure of catalyst-activity relationship for NiMo catalysts using Raman spectroscopy, X-ray absorption spectroscopy (XAS)

Abstract

Oxide and nitride phase of NiMo supported on Al_2O_3 were employed for hydrodeoxygenation (HDO) of oleic acid. Synthesized catalysts were characterized using Raman Spectroscopy, X-ray absorption near edge structure (XANES) and Extended X-ray Absorption Fine Structure (EXAFS). Raman spectroscopy was employed to understand the active-site distribution in NiMo catalysts and elucidate the relation between distribution of active species and catalytic activity. Raman maps were obtained for the oxide phase of catalyst and it indicates that the Mo supported on Al_2O_3 is present as polyanions ($[Mo_7O_{24}]^{6-}$ or $[Mo_8O_{26}]^{4-}$). XANES and EXAFS analyses were carried out to understand the oxidation state and coordination environment of the catalyst. The occurrence of Mo-Ni and Mo-Mo interactions were proved by the Mo K-edge EXAFS spectra and the bond lengths were determined.

Keywords: Hydrodeoxygenation, NiMo catalyst, oleic acid, spectroscopy

4.1 Introduction

Synthesis procedure and the local environment at the catalytic site alters the morphology of the catalyst. Chemical bonding information helps to project structural information about the reaction intermediates formed during a catalytic reaction (Koizumi et al. 2005). Generally, interaction between the support material and the active metals, calcination temperature and drying conditions (after metal impregnation) affect the migration of active metals on the catalyst surface (Bu et al. 2012; Chen et al. 2015).

Spectroscopic techniques are gaining attention as powerful tools to understand the dynamic nature of these solid catalytic materials and a correlation between the surface morphology and catalytic activity can be obtained (Hu and Wachs. 1995; Bergwerff et al. 2004). Catalyst imaging by vibrational spectroscopy techniques can help in monitoring the migration of active metals on the catalyst surface during their synthesis (Espinose-Alonso et al. 2010). Synchrotron radiation based X-ray techniques have played a crucial role to help us understand the nature and morphology of heterogeneous catalysts at molecular level. Moreover, they are powerful tools to reveal the nature of active metal species even at low concentration (Stavitski and Weckhuysen. 2010).

Techniques such as Raman, MRI and X-ray absorption imaging have been employed in past to understand the speciation of active metals on the surface of the supported catalysts and to obtain direct chemical information such as chemical bonding, redox state and degree of hydration (Mestl and Srinivasan. 1998). To date, it is challenging to obtain all the critical aspects of supported catalysts using single technique. Usually, a few techniques that have the potential to complement each other are used to elucidate important functionalities about the catalytic materials.

In this work, Raman spectroscopy was used to understand the distribution of metal species on the support material. The number and frequency of the vibrational modes in Raman spectroscopy can be used to obtain information about the structure of different species in catalysts. X-ray Absorption Near Edge Spectroscopy (XANES) was employed to obtain information about the electronic state and local site symmetry. XANES is also useful in studying the bulk oxidation states of nickel and molybdenum species present in the catalyst. Moreover, Extended X-ray Absorption Fine Structure (EXAFS) was employed to understand the coordination environment

and determine the bond length of the catalyst structure for NiMo nitride and oxide supported on γ-Al_2O_3. The primary objective of this study is to understand the influence of catalyst structure on the extent of hydrodeoxygenation reaction.

4.2. Experimental Procedure

4.2.1 Catalyst synthesis

Technical grade hydrogen (95%) was purchased from Praxair, Canada. Alumina support material was purchased from Alfa-Aesar (Canada). Nickel nitrate (99.9% purity). Commercial γ-Al_2O_3 (Alfa Aesar, Canada) was used along with the synthesized support materials. Nickel nitrate ($NiNO_3 \cdot 6H_2O$) and ammonium heptamolybdate ($(NH_4)_6Mo_7O_{24}$) were used as the precursors for nickel and molybdenum respectively.

The synthesis procedure for SBA-15 and HMS support materials are described elsewhere (Tanev and Pinnavaia. 1995; Taney et al. 1994; Boahene et al. 2011). Prior to impregnation with active metals, the support materials were dried for 5 h at 110 °C. Aqueous solution of nickel (4 wt%) and molybdenum (12 wt%) salts were added on the support materials using incipient wetness impregnation method. After impregnation, the materials were dried in oven at 110°C overnight and then calcined at 550°C for 6 h to form NiMoO supported catalysts. Temperature programmed reduction was carried out in the presence of NH_3 (100%) to obtain the NiMo nitride catalyst. Four stages of ramping were employed during temperature programmed reduction (Ramanathan and Oyama. 1995). The temperature was ramped to 200 °C and held for 2 h, then ramped to 700°C and held for 6 h. In the cool down cycle, the temperature was ramped down to 475 °C and then to 25 °C at the same ramping rate (1°C/min). Since the reduced catalyst can be pyrophoric, nitride catalysts were passivated at 25 °C with a mixture of 1% O_2 and 99% He for 2 h prior to storage. After nitridation, the synthesized catalysts are MoN/ γ-Al_2O_3, VN/ γ-Al_2O_3,

WN/ γ-Al_2O_3, NiMoN/ γ-Al_2O_3, NiMoN/ SBA-15 and NiMoN/ HMS. Before each reaction, the catalysts were activated by hydrogen inside the reactor.

4.2.2 Experimental setup and procedure

Raman microscopy images were collected with a Renishaw Invia Reflex Raman Microscope using 514.5 nm Ar^+ laser (Modulaser Stellar Pro, UT) and a 1800 l/mm grating, giving a spectral resolution of approximately 1 cm^{-1}. The laser was focussed onto sample using a 100X N PLAN objective (NA=0.90, Leica Microsystems Inc., Mannheim, Germany), and the backscattered Raman signals were separated by an edge filter and collected by a Peltier cooled CCD detector. Samples were dispersed onto Au-coated Si wafers, and Raman images were collected in Streamline^{TM} mode, using a detection time of 60 s, and a pixel resolution of 0.6 µm x 0.6 µm. The laser power was approximately 3.0 mW measured at the sample. The instrument's calibration was verified using an internal Si reference sample, which was measured at 520 cm^{-1}. The Renishaw Wire (V3.4) was used for data processing and image analysis.

Soft X-ray Micro-characterization Beamline (SXRMB) at the CLS, Canada was used to obtain the Ni-K edge and Mo-L_3 edge spectra of the catalyst (NiMo supported on γ-Al_2O_3). The energy range of the beamline was 1.7-10 keV. The data was recorded in the total electron yield (TEY) for Mo-L_3 edge and the Ni-K edge data was recorded in the fluorescence yield. The Mo K-edge EXAFS data was collected at the HXMA beamline at the Canadian Light Source. The monochromatic beam was produced by using a double crystal Si(111) monochromator with the second crystal detuned by 50% to reduce the high harmonic components in the X-ray beam. The beamline was configured in its focused mode with Rh mirrors (collimating and focusing mirrors) in the X-ray beam path. Data collection was performed in fluorescence mode by using 32 element Ge detector. The accumulation time was 0.15 s/step for Mo K-edge. To ensure edge

jump of 1, the thickness of the sample was adjusted based on absorption length calculation. The in-step energy calibration was made by using a Mo metal foil set downstream to the sample (Jiang et al. 2007). Hydrodeoxygenation of oleic acid was carried out in a batch system (300 ml, Parr Instruments). During each catalytic run, 20g of feedstock was used along with solvent (dodecane, 30g). Catalyst loading was maintained at 2 wt%. A constant agitation speed of 700 rpm and hydrogen pressure of 6.89 MPa were maintained for 8 h where the reaction temperature was varied from 350 to 410 °C.

4.3. Results and Discussion

4.3.1 Catalytic activity

Figure 4.1 indicates the influence of the catalysts on the hydrodeoxygenation of oleic acid. Nitride phase of molybdenum (MoN/ γ-Al_2O_3), vanadium (VN/ γ-Al_2O_3) and tungsten (WN/ γ-Al_2O_3) supported on γ-Al_2O_3 were evaluated for their hydrodeoxygenation activity. From the error bars in Fig. 4.1, it can be stated that change in oleic acid conversion for a temperature increase from 350 to 370 °C is not statistically significant. However, increase in temperature from 350 to 390°C resulted in non-overlapping error bars indicating that increase in temperature influences catalytic conversion to a good extent. The statistical significance was 95% confidence interval and the experiments were repeated twice. It is evident that molybdenum shows better catalytic activity in comparison to the other active metals (vanadium and tungsten). Hence, molybdenum was chosen to synthesize the bimetallic catalyst using nickel as the promoter. Performance of NiMoN/γ- Al_2O_3 was superior (>80%) in terms of conversion of oleic acid. Out of the support materials evaluated, performance of Al_2O_3 was proven to be superior in comparison to the other supports and one major reason is its moderate acidic nature that favors

the formation of desired NiMoN phase and decreased formation of agglomerates as indicated in Raman analysis.

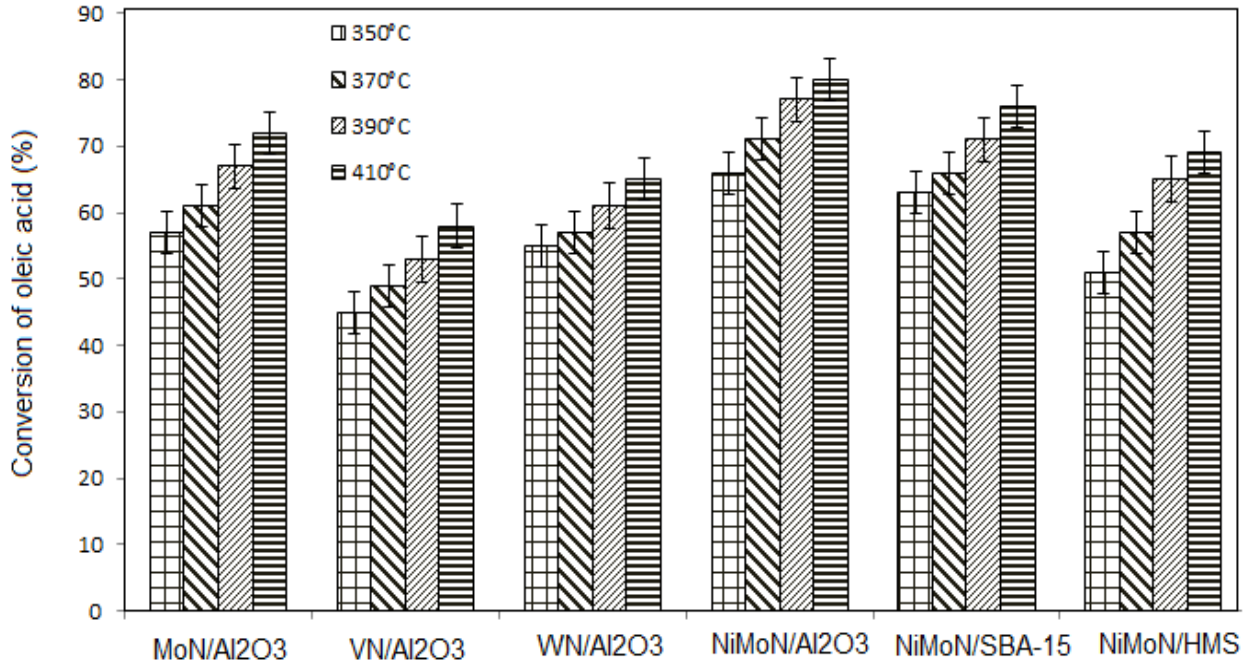

Fig. 4.1. Conversion of oleic acid using different catalysts at different temperatures. Reaction conditions: Oleic acid = 20 g, n-dodecane = 30g, catalyst loading = 2 (w/w)%, speed of agitation =700 rpm, initial hydrogen pressure = 6.89 MPa, reaction time = 8 h. The experiments were repeated twice with 95% confidence interval

The acidity of the catalyst support material aids in the agglomeration of the active metal species and since the performance of NiMoN/ γ- Al_2O_3 was better in terms of oleic acid conversion, it was extensively characterized using Raman and X-ray absorption spectroscopy.

4.3.2 Raman Spectroscopy

Raman spectroscopy measurements on different steps to make the NiMoN catalyst on γ-Al_2O_3 support is shown in Figure 4.2. The γ-Al_2O_3 support does not have any significant Raman bands. In general, the symmetric and asymmetric Mo-O bond stretches for different Mo-species generally occur in the 800-1000 cm^{-1}. In absence of Ni, the MoO_x Raman spectrum shows a broad peak envelope in the range of 700-1000 cm^{-1}.

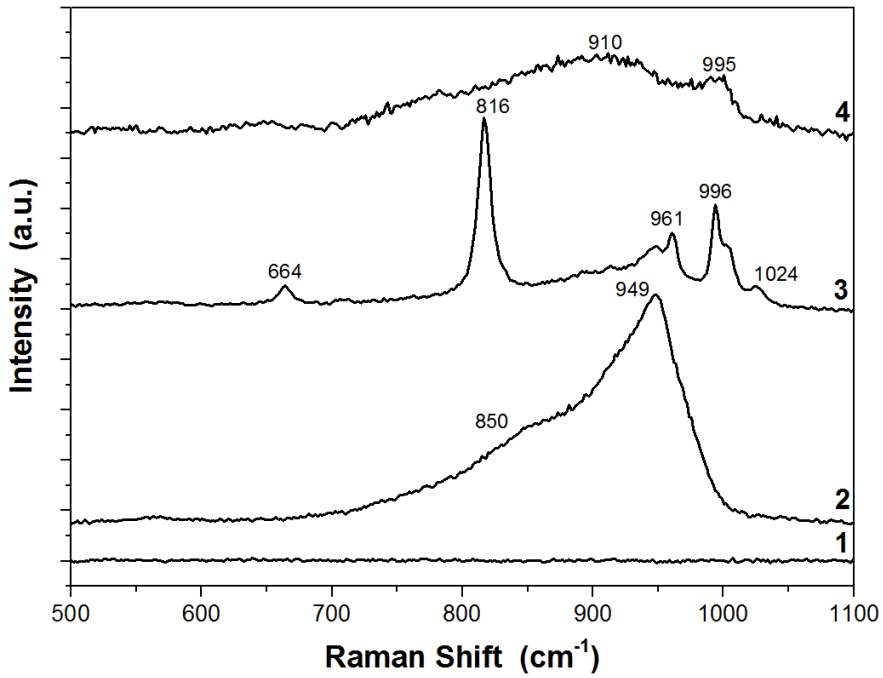

Fig 4.2. Raman spectra of bulk samples. (1) γ-Al_2O_3 (2) MoO/γ-Al_2O_3 (3) NiMoO/γ-Al_2O_3 (4) NiMoN/γ-Al_2O_3. The Raman intensity was very weak for sample No. 4. The laser power was increased by 2.5X to get suitable signal

This broad envelope has a significant shoulder at 850 cm^{-1} and a peak at 949 cm^{-1}, which are typical of polymeric molybdates (Hu et al. 1995). The addition of Ni to the synthesis shows a heterogeneous mixture of different NiMo-phases on the γ-Al_2O_3 support. The Raman bands at 664 cm^{-1}, 816 cm^{-1}, and 996 cm^{-1} correspond to the υ_s(Mo-O), υ_s(O-Mo-O), and υ_s(M=O) stretches for the tetrahedral MoO_3 (Hu et al. 1995). Another band located at 961 cm^{-1} is characteristic of the υ_s(Mo=O) bands of α-$NiMoO_4$ (Hu et al. 1995). The Raman spectrum of the NiMoO conversion to NiMoN shows a significant change in the Raman signature with a broad peak envelope in the 700-1000 cm^{-1} region. The distinct phases of NiMoO seem to have disappeared, which may indicate that the conversion of the oxide to nitride was successful. It should be noted that the peak intensity of this material was very weak, and it required approximately 2.5X higher laser power and this can be attributed to the formation of distorted

tetrahedral-octahedral species. Raman intensity is reduced as a molecule becomes less symmetric due to the reduced polarizability and the emergence of a net dipole moment.

The heterogeneous mixture of NiMoO/MoO on the γ-Al_2O_3 was investigated further by dispersing the material onto a flat substrate and allowed the acquisition of high resolution Raman images of the different NiMoO phases. Figure 4.3 shows a representative result from the Raman measurements completed on an individual γ-Al_2O_3 grain and shows that there are 3 distinct NiMoO/MoO phases on the γ-Al_2O_3 support.

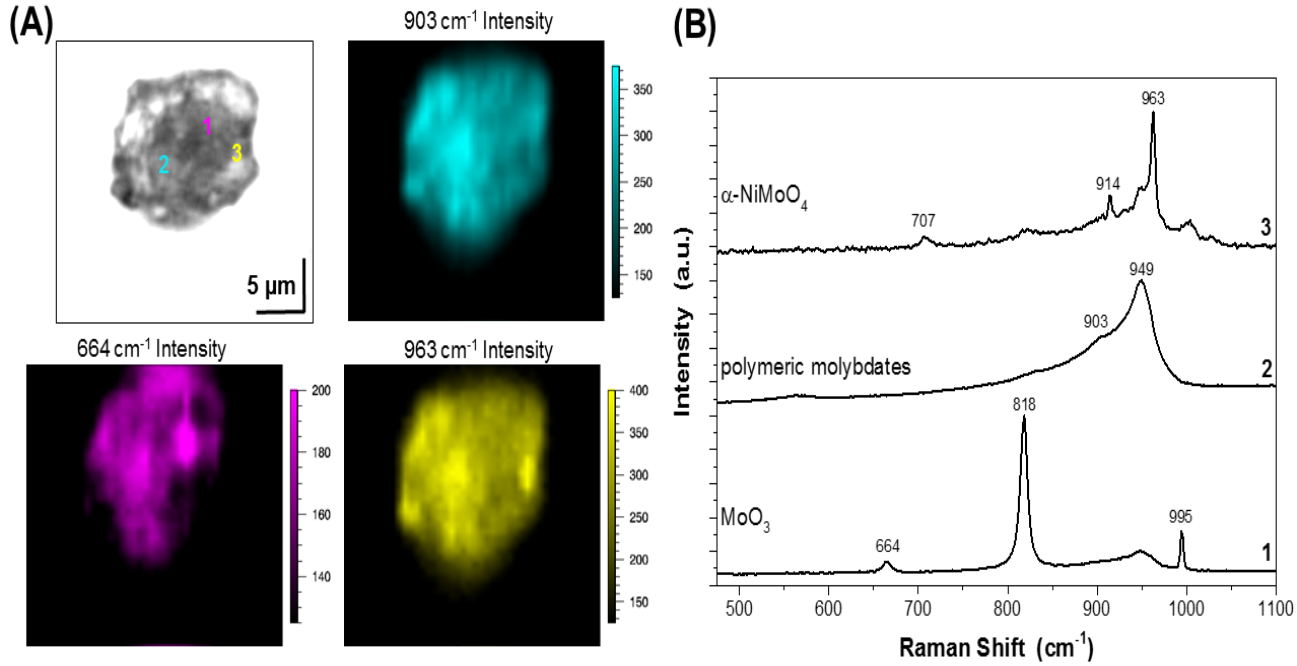

Fig 4.3. Raman spectroscopy performed on a single grain of γ-Al_2O_3 shows the presence of MoO_3, polymeric molybdates, and α-$NiMoO_4$. High-resolution Raman images (0.6 µm x 0.6 µm pixel size) were obtained for the relative amount of each MoO phase by using unique signature peaks for each phase. Individual MoO_3 hotspots can be observed, whereas the polymeric molybdates and α-$NiMoO_4$ distribution seem to correlate together, but there are some individual hotspots for each species

In region (1), there are 3 sharp Raman bands located at 664 cm^{-1}, 818 cm^{-1}, and 995 cm^{-1}. The narrow peak widths indicate that this phase is crystalline. Since the 664 cm^{-1} band is sufficiently away from the Raman bands for the other Mo-species present on the γ-Al_2O_3 support, the

intensity of 664 cm^{-1} peaks can be used to effectively map the distribution of MoO_3. In region (2) there is a broad Raman envelope between 800-1000 cm^{-1} with a prominent shoulder at 903 cm^{-1} and a peak at 949 cm^{-1}. This signature is typically observed for 2D polymeric molybdates [9]. The distribution of the polymeric molybdates can be imaged using intensity value of the shoulder located at 903 cm^{-1}. The Raman spectrum for region (3) shows distinct sharp peaks 707 cm^{-1}, 914 cm^{-1}, and 963 cm^{-1} which are attributed to the υ_s(Ni-O-Mo), υ_a(Mo=O), and υ_s(Mo=O) bands of α-$NiMoO_4$, respectively (Hu et al. 1995). The sharp peak widths indicate a crystalline, and the peak intensity at 963 cm^{-1} can be used to map the distribution of α-$NiMoO_4$.

The Raman images shown in Figure 4.3 indicate that polymeric molybdates and α-$NiMoO_4$ phases are relatively dispersed across the γ-Al_2O_3 grain. The higher intensity hotspots for both the polymeric molybdates and α-$NiMoO_4$ appear in the same regions, indicating that there is a heterogeneous mixture of these species in these areas. However, there are also distinct regions on the γ-Al_2O_3 where there are hotspots of each MoO phase. The MoO_3 phase appears to have some unique hotspots that contain lower amounts of polymeric molybdates and α-$NiMoO_4$.

4.3.3 X-ray Near Edge Spectroscopy (XANES) characterization of catalysts

Figures 4.4 and 4.5 shows the Ni K-edge and Mo L_3-edge spectra of NiMo supported on γ-Al_2O_3 respectively. From the nickel K-edge XANES spectrum, no pre-edge feature, suggesting a 1s-3d transition was observed. In Mo L_3-edge spectra, the change in the intensity indicates the change in the orientation of the metal species (octahedral to tetrahedral coordination). Based on the intensity of the split peaks, the geometry of the catalyst in oxide and reduced phase can be assigned. NiMo supported on γ-Al_2O_3 can be compared in it's oxidized and the reduced phase (Fig. 4.6). The shift towards lower energy indicates that the catalyst sample was reduced and molybdenum was present in its reduced state.

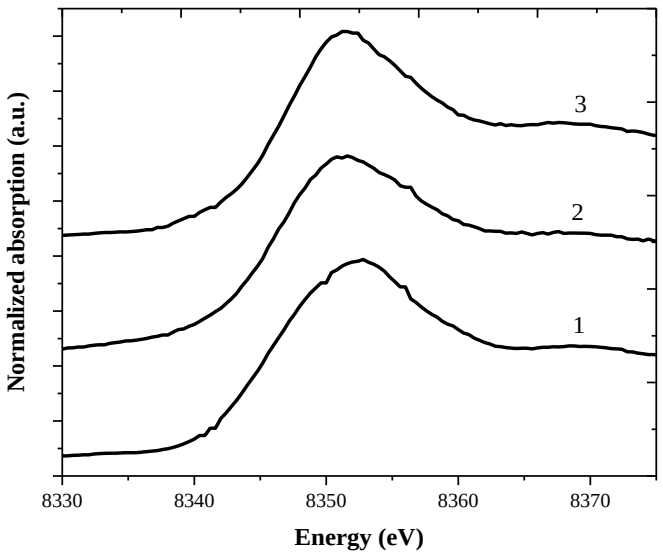

Fig. 4.4. Ni K-edge XANES spectra of catalysts (1-NiMoO/ γ-Al_2O_3; 2-NiMoN/ γ-Al_2O_3; 3-NiMoO/SBA-15)

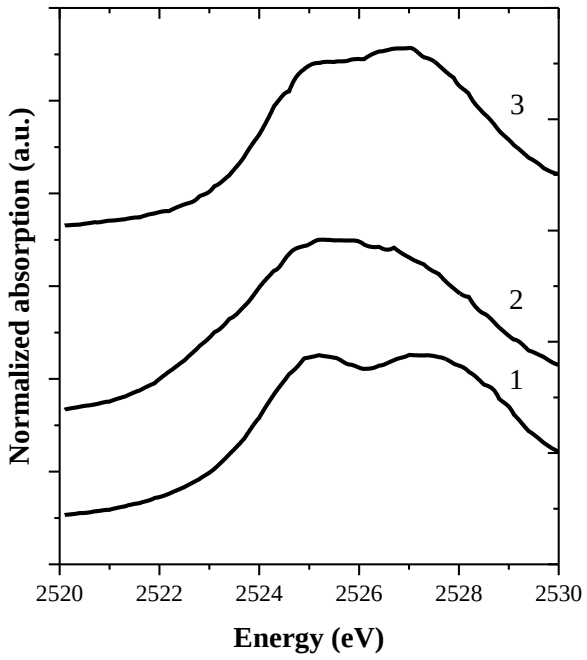

Fig. 4.5. Mo L_3-edge XANES spectra of catalysts (1-NiMoO/γ-Al_2O_3; 2-NiMoN/γ-Al_2O_3; 3-NiMoO/SBA-15)

In the oxide phase, molybdenum is present in +6 state and during reduction, it goes to +4 state which results in the shift in the peak towards lower absorption energy**.** Presence of primary peak at 2524 eV and a secondary peak at 2527 eV indicates that molybdenum existed in oxidation

states between +4 and +6 (Hu et al. 1995). Splitting of the peak to result in sharp intensity at 2525 eV and 2527 eV is due to the ligand field splitting of the Mo 2p orbitals, which is possible in the distorted octahedral symmetry (or Mo^{6+}) (Cattaneo et al. 2000).

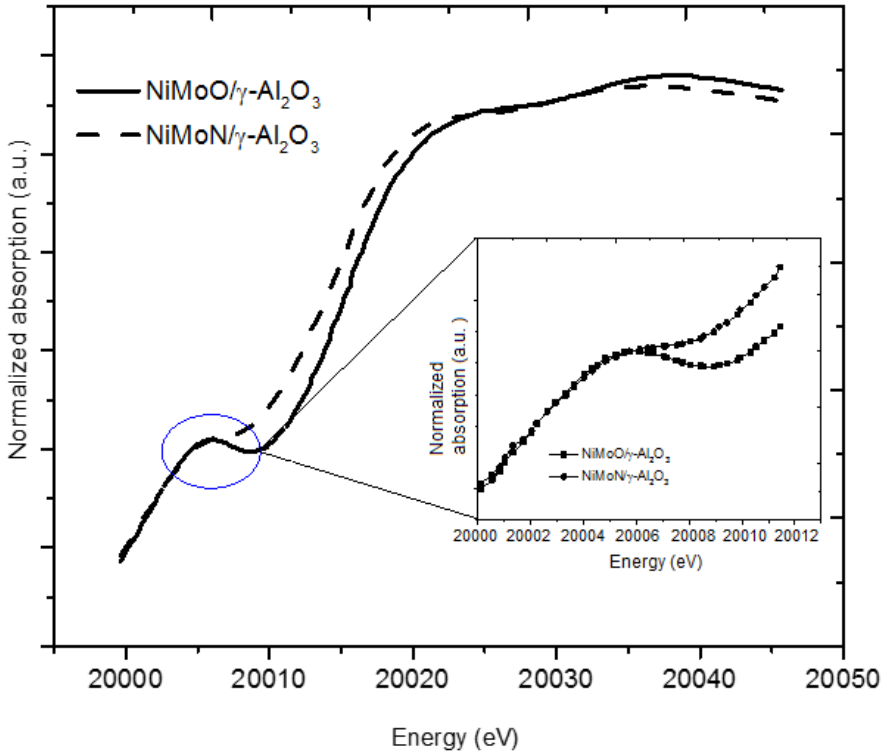

Fig.4.6. Mo K-edge plot indicating the change in oxidation state

4.3.4 Extended X-ray absorption fine structure (EXAFS) characterization of catalysts

For background removal, E^0 was fixed 20016 eV with k-weight spacing of 2 and edge step 0.699. Pre-edge region was fixed between -150 to -30 with normalization range from 150 to 858 and k spline range from 0.0-15.8. Forward Fourier transform was performed in the k-range of 2-15 and differential k (delta k) of 1 with hanning function and arbitrary k-weight of 0.5. During the forward Fourier transform, phase correction was not employed. For backward Fourier transform, the R-range was 1 to 5 with hanning window function. The accumulation time was 0.15 s/step for Mo K-edge and to ensure edge jump of 1, the thickness of the sample was adjusted based on absorption length calculation.

The EXAFS function was obtained from the absorption spectra after background removal, normalization and Fourier transformation and the k-spaced plot for the oxide and nitride samples are shown in Fig. 4.7.

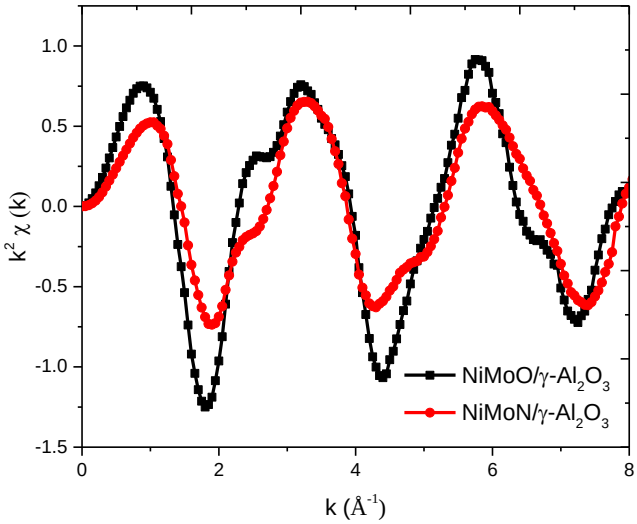

Fig. 4.7. k-spacing (Mo K-edge) plot of oxide and nitride phase of NiMo catalyst

If the structure of the standard molybdenum precursor (Ammonium heptamolybdate) is well-ordered, the Mo-Mo coordination number will be 3.3 (Cattaneo et al. 2000). However, in polymolybdates, the Mo-Mo bonds are not well ordered and a weak signal was obtained around 3Å and the Mo-Mo coordination number obtained from fit is 1 (Fig. 4.8). Mo-O bonds had a length of 1.7Å and the length of Mo-O bonds varied between 1.75-2.6 Å (Cattaneo et al. 2000). Table 4.1 indicates the detailed bond length calculation from EXAFS analysis. The Mo-N distance range from 2.152-2.206 Å and Mo-Mo distance is usually 2.605-3.008 Å. Polymolybdates are the most stable Mo species and they usually occur at an isoelectric point of 2 and the generalized form is $[Mo_7O_{24}^{-}{}_m (OH)_m]^{(6-m)-}$ (Cattaneo et al. 1999). EXAFS revealed no indication of Mo-support interaction. The Mo-Mo bond distance was determined to be 1.9 Å and the cluster heptamolybdate polyanion had an average Mo-Mo coordination of 3.4.

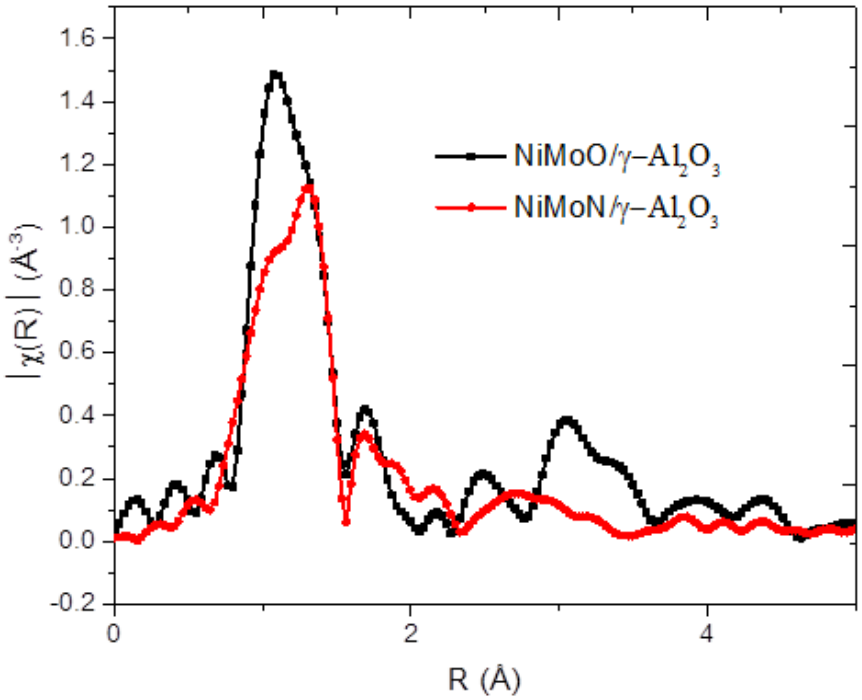

Fig. 4.8. Calculation of bond length for oxide and nitride phase of NiMo catalyst

Table 4.1. X-ray absorption fine structure parameters

Sample	Bond pair	CN	Distance (nm)	Debye-Waller factor (nm)
$Mo_2N/\gamma\text{-}Al_2O_3$	Mo-N	2.3	0.221	0.0092
	Mo-Mo	1.9	0.268	0.0083
$NiMoN/\gamma\text{-}Al_2O_3$	Mo-N	1.7	0.216	0.0089
	Mo-Mo or (Mo-Ni)	1.9	0.265	0.0080
$NiMoO/\gamma\text{-}Al_2O_3$	Mo-O	2.5	0.254	0.0085
	Mo-Mo or (Mo-Ni)	2.1	0.276	0.0086

4.3.5 Catalytic activity-structure relationship for hydrodeoxygenation of oleic acid

The conversion of oleic acid to the paraffin's (major product) occurs through several intermediate steps. Product analysis indicated that hydrogenation of oleic acid leading to the formation of stearic acid is the primary step.

$C_{17}H_{33}COOH + H_2 \rightarrow C_{17}H_{35}COOH$ (4.1)

Stearic acid undergoes decarboxylation and decarbonylation to yield n-$C_{17}H_{36}$ and $C_{17}H_{34}$ respectively. The schemes for the reactions are provided below.

$C_{17}H_{35}COOH \rightarrow CO_2 + n\text{-}C_{17}H_{36}$ (4.2)

$C_{17}H_{35}COOH \rightarrow CO + H_2O + C_{17}H_{34}$ (4.3)

At a reaction temperature of 300°C, the $\Delta G_{reaction}$ for decarboxylation and decarbonylation reactions are -83.5 and 17 kJ/mol respectively. The $\Delta H_{reaction}$ at the same conditions for decarboxylation and decarbonylation reactions are 9.2 and 179.1 kJ/mol (Snare et al. 2006). Additionally, the usage of NiMo/γ-Al_2O_3 resulted in the formation of octadecane ($C_{18}H_{38}$) by the direct hydrodeoxygenation as shown in Eq. (4.4) and similar reaction was reported by Ayodele et al. (2015).

$C_{17}H_{35}COOH + 3H_2 \rightarrow C_{18}H_{38} + 2H_2O$ (4.4)

The presence of the promoter (Ni) enhances the hydrogenation reaction and the excess hydrogen is used for the direct hydrodeoxygenation reaction. The possible reaction pathway for the hydrodeoxygenation of trioleic triglyceride was adopted from Kovács et al. (2011) with permission from publisher (Fig. 4.9). Reaction (I) indicates the direct HDO resulting in formation of water and reaction (II) and (III) indicates the decarboxylation and decarbonylation routes. A quick look at the scheme indicates that selectivity towards direct HDO (Reaction 1) can be increased by increasing the amount of hydrogen.

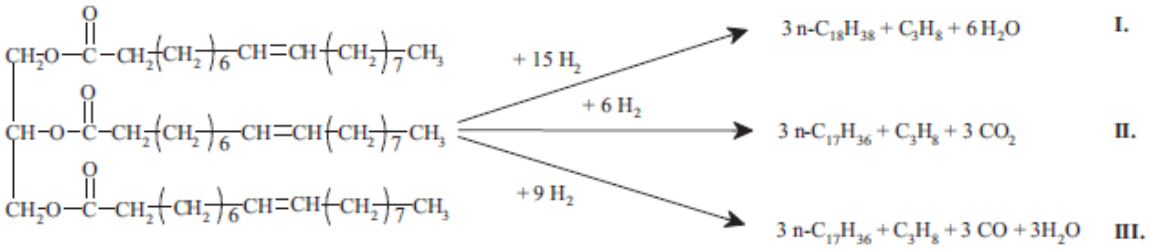

Fig. 4.9 Possible reaction pathways for oxygen removal by H_2 from trioleic triglycerides.

(Reproduced from Kovács et al. (2011) with permission from Elsevier)

The presence of the promoter metal (Nickel) aids in the hydrogenation of oleic acid to stearic acid and direct hydrodeoxygenation, decarboxylation and decarboxylation reactions were observed. The occurrence of polymeric molybdates as confirmed by the Raman spectroscopy leads to the decrease in the availability of active metals for the selective removal of water without breaking the carbon bond leading to the formation of $C_{18}H_{38}$.

From the reactions schemes (1-4), it can be said that direct hydrodeoxygenation is favored by the increased supply of hydrogen. In the NiMo/γ-Al_2O_3 system, the major product formed was n-octadecane (>40%) indicating that direct hydrodeoxygenation was favored. The Lewis acidity of the support material (γ-Al_2O_3) enhances the adsorption and subsequent splitting of hydrogen. Decreasing the occurrence of polymeric molybdates will enhance the availability of vacancy sites for hydrogen adsorption and spillover helping in minimization of decarboxylation and decarbonylation reaction.

During batch reaction, the bimetallic supported catalyst system performed better than the monometal systems in terms of HDO of oleic acid. The difference in the conversion of oleic acid on the different support materials can be attributed to the extent of hydrogen bonding between the acid (oleic/stearic acid) and the hydroxyl group from the support (Webber et al. 2016).

Hydrogen bonding between the reactant acid and the hydroxyl groups of the support material affects the extent of oleic acid conversion. Additionally, the bi-porous nature of SBA-15 and the decreased instability of HMS in comparison to γ-Al_2O_3 must have played a crucial role in governing the extent of HDO reaction on different support materials.

4.4. Conclusions

Raman analysis indicates that the active metals (Mo and Ni) are not uniformly distributed on the support material and there is a pattern governing the migration of the active metal species. No pre-edge peak was recognized in Ni K-edge XANES spectra indicating that tetrahedral geometry of nickel species was absent and the nickel species were present in octahedral geometry and the nickel species were co-ordinated with the oxygen atoms only. There is no ligand field splitting under tetrahedral symmetry. When the catalyst was reduced, there was a shift towards lower absorption energy and absence of the secondary peak. The chemical shift also indicates stronger bonding between the metal species and the support material. Mo L_3-edge clearly indicated that γ-Al_2O_3 support offered distorted tetrahedral-octahedral geometry and the SBA-15 offered tetrahedral geometry. Better catalytic performance of γ-Al_2O_3 supported catalyst can be attributed to the occurrence of distorted tetrahedral-octahedral geometry. Raman spectroscopy indicates that Mo is present in the form of clusters and these Mo clusters interact with the support material. The Mo-O and Mo-N coordination distance were estimated to be 2.5± 0.1Å and 2.1± 0.1Å respectively. The occurrence of particular oxidation states and the coordination environment governs the efficiency of the hydrotreating catalysts.

CHAPTER 5

PROMOTIONAL EFFECTS OF Cu, Cr AND Fe on NiMo/γ-Al_2O_3 FOR THE HYDRODEOXYGENATION OF OLEIC ACID

The outcome (manuscripts/conference presentations) from this phase of work are listed below:

1. N.Arun, H. Sulimma, Y. Hu, A. K. Dalai. Promotional effects of Cu, Cr and Fe on NiMo/γ-Al_2O_3 for the hydrodeoxygenation of oleic acid. (Under preparation for submission to *Journal of Cleaner Production).*
2. N. Arun, R. V. Sharma, U. Das, Y. Hu, A. K. Dalai. Mesoporous silica-alumina supported transition metallic nitride and mixed metal catalysts for the production of third-generation biofuels. *26th Canadian Material Science Conference*, University of Saskatchewan, Canada, June 1-4, 2014.

Contribution of the Ph.D. candidate and collaborators

All the experimental and characterization work was conducted by Naveenji Arun. Manuscript writing and revision work were done by Naveenji Arun based on the suggestions from Dr. R. V. Sharma, Dr. Ajay K. Dalai and Dr. Yongfeng Hu. H. Sulimma performed screening tests using mono-metallic catalyst systems for HDO of canola oil. Dr. U. Das offered key suggestions in the synthesis of mixed metal catalysts for the HDO reactions.

The contribution of this chapter to the overall Ph. D. work

This chapter focused on (1) Understanding the promotional effects of Cu, Cr and Fe, (2) Identifying the most influential process parameter, and (3) Optimizing the process parameter conditions for the best performing catalyst.

Abstract

Hydrodeoxygenation of oleic acid was carried out using transition metallic carbide and nitride catalysts in a continuous flow reactor (trickle bed system). Single metallic catalysts using Molybdenum (Mo), Vanadium (V) and Tungsten (W) supported on γ-Al_2O_3 were synthesized using incipient wetness impregnation method and were tested in trickle bed reactor. In continuous mode, hydrodeoxygenation reactions were carried out at the following conditions: Temperature = 390°C; LHSV = 0.46 h^{-1}; hydrogen pressure= 8.96 MPa. All the single metallic catalysts had a metal loading of 7.4 wt.%. MoN catalyst supported on γ-Al_2O_3 performed well in terms of oxygen removal (>90%) and alkane/olefin selectivity of 30%. In batch system, bimetallic catalyst (NiMo/ γ-Al_2O_3) promoted with Cu/Cr/Fe (CuNiMo/γ-Al_2O_3; CrNiMo/γ-Al_2O_3 and FeNiMo/γ-Al_2O_3) catalysts were used for the hydrodeoxygenation of oleic acid. Reactions were carried out at 300°C, hydrogen pressure of 6.89 MPa and agitation speed maintained at 600 rpm and maximum hydrodeoxygenation conversion of 92% was obtained using CuNiMo/γ-Al_2O_3. Optimization of the process parameters (reaction temperature, catalyst loading, hydrogen pressure, reaction time) was performed using orthogonal design matrix (OA_{16} matrix) for the best performing catalyst (CuNiMo/γ-Al_2O_3).

Keywords: NiMo, oleic acid, Hydrodeoxygenation, conversion, selectivity, optimization.

5.1. Introduction

Biomass is proven to be an efficient feedstock for renewable fuel production as it is easily available and carbon neutral (Ayodele et al., 2015). Higher oxygen content (>35 wt. %) in biooils obtained from biomass impose certain concerns related to their oxidative stability and engine usage (Bu et al., 2012). Present generation engines should be able to handle the bio-renewable fuels without any major modifications and the biofuels should not cause a decrease in

engine power (Case et al., 2014). It should be easily miscible with diesel fuels and should be of good quality in terms of CO_2 neutrality (Chen et al., 2015). To enhance the combustion and storage properties of alternate biofuels, it is mandatory to remove or lessen the oxygen content in biooils (De et al. 2015). Hydrodeoxygenation (HDO) of vegetable oils and biooils is an effective way to produce green diesel (hydrotreated renewable diesel) with desired combustion and engine properties. Hydrodeoxygenation of oils from renewable feedstocks is a catalytic process and mostly transition metallic catalysts have been employed (Dickson et al. 2014).

Production of transportation fuels from biooils obtained from biomass primarily involved deoxygenation reaction as a primary step. During direct deoxygenation, hydrogen reacts with the oxygen-rich reactant and water is formed as a by-product. Deoxygenation involves the removal of oxygen from the feedstock in the form of CO_2 (decarboxylation) and/or CO (decarbonylation). Design and development of catalyst with suitable physico-chemical properties are some of the most challenging tasks that affect the commercialization of hydrodeoxygenation process. Mostly, noble metals have been employed for hydrotreatment of biooils and vegetable oils. In addition to being expensive, noble metals (Pd, Pt and Rh) undergo considerable deactivation due to coke formation. However, it is reported that noble metal catalyst outperforms traditional hydrotreating catalysts in terms of yield and degree of deoxygenation (Do et al. 2012).

Hydrodeoxygenation of vegetable oils and canola oil yields wide range of products and the most desired products are paraffin and olefins (Duan et al. 2015). Diesel range carbon chains (C_{16}-C_{18}) and bio-aviation fuels (C_8-C_{15}) can be produced depending on the unsaturation in the feed oil, Free Fatty Acid (FFA) value nature of catalysts employed in the reaction (Table 5.1). Usually, hydrodeoxygenation reactions involve usage of model compounds. Guaiacol (Chiu et al. 2014),

oleic acid (Yang et al., 2015) and methyl laurate (Chen et al. 2015) were employed as model compounds in few earlier works to understand the mechanism of hydrodeoxygenation reaction.

Table 5.1. Physicochemical properties of canola oil (Roiaini, 2015)

Properties	Canola oil
Relative Density (g/cm^3; 20°C/water at 20°C)	0.914 - 0.917
Viscosity (Kinematic at 20°C, mm^2/sec)	78.2
Iodine value (g I_2/100 g)	114.47 ±1.423
Peroxide value (m eq O_2/kg)	5.73±0.949
FFA Value (%)	0.16±0.011

Some studies have employed real feedstocks such as castor oil (Liu et al. 2015) and jatropha oil (Guo et al. 2015). Mostly single and bi-metallic catalysts in reduced phase are used during reactions and the reduced phases are usually sulfide, carbide, nitride or phosphide. Zarchin et al. (2015) investigated on hydrotreatment of soybean oil using nickel phosphide catalysts (Ni_2P) supported on silica and HY zeolite. Metal loading (Ni) was maintained at 25 wt. % and it was reported that silica support did not offer any cracking activity. However, acidic support (HY zeolite) exhibited hydrocracking and isomerization activities. It is evident that the acidity of support material affects the extent of hydrotreatment and subsequent oxygen removal reactions. Ayodele et al. (2015) employed palladium supported on zeolite catalysts for the hydrodeoxygenation of oleic acid in a semi-batch reaction system. To increase acidity of the material, palladium was functionalized with oxalic acid. Addition of fluoride (to increase acidity) caused increased dispersion of palladium and it was confirmed through Energy-dispersive X-ray (EDX) spectra.

Duan et al. (2015) carried out hydrodeoxygenation of octanoic acid using Ni/ZrO_2 catalysts. Contrary to most catalytic systems, Molybdenum (Mo) was used as promoter to Ni/ZrO_2 to

analyze the influence of Mo. It was reported that addition of Mo favored hydrogenation and dehydration reaction. Moreover, it was reported to increase the hydrogen adsorption capacity of Ni/ZrO_2 catalyst. In our screening studies using continuous trickle bed system, γ-Al_2O_3 (moderate acidity) was employed as the support material and carbide and nitride phase of Mo, V and W were employed to evaluate the HDO performance of single metal catalysts using oleic acid. Once the best performing catalyst was confirmed in continuous phase, the catalyst was impregnated with Ni (primary promoter) and further impregnated with Cu/Cr/Fe (secondary promoter) and the reactions were performed in batch system to optimize process parameters.

Reports on optimization of process conditions for hydrodeoxygenation reaction is scarce. A stepwise approach is a commonly used optimization method though it is highly time consuming. Orthogonal array design has the ability to evaluate parameters individually and it ensures uniform distribution of combination of each level. Full-scale test in an orthogonal array design involves analysis of the combination of all factors and levels and is very time consuming and its feasibility is highly questionable (Wu and Leung, 2011). A unique feature of orthogonal array is the selection of few selective combinations of parameters and their levels. It is ensured that these selected combinations are uniformly distributed and is a good representation of the complete examination area. Recently, chemometric approach such as orthogonal array experimental design has gained importance and this chapter deals with the application of orthogonal array design for optimization of process condition for hydrodeoxygenation process. The main objective of this chapter is to optimize four parameters (reaction temperature, catalyst loading, hydrogen pressure, reaction time) for the hydrodeoxygenation of oleic acid.

5.2. Experimental Details

5.2.1 Catalyst Synthesis and Characterization

Single metal catalyst systems (Mo, V and W supported on γ-Al_2O_3) were prepared using commercial γ-Al_2O_3 (Alfa Aesar, USA) as support material. Incipient wetness impregnation method was employed to load metal salt solutions on the support material. Impregnated catalysts were dried at 110°C (2h) and calcined for 6h at 550°C. In single metal catalyst synthesis, the oxide phase of the catalysts obtained after calcination was converted to nitride and carbide phase in a temperature programmed reduction setup. Carbide phase of catalyst was produced using a gas mixture (85% H_2, 10% C_2H_4 and 5% N_2) and 100% ammonia (NH_3) was employed to produce nitride catalyst and the reduced catalysts were passivated using 1% by volume oxygen. Before hydrodeoxygenation reactions, the passivated catalysts were reduced again using hydrogen (6.89 MPa) at 270°C for 4h. X-ray fluorescence (XRF) analysis was performed using Rigaku RIX 3000 WD-XRF with 3 kM generator to analyze the metal loading on the catalyst. XRD analysis was performed using BRUKER D500TT and D5000 diffractometers with Cu (Kα) radiation at 1.54 Å (Sulimma, 2008). Physico-chemical properties of the catalysts were analyzed using BET analysis performed with Micromeritics ASAP 2000 system.

5.2.2 Experimental setup

High-pressure stainless steel tubular reactor (I.D.= 6.0 mm; total length = 395 mm) was employed for continuous hydrotreatment reactions and the experimental apparatus is shown in Fig. 5.1. The catalyst of particular loading (2 g) mixed with 15g of silicon carbide (0.425-0.850 mm) was loaded and the setup is shown in Fig. 5.1 (b). The available reaction volume was approximately 10 ml.

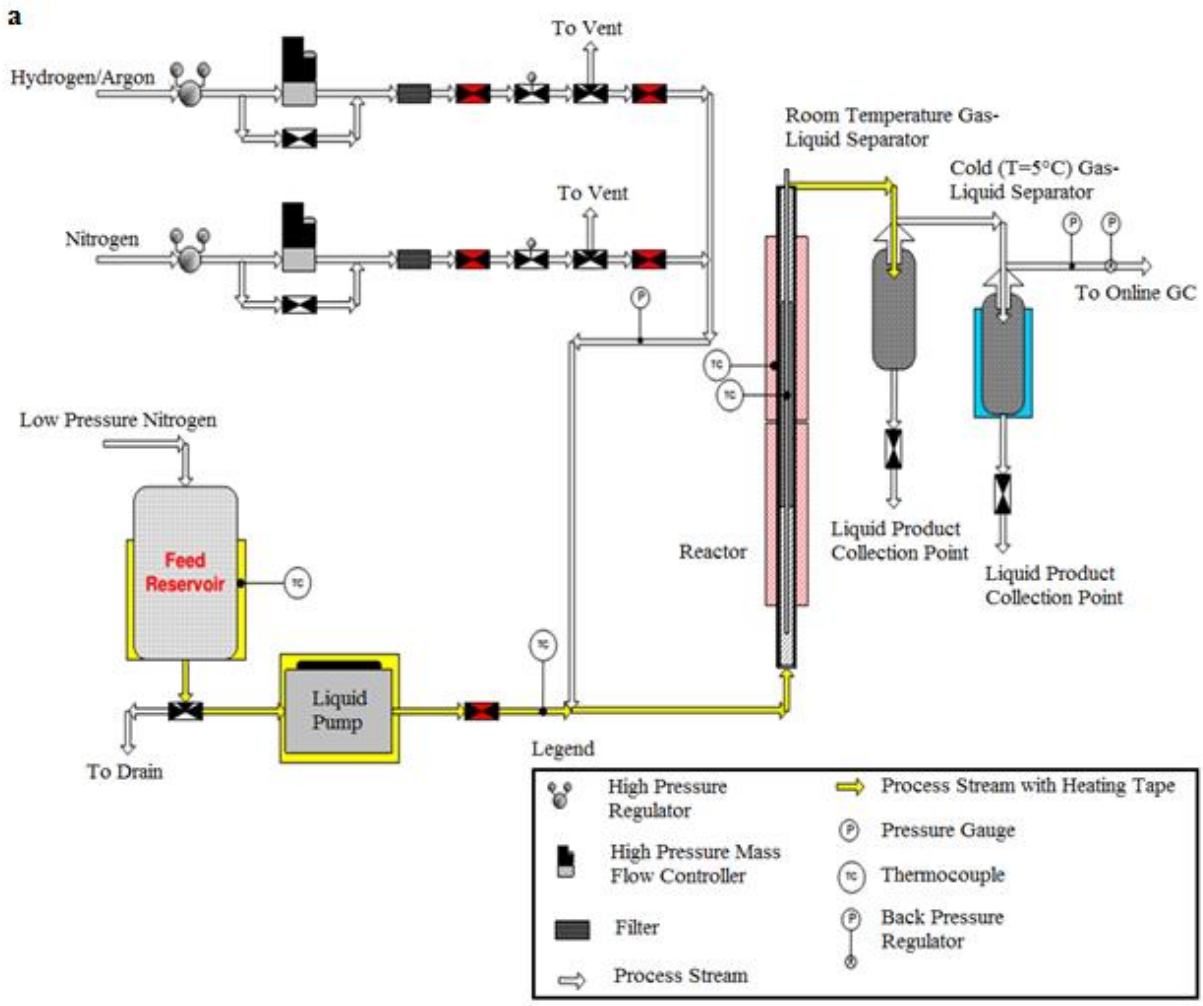

Fig.5.1.a Experimental setup for continuous reactor system (Sulimma 2008)

Liquid reaction samples were pumped upflow through the reactor for uniform flow distribution and increase the contact time with the catalyst bed. To prevent solidification of heavier products in the lines, heating tapes controlled by manual rheostats were used. Gas samples were analyzed using HP5890 gas chromatograph equipped with TCD and FID setups. Additionally, analysis of light end gases was carried out using Agilent micro gas chromatograph model 3000A. Pre-reduction of catalyst was carried out using 90% H_2 to reduce the catalyst. The liquid samples

were analyzed using GC system and the oxygen content change was obtained using C/H/N elemental analyzer.

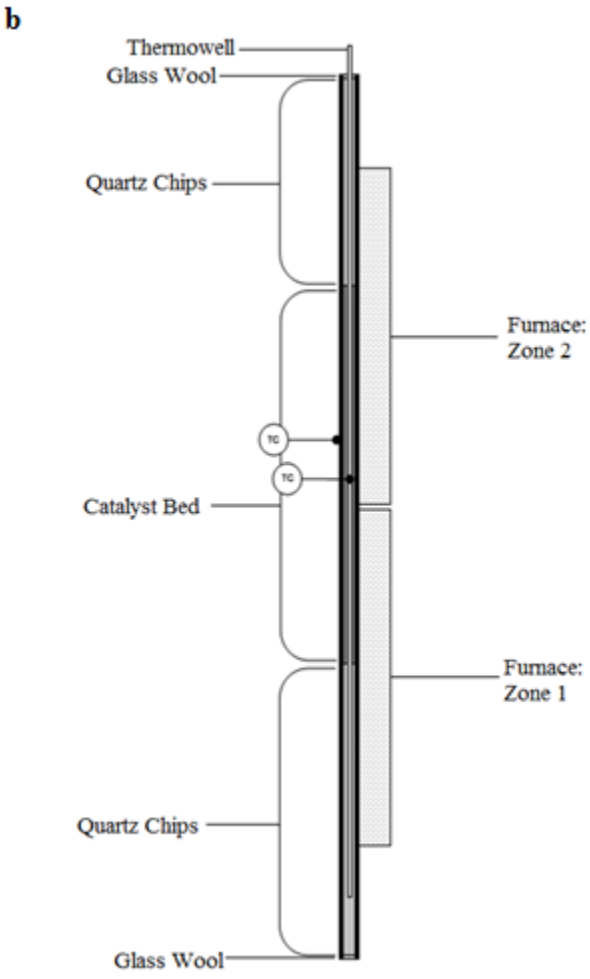

Fig.5.1.b Representation of catalyst bed (Sulimma. 2008)

Conversion (%), selectivity (%) and yield (wt. %) were calculated based on the equations (Eq.5.1, 5.2 and 5.3) (Sulimma. 2008).

$$\text{Conversion (\%)} = \frac{\text{Change in the molar amount of oleic acid after reaction}}{\text{Initial molar amount of oleic acid}} \times 100\% \qquad (5.1)$$

$$\text{Selectivity (\%)} = \frac{\text{molar amount of each product}}{\text{molar amount of oleic acid converted to products}} \times 100\% \qquad (5.2)$$

$$\text{Yield (wt.\%)} = \frac{\text{weight of each product formed after reaction}}{\text{weight of oleic acid used in the reaction}} \text{ x } 100\% \quad (5.3)$$

Best performing single metallic catalyst was impregnated with Ni (primary promoter) and subsequently with Cu/Cr/Fe (Secondary promoters) and HDO reactions were performed in batch system using oleic acid and the performance of the catalysts was compared in terms of oleic acid conversion and selectivity towards n-octadecane. Studies were done in batch and continuous mode in order to evaluate the performances the catalysts for HDO process.

5.2.3 Experimental design using orthogonal array

Influence of process parameters such as catalyst loading (A), time of reaction (B), temperature (C) and hydrogen pressure (D) on oleic acid conversion and selectivity towards n-octadecane from oleic acid for best performing trimetallic catalyst was analyzed using orthogonal array design (OA_{16}) matrix. All the levels for each variable were covered in this design. To complete optimization process, 16 trials were carried out with randomized run orders to avoid subjective bias. Range analysis and analysis of variance (ANOVA) were performed to predict the optimal values for reaction condition and experiments were repeated thrice at optimal condition to confirm the repeatability of data. In range analysis, the parameter K_{ji} is the total of evaluation indexes in various levels (i=1, 2, 3, 4) for various factors. In range analysis, larger the value of range parameter (R_j), greater is the importance of that particular factor. Owing to the limitations involved with range analysis, ANOVA analysis was performed to understand the factor's magnitude affecting the index. During ANOVA analysis, factors and experimental errors influence the output, and F-test was performed to quantitatively determine the influence of a factor (Wu. 2011).

5.3. Results and Discussion

5.3.1 Screening tests in continuous mode

Physico-chemical properties of the monometallic catalytic systems are shown in Tables 5.2 and 5.3.

Table 5.2. Physico-chemical properties of monometallic catalysts

Phase of catalyst	Catalyst	BET surface area (m^2/g)	Pore volume (x 10^{-6} m^3/g)	Loading of metal x 10^6 (moles/m^2)	Average Pore diameter (nm)
Nitride	7.6 wt% Mo/γ-Al_2O_3	187	0.443	4.11	10.3
	10.4 wt.% W//γ-Al_2O_3	188	0.487	2.91	9.8
	3.4 wt.% V/γ-Al_2O_3	191	0.532	3.15	11.1
Carbide	7.6 wt% Mo/γ-Al_2O_3	176	0.491	4.19	10.8
	10.4 wt.% W//γ-Al_2O_3	181	0.499	2.87	10.2
	3.4 wt.% V/γ-Al_2O_3	187	0.534	3.03	11.9

Table 5.3. Chemical composition of the catalysts

Catalyst precursor	γ-Al_2O_3 (wt.%)	MoO_3 (wt.%)	WO_3 (wt.%)	V_2O_5 (wt.%)	SiO_2 (wt.%)	P_2O_5 (wt.%)	Cl (wt.%)
Mo	90.1	10.9	-	-	0.2	0.3	0.2
W	88.4	-	11.9	-	0.2	-	-
V	93.1	-	-	5.7	0.2	-	-

The metal loading of Mo, W and V were 7.4, 10 and 3.1 wt.% respectively in order to ensure equal availability of active sites for all the catalysts (Sulimma, 2008). In continuous setup, catalyst loading (MoN/γ-Al_2O_3 – 2 g; WN/γ-Al_2O_3- 1.44 g; VN/γ-Al_2O_3 – 1.28 g; MoC/γ-Al_2O_3 –

2 g; WC/γ-Al_2O_3- 1.44 g; VC/γ-Al_2O_3 – 1.28 g) was modified to ensure availability of same number of active sites for all the catalysts (Table 5.4).

Table 5.4. Calculation of catalyst loading in continuous system

Phase of catalyst	Catalyst	Metal molecular weight (g/mol)	Active site coordination	Reactor loading (g)
Nitride	7.6 wt% Mo/γ-Al_2O_3	95.94	2	2.00
	10.4 wt.% W/γ-Al_2O_3	183.85	1	1.44
	3.4 wt.% V/γ-Al_2O_3	50.94	1	1.28
Carbide	7.6 wt% Mo/γ-Al_2O_3	95.94	2	2.00
	10.4 wt.% W//γ-Al_2O_3	183.85	1	1.44
	3.4 wt.% V/γ-Al_2O_3	50.94	1	1.28

Table 5.5. Percentage removal of oxygen (T=380°C, LHSV=0.45 h^{-1}, P_{H2}=6.89 MPa)

Catalyst	Mo_2C/ γ-Al_2O_3	WC/ γ-Al_2O_3	VC/ γ-Al_2O_3	Mo_2N/ γ-Al_2O_3	WN/ γ-Al_2O_3	VN/ γ-Al_2O_3
% HDO	94	81	61	95	85	68

In comparison of Molybdenum (Mo), Vanadium (V) and Tungsten (W) supported on γ-Al_2O_3 in carbide and nitride phase, performance of nitride phase of Mo supported on γ-Al_2O_3 was better in terms of paraffin yield and overall HDO conversion (Table 5.5 and 5.6). Hollak, 2013 compared Mo_2C and W_2C supported on carbon nanofiber (CNF) for the hydrodeoxygenation of oleic acid and it was shown that W_2C favored formation of olefin products and expressed higher deactivation rate.

Table 5.6. Gas by-product (Reaction temperature=390°C, LHSV=0.45 h^{-1}, P_{H2}=6.89 MPa)

Catalyst	CO*	CO_2*	Methane*	Ethane*
$Mo_2C/\gamma\text{-}Al_2O_3$	3.47	8.01	4.77	5.23
$WC/\gamma\text{-}Al_2O_3$	10.99	11.23	2.32	2.23
$VC/\gamma\text{-}Al_2O_3$	11.02	12.16	1.77	1.87
$Mo_2N/\gamma\text{-}Al_2O_3$	4.67	6.98	2.13	2.12
$WN/\gamma\text{-}Al_2O_3$	10.98	9.89	1.45	1.34
$VN/\gamma\text{-}Al_2O_3$	12.06	11.89	1.35	1.56

*Units of all values: L of gas produced at STP/L of liquid feed

Overall, it was concluded that Mo_2C/CNF is better than W_2C/CNF in terms of HDO activity and catalyst stability. Similarly, in our screening tests, performance of Mo was observed to be better than W and V in terms of catalytic activity and our results in agreement with the results reported by Hollak et al., 2013. As reported by Duan et al., 2015, higher loading of molybdenum can cause decrease in catalytic activity due to the preferential occupation of molybdenum species over anionic vacancy sites and also increased coverage of nickel active sites. Increase in molybdenum loading from 1 wt.% to 15 wt.% on Ni/ZrO_2 catalyst, substantially decreased the catalytic activity and selectivity. At an optimized metal (Mo) loading of 10 wt.%, the catalytic conversion and selectivity were reported to be maximum (> 75%). In commercial hydrotreating catalysts, the molybdenum loading is usually around 13 wt.%.

At steady state, the HDO conversion in continuous system was approximately 96%. At the same reaction conditions, single metallic catalyst ($MoN/\gamma\text{-}Al_2O_3$) gave a conversion of 87% in continuous mode and in batch mode, the conversion was 65%. During hydrodeoxygenation of

oleic acid, formation of carboxylate anion is evident as the hydrogen in the carboxyl group is acidic and the oxygen in the carboxylic group can coordinate with metal cation. Unidentate type of coordination is proposed to occur in the coordination structure. In transition metallic catalyst system, only one coordination site is generally available. Once the metal carboxylate is formed, they can decompose at elevated temperature and two reaction pathways can happen

$$M(RCOO)_2 \rightarrow R_2C{=}O + H_2O + CO_2 + MO \quad (12)$$

Since there is considerable availability of carboxylic acid and the decomposition is usually catalytic. The reaction scheme can be as follows.

$$M(RCOO)_2 \rightarrow R_2C{=}O + H_2O + MCO_3 \quad (13)$$

Once the metal carboxylate is formed, it gets suspended in the unreacted carboxylic acid and in the presence of hydrogen, and further reaction can take place to yield the desired products.

5.3.2 Screening tests in batch mode

In batch system, maximum conversion of 80% was achieved over 8 h reaction time. Fig. 5.2 indicates the temperature dependence of oleic acid conversion and selectivity towards n-octadecane using CuNiMo/γ-Al_2O_3 catalyst. Higher temperature (>300 °C) is required for the splitting of gaseous hydrogen molecule and further spill over of hydrogen species on the active metal sites. Presence of nickel promotes the migration of hydrogen species (spill over) and reduced sites on Mo metals promotes sites for the adsorption of oxygen containing molecules (Prins, 2012). The steady rise in temperature from 260°C to 320°C at hydrogen pressure of 6.89 MPa and reaction time of 8 h in batch setup caused increase in conversion from 75% to 92%. However, the selectivity towards n-octadecane was found to decrease once the reaction temperature was maintained above 300°C. Cracking reactions are favored at higher temperatures (>300°C) resulting in formation of other products.

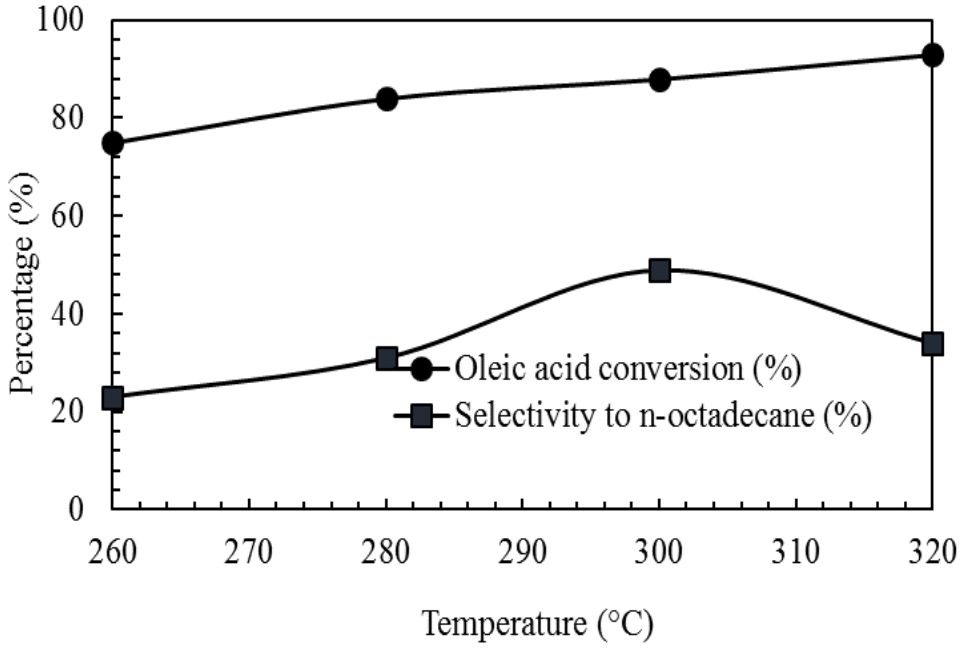

Fig. 5.2 Influence of reaction temperature on conversion and selectivity
(Reaction conditions: Oleic acid = 20 g, n-dodecane = 30g, catalyst: CuNiMo/γ-Al_2O_3, catalyst loading = 2 (w/w) %, speed of agitation =700 rpm, initial hydrogen pressure = 6.89 MPa, reaction time = 8 h)

From the GC-MS analysis, it was confirmed that n-dodecane was the major product formed for reaction temperature above 300°C indicating that cracking reactions were favored resulting in formation of products with decreased carbon number. Fig. 5.3 indicates the comparison between the performances of trimetallic catalysts containing 6 wt.% of secondary promoters at different reaction times. Metals such as Cu, Fe and Cr were chosen as they tend to have high affinity towards oxygen and also offers unsaturated vacancy sites for the adsorption of oxygen (Saidi, 2014). The performance of trimetallic catalysts systems did not follow any pattern.

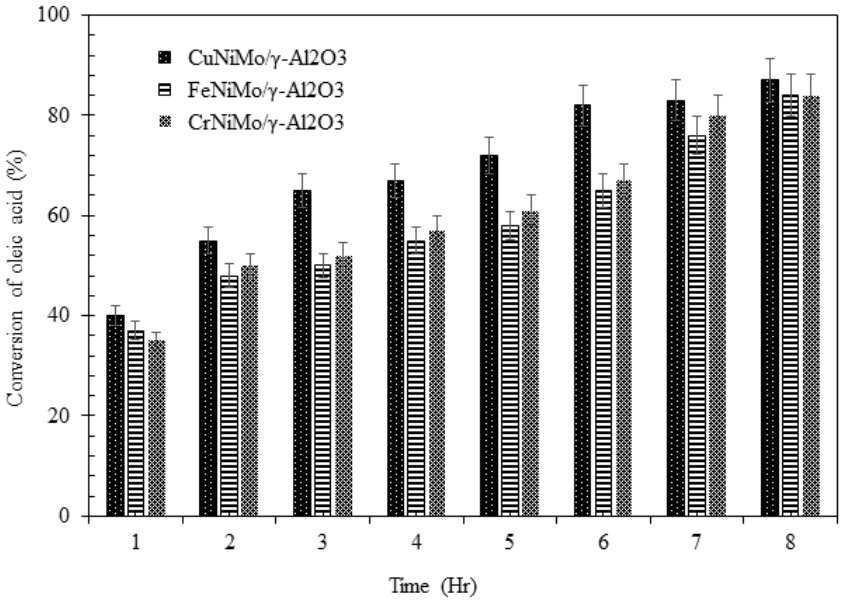

Fig. 5.3 Evaluation of Cu/Fe/Cr supported NiMo/γ-Al_2O_3 for the hydrodeoxygenation of oleic acid
(Reaction conditions: Oleic acid = 20 g, n-dodecane = 30 g, catalyst loading = 2 (w/w) %, speed of agitation =700 rpm, initial hydrogen pressure = 6.89 MPa, Reaction temperature = 300°C)

Hydrogen activation and dissociation of hydrogen molecule are aided by copper, and Fe helps in the abstraction of oxygen to form oxides, and the oxides are reduced by the continuous supply of hydrogen by reverse Mars-van krevelen mechanism (Hinokuma et al. 2015). However, impregnation of copper was found to be beneficial in comparison to other metals (Fe and Cr).

5.3.3 Statistical analysis on conversion of oleic acid

The process parameters and their levels for optimization are as follows: Catalyst loading A: 2-8 wt.%; Reaction time B: 4-10 h; Reaction temperature C: 250-325 °C; Hydrogen pressure D: 4.14-8.27 MPa. Orthogonal design of experiments for conversion of oleic acid is shown in Table 5.7. The range of oleic acid conversion varies from 61-88% depending on the process parameter conditions. Table 5.8 indicates the different mean values of K.

Table 5.7 Conversion of oleic acid using CuNiMo/γ-Al_2O_3 catalyst in OA_{16} matrix

Trial No.	Factors					Response (Y_i)
	Catalyst loading A (wt.%)	Reaction time B (h)	Reaction temperature C (°C)	Hydrogen pressure D (MPa)	Error	Conversion of oleic acid (%)
1	2	6	300	6.89	2[a]	81
2	4	10	250	5.51	2	72
3	6	10	300	8.27	3[a]	85
4	8	6	250	4.14	3	67
5	2	8	250	8.27	4[a]	75
6	4	4	300	4.14	4	76
7	6	4	250	6.89	1[a]	61
8	8	8	300	5.51	1	81
9	2	4	325	5.51	3	78
10	4	8	275	6.89	3	87
11	6	8	325	4.14	2	88
12	8	4	275	8.27	2	74
13	2	10	275	4.14	1	79
14	4	4	325	8.27	1	87
15	6	4	275	5.51	4	73
16	8	10	325	6.89	4	79

[a] It is the number of trials 'I' when calculates the experimental error (like the different levels for the definite factor).

Table 5.8. Range analysis data of the oleic acid conversion in a batch reactor

Value name	Catalyst loading A (wt. %)	Reaction time B (h)	Reaction temperature C (°C)	Hydrogen pressure D (MPa)
$K_{1\ mean}$	78.9	72.9	69.0	77.7
$K_{2\ mean}$	80.6	77.2	78.8	79.0
$K_{3\ mean}$	76.9	83.0	80.7	79.5
$K_{4\ mean}$	75.5	78.8	83.4	76.4
R_j	5.0	10.0	14.4	2.6

Higher the mean value, larger the effect of parameter on the oleic acid conversion. The levels of significance of factors are: reaction temperature (14.4) > reaction time (10.5) > catalyst loading (5.05) > hydrogen pressure (3.6). Detailed methodology to perform range analysis is illustrated by Wu and Leung, 2015. The reaction temperature is the most influential parameter based on the Rc values. Furthermore, from the percentage contribution, it can be deduced that the most important factor contributing to the oleic acid conversion is factor C.

5.3.4 Statistical analysis on selectivity towards n-octadecane

Orthogonal design of experiment and range analysis for selectivity are shown in Tables 5.10 and 5.11 respectively. Highest selectivity (47%) was observed at reaction temperature of 300°C, hydrogen pressure of 8.27 MPa catalyst loading of 6 % and reaction time of 10 h. For the various sets of experiments performed, range of selectivity varied from 20 to 47%. Range analysis and ANOVA were performed on this data and the order of influence of parameters influencing selectivity are reaction temperature (20.7) > reaction time (17.1) > hydrogen pressure (13.2) > catalyst loading (11.2). The largest R_C and smallest R_A value indicated that reaction temperature had the highest effect and catalyst loading had the least effect. The ANOVA table for selectivity

towards n-octadecane is shown in Table 5.12. The reaction temperature is found to be the most significant factor affecting selectivity towards n-octadecane.

Table 5.9. Analysis of variance (ANOVA) of oleic acid conversion in OA_{16} matrix in a batch reactor

Source	SS	*df*	V	F	$F_{0.01}$ (3,6)=9.78	SS′	P (%)
A	59.5	3	19.8	11.1	>	130.4	20.3
B^{Δ}	206.8	3	68.9	-		-	-
C	473.78	3	157.9	20.2	>	245.6	38.4
D	39.9	3	13.3	18.4	>	198.0	30.9
e	26.4	3	8.8	-		-	-
e^{Δ}	233.3	6	77.7	-		65.0	10.1
T	1039.7	15	-	-		639.0	100.0

SS: the sum of square deviation; *df*: the degree of freedom; V: the variance; F: the F ratio; SS′: the purified sum of squares deviation; P: the percent contribution; B^{Δ}: the variance of reaction time, but the value is less than twofold of the experiment error (e); e^{Δ}: the new value of the experimental error, which is the sum of B^{Δ} and e.

5.3.5 Process optimization study

Increase/decrease in temperature has the most significant influence on conversion and selectivity. However, cracking reactions occurs at temperature above 325°C and thus selectivity towards n-octadecane decreased. Hence, it is not recommended to use higher reaction temperature (>300°C) for hydrodeoxygenation of oleic acid. Higher loading of catalyst (6 wt.%) aids in conversion of oleic acid and selectivity towards n-octadecane. Increase in loading to 8 wt.% is beneficial; however, considering the cost involved we choose to perform reactions with catalyst loading of 6 wt.%.

Table 5.10 Selectivity towards n-octadecane using CuNiMo/γ-Al_2O_3 catalyst in OA_{16} matrix for a batch reactor study

Trial No.	Factors					Response (Y_i)
	Catalyst loading A (wt.%)	Reaction time B (h)	Reaction temperature C (°C)	Hydrogen pressure D (MPa)	Error	Selectivity towards n-octadecane (%)
1	2	6	300	6.89	2[a]	31
2	4	10	250	5.51	2	40
3	6	10	300	8.27	3[a]	47
4	8	6	250	4.14	3	27
5	2	8	250	8.27	4[a]	36
6	4	4	300	4.14	4	36
7	6	4	250	6.89	1[a]	35
8	8	8	300	5.51	1	45
9	2	4	325	5.51	3	27
10	4	8	275	6.89	3	20
11	6	8	325	4.14	2	25
12	8	4	275	8.27	2	32
13	2	10	275	4.14	1	41
14	4	4	325	8.27	1	30
15	6	4	275	5.51	4	35
16	8	10	325	6.89	4	27

[a] It is the number of i when calculates the experimental error (like the different levels for the definite factor).

Table 5.11 Range analysis on selectivity

Value name	Catalyst loading A (wt.%)	Reaction time B (h)	Reaction temperature C (°C)	Hydrogen pressure D (MPa)
K1 mean	26.3	25.7	26.6	31.9
K2 mean	27.4	33.7	37.6	30.3
K3 mean	35.3	37.8	42.4	42.4
K4 mean	37.5	42.9	35.2	43.5
Rj	11.2	17.1	20.6	13.1

Table 5.12. Analysis of variance (ANOVA) of selectivity towards n-octadecane in OA_{16} matrix

Source	SS	*df*	V	F	$F_{0.01}$ (3,3)=20.5	SS′	P (%)
A	16.5	3	5.5	7.8	<	11.5	2.5
B^{Δ}	114.2	3	38.1	36.5	>	104.3	21.1
C	11.2	3	3.7	8.5	>	8.7	1.9
D	358.1	3	119.3	175.2	<	361.5	73.1
e	1.6	3	0.53	-		9.2	2.0
T	501.6	15	-	-		494.1	100

Hydrogen pressure plays a major role in aiding hydrogenation and deoxygenation reaction. Higher hydrogen pressure (6.89 MPa) indicates abundant availability of hydrogen and thus spillover of H_2 is aided favoring hydrogenation and deoxygenation reaction. Reaction time had a significant influence on oleic acid conversion and n-octadecane selectivity and the optimal values for the factors are reaction temperature 300°C, reaction time 8 h, catalyst loading 8 wt.%, hydrogen pressure of 6.89 MPa.

5.4. Conclusions

Comparison of the metal precursors (Mo, V and W) indicated that molybdenum nitride is the best choice for hydrotreating of oleic acid as it gave higher conversion and product selectivity. Hence, from the continuous phase, $Mo_2N/\gamma\text{-}Al_2O_3$ was chosen as the best. $NiMo/\gamma\text{-}Al_2O_3$ showed higher conversion (80%) in comparison to NiMo supported on during the HDO of oleic acid at reaction temperature of 300°C, hydrogen pressure of 6.89 MPa and reaction time of 8 h with 8 wt. % catalyst loading. At higher reaction temperature (>320°C), undesired cracking reactions were observed resulting in formation of lower carbon number products. Orthogonal design matrix (OA_{16}) was developed and statistical analysis was performed to optimize process parameters for the hydrodeoxygenation of oleic acid. Range analysis indicated that the conversion and selectivity steadily increased with reaction temperature. However, with catalyst loading, they increased steadily until an optimum point and then decreased. The selectivity remained constant with reaction pressure. ANOVA indicated that reaction temperature is the most important factor in hydrodeoxygenation reactions. Another most significant parameter is catalyst loading. The final order of influential parameter is reaction temperature> catalyst loading>hydrogen pressure> reaction time. Maximum conversion was obtained at reaction temperature of 325 °C, hydrogen pressure 6.89 MPa, reaction time of 8 h and catalyst loading of 8 wt.%.

CHAPTER 6

COMPARISON OF COMMERCIAL NiMo/γ-Al_2O_3, NOVEL MIXED- METAL CATALYST AND FeCu/γ-Al_2O_3 FOR THE HYDRODEOXYGENATION OF OLEIC ACID

The outcome (manuscripts/conference presentations) from this phase of work are listed below:

1. N. Arun, R. V. Sharma, Y. Hu, A. K. Dalai. Comparison of commercial NiMo/γ-Al_2O_3, novel mixed-metal catalyst and FeCu/γ-Al_2O_3 for the hydrodeoxygenation of model compound (oleic acid) and canola oil study (In preparation).
2. N. Arun, R. V. Sharma, A. K. Dalai. Comparison of commercial NiMo/γ-Al_2O_3 and Cu: Zn: Cr: Zr mixed oxide catalyst for the hydrodeoxygenation of oleic acid. *23rd Canadian Symposium on Catalysis*, Edmonton, Canada, May 11-14, 2014.

Contribution of the Ph.D. candidate and collaborators

All the experimental and characterization work was conducted by Naveenji Arun. Manuscript writing and revision work were done by Naveenji Arun based on the suggestions from Dr. Ajay K. Dalai and Dr. Yongfeng Hu. Dr. R. V. Sharma offered key suggestions in catalyst synthesis and characterization.

The contribution of this chapter to the overall Ph. D. work

This research work focused on the evaluation of the performance of NiMo/γ-Al_2O_3, mixed-metal catalyst and FeCu/γ-Al_2O_3 for the HDO of oleic acid and statistical modeling of the process parameter for best performing catalyst using RSM, ANN techniques and understand their ability to predict the response (conversion) of the system.

Abstract

HDO reactions were performed in a batch setup using commercial NiMo/γ-Al_2O_3, novel mixed-metal catalyst (MMC) and FeCu/γ-Al_2O_3 catalysts using oleic acid as feedstock. The performance of commercial NiMo/γ-Al_2O_3 and novel mixed-metal catalyst was compared in batch and continuous mode of operation at the H_2 pressure of 6.89 MPa and catalyst loading of 6 wt.%. Commercial NiMo/γ-Al_2O_3 catalyst was chosen as the reference material to compare the performance of the synthesized catalysts. During hydrodeoxygenation of oleic acid at different reaction temperatures, the conversion obtained using a mixed metal catalyst (MMC) was usually higher (>90%) in comparison to commercial NiMo/γ-Al_2O_3 (80-85%). A novel FeCu/ γ-Al_2O_3 was synthesized based on wetness impregnation method and the influence of process parameters on the performance of FeCu/γ-Al_2O_3 was investigated. In comparison to RSM, ANN model was more accurate in predicting the conversion of oleic acid and selectivity. ANN coupled with genetic algorithm optimization was able to predict highest oleic acid conversion of 90% and in experimental works, the conversion was found to be 89%.

Keywords: Hydrodeoxygenation, mixed-metal catalysts, transition metals

6.1. Introduction

In the 21st century, the major problem that we are facing is the development of sustainable energy sector that is commercially and technologically feasible (Ayodele et al. 2015). It is well documented that usage of alternative fuels such as biodiesel will help in the reduction of GHG emissions especially particulates and SOx in comparison to gasoline and diesel fuels (Bu et al. 2012; Case et al. 2014; Chen et al. 2015). Biofuels have been proven as an efficient alternative for fossil fuels to meet the energy demands of the present and future generations. It has been estimated that contribution of biomass energy will be 60% of the overall energy from renewable

resources to the energy consumption totally in 2020 (De et al. 2015; Dickinson and Savage. 2014). Third generation biofuels are produced by hydroprocessing of the feedstocks (that does not pose food versus fuel concerns) such as bio-oils (Do et al.2012; Duan et al. 2015).

Development of commercially feasible novel catalytic materials for the production of third generation biofuels is considered to be a demanding task owing to the limited theoretical understanding of these materials (Guo et al. 2015; Hollak et al. 2013). Hydrodeoxygenation of oils from renewable feedstocks is a catalytic process and mostly transition metallic (single and bi-metals) catalysts have been employed (Liu et al. 2015; Mu et al. 2014). Traditionally, hydrotreating reactions employ NiMo supported on different materials as catalysts and the catalyst hold good for hydrodeoxygenation reactions. Production of transportation fuels for biooils obtained from biomass primarily involved deoxygenation reaction as a primary step (Zarchin et al. 2015). During direct deoxygenation, hydrogen reacts with the oxygen-rich reactant and water is formed as a by-product. Indirect deoxygenation involves the removal of oxygen in the form of CO_2 (decarboxylation) and/or CO (decarbonylation). To increase process efficiency, reduce operating costs and make process profitable, all process needs to be conducted under optimal conditions (Zhao et al. 2013). Based on the results from the previous chapter, it can be concluded that promotional effects of Cu and Fe are superior and based on the synergy between Cu and Fe, a novel FeCu supported catalyst system was developed The synergism between metallic Fe sites that are strongly oxyphilic and metallic Cu sites that favour activation of hydrogen was investigated by Manikandan et al. 2016.

RSM is one of the most widely used statistical technique and during RSM modeling, experiments are statistically designed and the coefficients of the developed mathematical model are evaluated followed by response prediction and testing the accuracy of the model (Avramovic

et al. 2015). RSM can predict the optimum values for the parameters that can maximize or minimize the objective function (process response). Moreover, two and three-dimensional plots are used to represent the direct and interactive effects of parameters. It is imperative to have necessary data points to construct RSM and perform optimization.

ANN is proven to have the ability to simulate non-linear multivariate processes and have better generalization ability than RSM. Application of Artificial Neural Networks (ANN) coupled with Genetic Algorithm (GA) is gaining importance as a powerful optimization tool to understand the influence of process parameters in any complex multivariate process. ANN coupled with GA works similar to the brain functioning process. Till date, no report is available on the usage of RSM and ANN for modeling and optimization of hydrodeoxygenation process. Main goals of this work are to evaluate the performance of different catalysts and optimize process conditions for the best performing catalyst. Through analysis of variance (ANOVA), we attempt to evaluate the effect of process parameters on conversion of oleic acid and optimize process conditions to achieve maximum conversion using RSM and ANN.

6.2. Materials and Methods

6.2.1 Materials

Commercial γ-Al_2O_3 was purchased from Alfa Aesar. As described by Sharma et al. 2013, "Copper (II) nitrate trihydrate (purity ≥ 99% from VWR, Canada), zinc (II) nitrate hexahydrate (reagent grade, 98% purity from VWR, Canada), chromium nitrate nonahydrate (reagent grade ≥ 98% purity, from VWR, Canada), zirconium nitrate (reagent grade ≥ 98% purity, from VWR, Canada) and iron (III) oxide (reagent grade ≥ 98% purity, from Alfa Aeser, USA)" are the chemicals used in this chapter.

6.2.2 Catalyst Synthesis, Characterization, and Evaluation

The detailed procedure for the synthesis of mixed metal oxide catalyst is described elsewhere (Sharma et al. 2013). Usually supported catalyst systems are employed for HDO reactions as they offer surface area, stability and favors hydrogen spill over. The unsupported mixed metal oxide catalyst was employed for the HDO reaction to elucidate the possibilities for developing cost-effective catalyst with high stability and desired physico-chemical properties for HDO reactions. For the synthesis of FeCu/γ-Al_2O_3, copper (II) nitrate trihydrate was used as the precursor for copper and iron (III) oxide was used as the precursor for iron. Wetness impregnation method was employed to synthesize the catalysts. In a typical synthesis procedure, 20 ml of 1.0 M copper (II) nitrate trihydrate and 30 ml of 1.2 M iron (III) oxide solution was prepared. Commercial γ-Al_2O_3 was used as the support material. After impregnation with a copper solution, the support material was dried at room temperature for 12 h and then calcined at 550°C for 5 h. After calcination, 20 ml of iron (III) oxide solution was added to 30 g of catalyst material (Cu/γ-Al_2O_3) and then same drying and calcination procedure was carried out to obtain FeCu/ γ-Al_2O_3 and by theoretical calculations, the synthesized catalysts has Cu loading of 13 wt.% and Fe loading of 3 wt%. All the synthesized catalysts were characterized to understand their physico-chemical properties. A standard batch reaction was carried out with using oleic acid (40 g), dodecane (50 g), catalyst (6 wt.%), temperature (250°C), H_2 pressure (6.89 MPa) and time (6 h). The typical reaction conditions in continuous mode are oleic acid (20 g), dodecane (80 g), catalyst bed volume (15 ml), hydrogen pressure (6.89 MPa), feed flow rate (20 g/h).

6.2.3 RSM, ANN and ANN-GA modeling

Face centered Central Composite Design (CCD) was used for the collection of data and second order polynomial regression model (quadratic model) was used for approximation. The relation

between the conversion of oleic acid and the process parameters can be modeled using the equation (6.1). Y indicates the conversion of oleic acid. X indicates the process parameters (reaction temperature, catalyst loading, and hydrogen pressure). Regression coefficients are a_o, a_i, a_{ij} and a_{ii} (i=1, 2, 3 and j > i).

$$Y = a_0 + \sum_i a_i X_i + \sum_i \sum_{j>i} a_{ij} X_i X_j + \sum_i a_{ii} X_i^2 \tag{6.1}$$

In RSM modeling, the second-order polynomial regression model (quadratic model) for model f can be generally represented as (Avramovic et al. 2015)

$$f = a_o + \sum_{i=1}^{n} a_i x_i + \sum_{i=1}^{n} a_{ii} x_i + \sum_{i<j}^{n} a_{ij} x_i x_j + \varepsilon \tag{6.2}$$

Where a_i represents the linear effect of x_i, a_{ii} represents the quadratic effect of x_i and a_{ij} represents the linear interactions between x_i and x_j and ANOVA was performed to find the significance of process variables. The trial version of Design-Expert 7.0.0 (Stat-Ease Inc., Minneapolis, MN) was employed for modeling and simulation using RSM and ANN techniques. As mentioned in Avramovic et al. 2015, “MATLAB's Neural Network and Genetic Algorithm Toolboxes (MATLAB 8.1.0.604) were employed for modeling and optimization. A feedforward, back-propagation multi layer ANN was developed and Levenberg-Marquardt (LM) algorithm as employed for modeling and training". For input, hidden and output layers, hyperbolic tangent transfer function (tan h) was employed. Input layer had three neurons (reaction temperature, catalyst loading, and hydrogen pressure). The output layer is the conversion of oleic acid. ANN simulation and optimization is based on biological neural systems and the method by which ANN works is similar to biological neurons in humans. Each neuron receives input from previous neurons in proportion to connection weights and feed forward with backward propagation is one of the most common networks used in chemical engineering processes

optimization. In neural network analysis, all data were normalized as they have several physical units and range. As far as in the training procedure of the neural networks, the input and output data had several physical units and range sizes, and all data are generally normalized in the 0-1 range to avoid any computational difficulty.

The Levenberg–Marquardt back propagation algorithm was used for the preparation of the ANN and in this method, weights and biases were iteratively adjusted to reduce diversion of the predicted values from the desired values according to the Levenberg–Marquardt optimization procedure. Normalization of data was done for the input and output data in the range [-1, 1] and [0,1] respectively in order to obtain minimum mean square error at a fast convergence rate. Normalization makes the datasets uniformly distributed within an acceptance range for the neural network. Due to normalization, all the chosen process variables are considered significant to the same level during neural network learning. The main objective of training neural network is to obtain the minimum error. During training and examination, the ANN parameters such as the number of hidden neurons, type of transfer function and learning rate were changed based on trial and error method to achieve optimum values. Values of mean square error (MSE) and regression coefficient (R^2) were used to statistically measure the performance of the developed ANN and they were obtained using the equations 6.3 and 6.4.

$$MSE = \frac{1}{N}\sum_{i=1}^{N}(y_o - y_e)^2 \tag{6.3}$$

$$R^2 = 1 - \frac{\sum_{i=1}^{N}(y_o - y_e)^2}{\sum_{i=1}^{N}(y_o - y_m)^2} \tag{6.4}$$

In the above expressions, N indicates the number of experiments allocated for training the neural network, 'y_e' indicates the experimental value for conversion of oleic acid, 'y_0' indicates the

predicted value for conversion and 'y_m' indicates the average of actual oleic acid conversion. The network that gave the lowest error during training was selected. During initial neural runs, it was indicated that one hidden layer network offered better learning and prediction ability in comparison to multi-hidden layer networks. Hence, for our design, single hidden layer network was studied.

6.3. Results and Discussion

6.3.1 Characterization and Screening tests

Table 6.1 illustrates the metal dispersion, metallic surface area and crystallite size for mixed metal catalyst and FeCu/γ-Al_2O_3. In the case of MMC, interaction with other metals such as chromium, zinc, and zirconium hinders the dispersion of Cu causing agglomeration of metallic copper. Synthesized FeCu/γ-Al_2O_3 has a metal dispersion of 8.1 % which is comparatively higher than in the case of MMC.

Table 6.1. Physico-chemical properties of the catalysts

Catalysts	Metal dispersion (%, Cu)	Metallic surface area (m^2/g, Cu)	Crystallite size (nm, Cu)	Adsorption of CO (μmol/g)
Mixed metal catalyst (MMC)	6.10	1.30	14.4	28.3
FeCu/γ-Al_2O_3	8.10	2.12	15.4	29.7

One of the reasons being the usage of support material which aids in the dispersion of active metals. Table 6.2 represents the comparative study on the BET surface area of reduced, used and regenerated MMC and FeCu/γ-Al_2O_3. No major changes in surface area between reduced and used catalyst were observed. About 25% decrease in surface area was noticed in the case of MMC and the decrease in surface area in the case of FeCu/γ-Al_2O_3 was only 6%.

Table 6.2. Comparison of reduced, used and regenerated catalysts

Catalysts	BET (m^2/g)
MMC (Reduced)	42.5
MMC (Used)	40.1
MMC (Regenerated)	31.9
FeCu/γ-Al_2O_3 (Reduced)	220.1
FeCu/γ-Al_2O_3 (Used)	217.1
FeCu/γ-Al_2O_3 (Regenerated)	205.1

Reduction of CuO to metallic copper increases the BET surface area. BET surface area of the regenerated catalyst is less (31.9 m^2/g) in comparison to freshly reduced and used catalyst indicating the transformation of metallic Cu to CuO during calcination. These results indicate that usage of support materials is beneficial for the hydrodeoxygenation reactions and prolonged usage of unsupported catalysts may not be economically beneficial due to the rapid loss in surface area. Fig. 6.1 illustrates the comparison of the performance of mixed metal catalyst and commercial NiMo/γ-Al_2O_3 at a different reaction temperature in continuous mode. Fig. 6.2 represents the comparison in the batch system at different reaction time. It is evident that performance of MMC is superior to commercial NiMo/γ-Al_2O_3 in terms of oleic acid conversion. This superior performance may be attributed to the higher affinity of copper and zinc towards oxygen and this favors extraction of oxygen from the oleic acid. In batch mode, increase in agitation speed does not have major influence the conversion of oleic acid. Increase in agitation speed (400-1000 rpm) has no major influence on the conversion of oleic acid and product selectivity (Table 6.3).

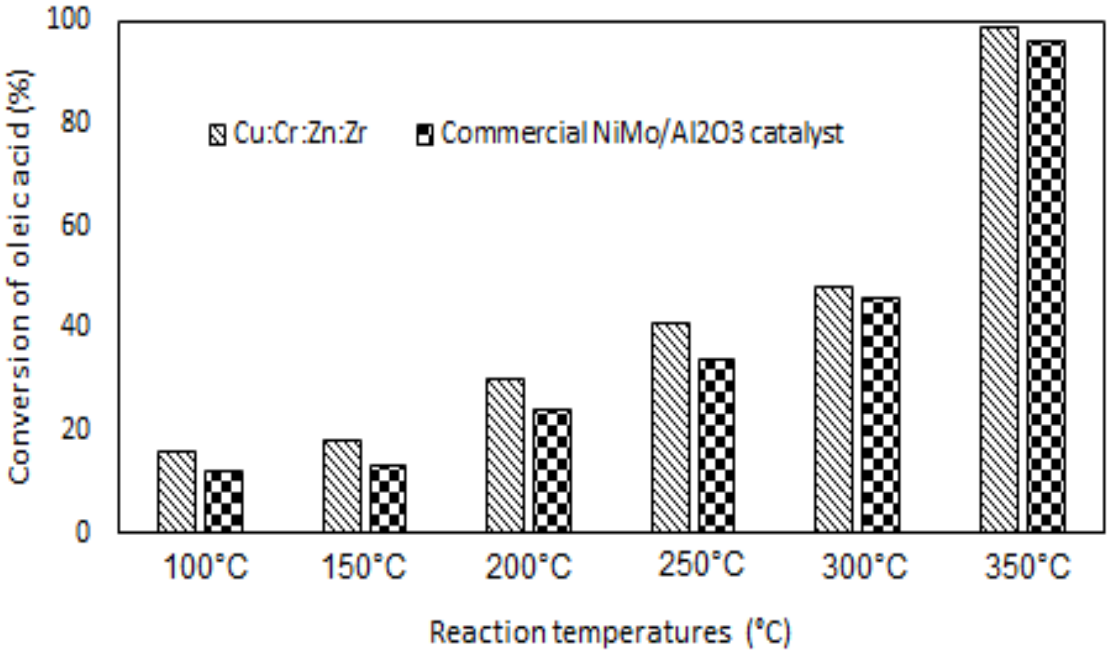

Fig. 6.1 Comparison of Cu (3): Zn (2): Cr (1): Zr (3) and commercial NiMo/γ-Al_2O_3 catalyst for the hydrodeoxygenation of oleic acid in the continuous system.
Reaction condition: Oleic acid (20 g), dodecane (80 g), catalyst bed volume (15 ml), hydrogen pressure (6.89 MPa), feed flow rate (20 g/h)

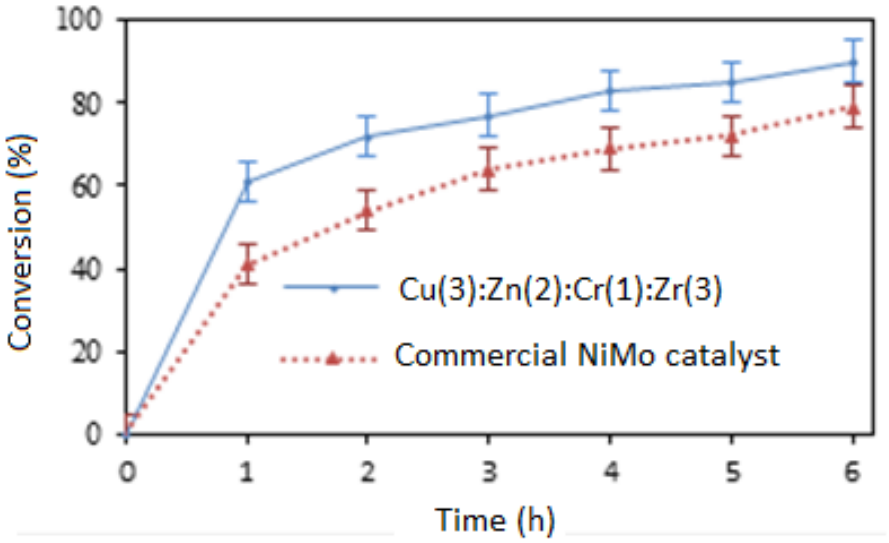

Fig. 6.2 Comparison of Cu (3): Zn (2): Cr (1): Zr (3) and commercial NiMo/γ-Al_2O_3 catalyst on the conversion of oleic acid in the batch system.
Reaction condition: Oleic acid (40 g), dodecane (50 g), catalyst loading (6 g), reaction temperature (250°C), hydrogen pressure (6.89 MPa), agitation speed (600 rpm) and reaction time (6 h)

Table 6.3. Effect of agitation speed on conversion and selectivity during hydrodeoxygenation reaction

S.No	Speed of agitation (rpm	Conversion, mole % (Oleic acid)			Selectivity, % (n-Octadecane)		
		Commercial NiMo/γ-Al_2O_3	Cu:Zn:Cr:Zr (Cat A)	Cu:Zn:Cr: Zr (Cat B)	Commercial NiMo/γ-Al_2O_3	Cu:Zn:Cr:Zr (Cat A)	Cu:Zn:Cr:Zr (Cat B)
1	400	76	81	87	62	67	67
2	600	80	82	91	62	67	68
3	800	80	84	92	63	67	68
4	1000	81	84	92	63	67	68

Reaction condition: Oleic acid (40 g), dodecane (50 g), catalyst (6 wt.%), temperature (250°C), H_2 pressure (6.89 MPa), time (6 h)

Comparison of commercial NiMo and MMC indicates that mixed catalyst is superior in terms of their reusability (Table 6.4).

Table 6.4. Comparison of commercial NiMo/γ-Al_2O_3 and mixed oxide catalysts on their reusability

S.No.	Reusability	Conversion, mole % (Oleic acid)			Selectivity, % (n-Octadecane)		
		Commercial NiMo/γ-Al_2O_3	(Cat A)	(Cat B)	Commercial NiMo/γ-Al_2O_3	(Cat A)	(Cat B)
1	Fresh	80	82	91	62	67	68
2	1st reuse	77	77	89	58	61	61
3	2nd reuse	72	70	87	57	59	60

Reaction condition: Oleic acid (40g), dodecane (50g), catalyst (6 wt.%), temperature (250^0C), H_2 pressure (6.89 MPa), speed of agitation (600 rpm), time (6h)

Performance of mixed metal catalyst (Cu: Zn: Cr: Zr) was superior (HDO conversion~90 %) in comparison to commercial NiMo catalyst (HDO conversion~75 %) for the HDO of oleic acid. Comparison of commercial NiMo and mixed metal oxide catalyst indicates that mixed catalyst is

superior in terms of their reusability. The elemental molar composition of the regenerated catalyst is almost same as the fresh catalyst (Table 6.5).

Table 6.5. Elemental molar composition of fresh (reduced) and regenerated catalyst

Elements	Cu	Zn	Cr	Zr
MMC (Fresh)	2.98	2.02	0.99	2.89
MMC(Regenerated)	2.86	1.98	0.97	2.84

By difference, there is a differential loss of 4% in copper content and 1.7% in zirconium content. A minor decrease in the catalytic activity of the regenerated catalyst can be attributed to the loss of the active metal content of the regenerated catalyst.

6.3.2 RSM, ANN and ANN-GA modeling

The effects of process variables on the hydrodeoxygenation of oleic acid and the levels of process parameters investigated are shown in Table 6.6.

Table 6.6. Variables affecting the process and their levels

Process variable	Notation for each factor	Levels		
		Lower level (-1)	Middle level (0)	High level (+1)
Reaction temperature (°C)	A	250	275	300
Catalyst loading (wt.%)	B	2	6	10
Hydrogen pressure (MPa)	C	5.51	6.89	8.27

The design matrix and the results for different values of parameters are shown in Table 6.7. Commercial NiMo/γ-Al_2O_3 catalyst gave 80% conversion of oleic acid at 6 wt.% loading, a temperature of 250°C and H_2 pressure of 6.89 MPa (Table 6.4). In the case of FeCu/γ-Al_2O_3 catalyst, the conversion was 55% (Table 6.7). However, conversion of 83% was achieved at a reaction temperature of 300°C and catalyst loading of 10 wt.% indicating that the performance of FeCu/γ-Al_2O_3 is comparable to commercial NiMo/γ-Al_2O_3 catalyst system.

Table 6.7. List of experiments used for RSM and ANN analysis for FeCu/γ-Al_2O_3 catalyst

Sample number	Reaction temperature (°C)	Catalyst loading (wt. %)	Hydrogen pressure (MPa)	Conversion of oleic acid (%)
1	250	2	5.51	50.55
2	250	4	5.51	52.34
3	250	6	5.51	55.76
4	250	8	5.51	60.91
5	250	10	5.51	62.87
6	275	2	5.51	54.56
7	275	4	5.51	55.87
8	275	6	5.51	58.34
9	275	8	5.51	63.45
10	275	10	5.51	67.7
11	300	2	5.51	71.7
12	300	4	5.51	75.67
13	300	6	5.51	78.65
14	300	8	5.51	81.23
15	300	10	5.51	83.32
16	250	2	6.89	51.23
17	250	4	6.89	53
18	250	6	6.89	55.24
19	250	8	6.89	60.08
20	250	10	6.89	63.25
21	275	2	6.89	55.34
22	275	4	6.89	56.5
23	275	6	6.89	61.25
24	275	8	6.89	64.55
25	275	10	6.89	68
26	300	2	6.89	72

27	300	4	6.89	75.34
28	300	6	6.89	81.23
29	300	8	6.89	82.45
30	300	10	6.89	83
31	250	2	8.27	53
32	250	4	8.27	54.45
33	250	6	8.27	57.56
34	250	8	8.27	61.23
35	250	10	8.27	64.71
36	275	2	8.27	55.45
37	275	4	8.27	56.56
38	275	6	8.27	62.23
39	275	8	8.27	64.45
40	275	10	8.27	67.01
41	300	2	8.27	73.12
42	300	4	8.27	75.67
43	300	6	8.27	79.34
44	300	8	8.27	82.25
45	300	10	8.27	84

During initial analysis, a different number of hidden neurons was tried to find the one that offers least mean relative percentage deviation (MRPD).Sum of squares, degrees of freedom, mean square, F value and p-value are the indicators that were evaluated for variations in parameters. The interaction between factors and squares of factors were obtained from the F- and p-values. Table 6.9 indicates the parameters for ANN coupled with GA model. The values RSM and ANN are compared for 30 runs of experiments suggested in CCD design of RSM. The deviation in predictive values for conversion of oleic acid is more in the ANN predictive model than in the

RSM design. The datasets were divided into three subsets: 70% of the data points are used for training the network and 15% of the data points were used for testing and 15 of data points were used for validation of the network. "Sensitivity analysis was employed to optimize genetic algorithm parameters such as population size, a number of generations, crossover rate and mutation probability" and the values are found to be 20, 50, 8 and 0.01 respectively (Avramovic et al. 2015). Fifty generations were sufficient to optimize the process parameter conditions.

Table 6.8. ANOVA results for the screening tests using FeCu/γ-Al_2O_3 catalyst

Parameter variations	Sum of squares	Degree of freedom	Mean square	F value	p-value
Model	17926.0	14	1280.4	13.05	<0.0001
A	327.9	1	327.9	3.34	0.072
B	2713.6	1	2713.6	27.66	<0.0001
C	6571.2	1	6571.2	66.97	<0.0001
D	3706.5	1	3706.4	37.77	<0.0001
AB	37.3	1	37.3	0.38	0.539
AC	24.3	1	24.3	0.25	0.620
AD	100.8	1	100.8	1.03	0.314
BC	1762.6	1	1762.6	17.96	<0.0001
BD	527.3	1	527.3	5.37	0.023
CD	943.8	1	943.8	9.62	0.003
A2	4.0	1	4.0	0.04	0.839
B2	120.3	1	120.3	1.23	0.272
C2	804.5	1	804.5	8.20	0.006
D2	87.1	1	87.1	0.89	0.349
Lack of fit	6791.5	66	102.9	2.94	0.113
Pure error	175.0	5	35.02		
Corrected total	24892.6	85			

A- Catalyst loading; B-reaction pressure; C-Hydrogen pressure

Table 6.9. ANN-GA parameters.

Model	Property	Value/Comment
ANN	Algorithm	Levenberg-Marquardt back-propagation
.	Number of input	4
	Number of hidden	1-20
	Number of output	1
Genetic Algorithm	Population Size	10-600
	Generations	1-600
	Crossover Rate	0-1
	Mutation Probability	0.01-1

6.4. Conclusions

Performance of mixed metal catalyst (Cu: Zn: Cr: Zr) was superior (HDO conversion~90 %) in comparison to commercial NiMo catalyst (HDO conversion~75 %) for the HDO of oleic acid in batch and continuous mode. Change in agitation speed (400-1000 rpm) does not have any influence on the performance of the catalysts (commercial NiMo and mixed metal catalyst). Hence, the reaction is free from external mass transfer resistance. The quadratic model generated by RSM is used to predict the process parameters, i.e. reaction temperature, hydrogen pressure and catalyst loading with reasonably good accuracy. Both models seem to predict the same level of conversion of oleic acid and it is in agreement with the experimental results.

CHAPTER 7

TECHNO-ECONOMIC AND LIFE CYCLE ANALYSIS OF HDO PROCESS

This part of the work is to be published as research article and was presented at the following conference:

N. Arun, M. Jhalaria, U. Das, Y. Hu, A. K. Dalai. Techno-economic and life-cycle assessment of production of diesel fuel substitutes from canola oil through HDO process. (Under preparation).

N. Arun, M. Jhalaria, A. K. Dalai. Life cycle analysis of hydrotreated renewable diesel production from canola oil through HDO process, *64th Canadian Chemical Engineering Conference*, Niagara Falls, Canada, October 19-22, 2014.

Contribution of the Ph.D. candidate and collaborators

The process plant design and economic evaluations were performed by Mayank Jhalaria and Naveenji Arun. Dr. U. Das offered suggestions in economic analysis and process design. Manuscript writing and revision work were done by Naveenji Arun based on the suggestions from Dr. Ajay K. Dalai and Dr. Yongfeng Hu.

The contribution of this chapter to the overall Ph. D. work

This research work was focused on

- Performing techno-economic analysis of hydrotreated-vegetable oil (HVO) production plant using canola oil as feedstock.
- Analyzing the environmental impact of alternative fuels production plants (biodiesel and hydrotreated-vegetable oil) that use canola oil as feedstock.

Abstract

Techno-economic analysis of catalytic hydrotreatment process (hydrodeoxygenation) for green diesel production from canola oil was performed using Aspen Plus V.2006 and Icarus V.2006.

Hydrotreatment plant was developed with a feedstock processing capacity of 10000 kg/h and sensitivity analysis was performed to evaluate uncertainty in input-output relationships. The payback period for the process at current costs was 3 years which is within the viable range for high-risk ventures. The internal rate of return for hydrodeoxygenation process to produce green diesel was estimated to be 210% based on the current oil price. From energy analysis, it was found that production of 1 kJ of green diesel from canola oil requires an energy input of 1.078 kJ. Power generation from the hydrotreatment plant was found to be 197.2 kW. Energy efficiency of hydrodeoxygenation process was found to be higher (95%) in comparison to the transesterification process (85%). Gram equivalent CO_2 emissions per kilometer were higher for hydrodeoxygenation process in comparison to transesterification process and this could be due to the involvement of hydrogen during hydrodeoxygenation process and also extensive reaction conditions (T>300°C and H_2 pressure> 6.89 MPa). From the LCA analysis, it was found that the usage of diesel fuel blended with green diesel has a lower environmental impact in terms of eutrophication, acidification, and energy usage as compared to fossil fuels.

Keywords: Techno-economic analysis, Life cycle assessment, hydrodeoxygenation, Transesterification, green diesel

7.1 Introduction

Alternative fuels are increasingly in great demand due to diminishing petroleum reserves, stringent governmental norms on environmental impact and environmental consequences of exhaust gases from automobiles. Presently the automobile industry is dominated by the usage of fossil fuels and this scenario will continue for the next 4-10 years as the alternate fuels sector continues to gain attention (Black et al. 2011; Cherubini and Stromman, 2011, Foteinis et al. 2011; Garcia et al. 2011; Gonzalez-Garcia et al. 2012; Grau et al.2013; Holma et al. 2013; Khoo

et al. 2011). First generation biofuels were dominated by biodiesel and bioethanol. One major drawback associated with the sustainable usage of biodiesel is its high oxygen content (> 10 wt. %) which results in increased thermal and chemical instability, corrosive properties and an increased tendency towards polymerization. Owing to these drawbacks, researchers focus on the development of alternate processes (hydrodeoxygenation) for the removal of oxygen from bio-based fuels to enhance fuel properties (Sebos et al. 2009). Before validating the commercialization of fuels, produced by hydrodeoxygenation (HDO) of vegetable oils, a justification based on the environmental impacts of alternative and fossil fuels is essential and hence life cycle analysis/assessment (LCA) is crucial (Singh and Olsen, 2011; Sobrino et al. 2011).

Research on HDO of vegetable oils had not gained much attention until this decade as the global energy demands were mainly catered by petroleum products which contain less oxygen (< 1 wt.%) content. Most of the crude oil worldwide contains 98 wt. % carbon and hydrogen, 1.8 wt. % sulfur and only 0.1 wt. % oxygen. Hydrodeoxygenation reaction involves the treatment of feedstock (vegetable oils/plant oils) using hydrogen and the reaction is carried out at high temperature (523-673 K) and pressure (5.51-8.96 MPa) that produces hydrocarbons such as paraffin and olefins as main products and oxygen is removed in the form of water and CO_2 (direct HDO and decarboxylation, Eq. 7.1 & 7.2). Transesterification of vegetable oil to produce biodiesel is represented by Eq. 7.3.

$$CH_3\text{-}(CH_2)_m\text{-}COOH \xrightarrow{H_2} CH_3\text{-}(CH_2)_m\text{-}CH_2OH + H_2O \xrightarrow{H_2} CH_3\text{-}(CH_2)_m\text{-}CH_3 + H_2O \quad (7.1)$$

$$CH_3\text{-}(CH_2)_m\text{-}COOH \xrightarrow{H_2} CH_3\text{-}(CH_2)_{m-1}\text{-}COOH + CO_2 \quad (7.2)$$

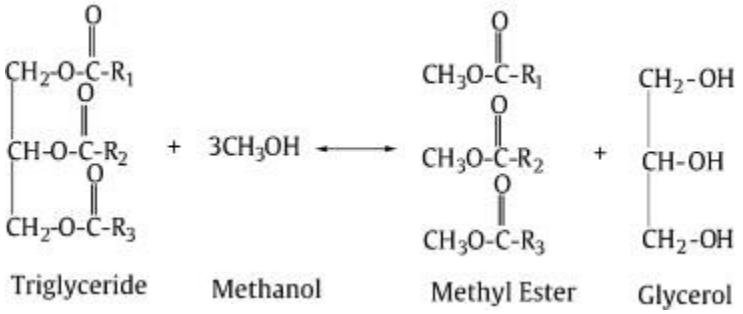

(7.3)

Few studies have been reported on the techno-economic evaluation of a biodiesel process plant using Aspen Plus simulation software (García et al. 2010, Vlysidis et al. 2011, Yun et al. 2013). Any chemical process makes a direct and indirect impact on the environment and it is crucial to understand this impact. Life cycle analysis is an effective means to understand the impact of a chemical process on its surrounding. LCA models that are used for the analysis of the environmental impact of a process should be open, user-friendly, verifiable, periodically updated and should be based on technical data measurements (Souza et al. 2012; Uchida and Hayashi, 2012). Alvarado-Morales et al. (2013) performed LCA of brown seed weed in Nordic regions for the production of biogas and biomethanol. Two processes (scenario 1: biogas production; Scenario 2: biomethanol and biogas production) were compared based on factors such as greenhouse gas emissions, eutrophication, and acidification. It was concluded that scenario 1 was energy efficient than scenario 2 due to the incorporation of energy intensive biomethanol production process in scenario 2. Hsu (2012) studied on the life cycle assessment of gasoline and diesel production through fast pyrolysis and hydroprocessing reactions. Through the pyrolysis route, the GHG emissions equivalents for gasoline and diesel productions were found to be 117 $g.km^{-1}$ and 98 $g.km^{-1}$ respectively. These values indicate that the diesel production through pyrolysis route is more energy efficient in comparison to the production of gasoline. Iglesias et al. (2012) performed "LCA of biodiesel production using raw sunflower oil and waste cooking

oil" as feedstocks in a centralized and decentralized production system. It was concluded that usage of waste cooking oil adds credit in terms of its impact on climatic changes.

Kauffman et al. (2011) studied the LCA of advanced biofuels production from a hectare of corn. From the cultivation of corn, two important products such as corn seeds and corn stover are obtained. Corn seeds are used for the production of corn oil which acts as a feedstock for biofuel (bioethanol) production and corn stover can be used for the production of biochar and biooil through the fast pyrolysis process. Krohn and Fripp (2012) carried out life cycle assessment for biodiesel production using *Camelina sativa (L.).* The major advantage of using *Camelina sativa* is the absence of food versus fuel issues. Three major cropping systems (spring, dryland, and dual cropping) were compared based on their environmental impacts and it was concluded that the spring and dual cropping system resulted in significant reduction of greenhouse gas emissions than dryland system.

Liang et al. (2013) performed life cycle analysis for the production of biodiesel from four different feedstocks: Jatropha seed, castor seed and waste cooking oil. It was concluded that algae are the promising feedstock for long term production of alternate fuels based on its positive environmental impacts and minimum demands on land usage.

The main goal of this work is to compare the techno-economic and environmental impacts of two pathways (hydrodeoxygenation and transesterification) for the conversion of canola oil to biofuels. Hydrodeoxygenation of canola oil yields n-C_{18} paraffin (green diesel) as major product and transesterification of canola oil produces biodiesel that can be blended with traditional diesel and used in commercial engines. In our study, the LCA analysis was performed on both the processes (transesterification and hydrodeoxygenation) to understand their environmental impact by analyzing some parameters such as eutrophication rate, acidification, energy usage and

greenhouse gas emissions. This comparative study will help in understanding the key issues and challenges associated with the development and commercialization of biofuel from canola oil.

7.2. Methodology

7.2.1 Techno-economic analysis

Mass and energy balance was performed using Aspen Plus v.2006 for hydrodeoxygenation of Triolein using hydrogen and thereafter, the technical assessment was performed for the same process. Triolein was taken as the model feedstock as its structure is similar to that of a vegetable oil. The process plant was designed based on the production rate of canola oil in Saskatchewan. The simulation study was carried out for a continuous system. All the reactants and products in the simulation were present in the Aspen Plus databank library. The components incorporated into the simulation are triolein, oleic acid, stearyl alcohol, glycerol, hydrogen, water, octadecane and 1-octadecene with NRTL as a thermodynamic model. A two liquid (NRTL) thermodynamic model was chosen as the base model for the simulation of hydrodeoxygenation process (Lee et al. 2011).

The process flow diagram is shown in Fig. 7.1 and the simulation study for the HDO of triolein were based on a feed (triolein) flow rate of 10,000 kg/h to the reactor. Fig. 7.2 indicates the process flow diagram for the transesterification process to produce biodiesel as main product and glycerol as a by-product. The processing unit (Fig. 7.1) was designed to maximize the production of paraffin with minimum costs and energy losses in the process. Hydrogen was supplied in a 4:1 mole ratio to the reactants (oleic acid, stearyl alcohol) in reactors R-101 and R-102.

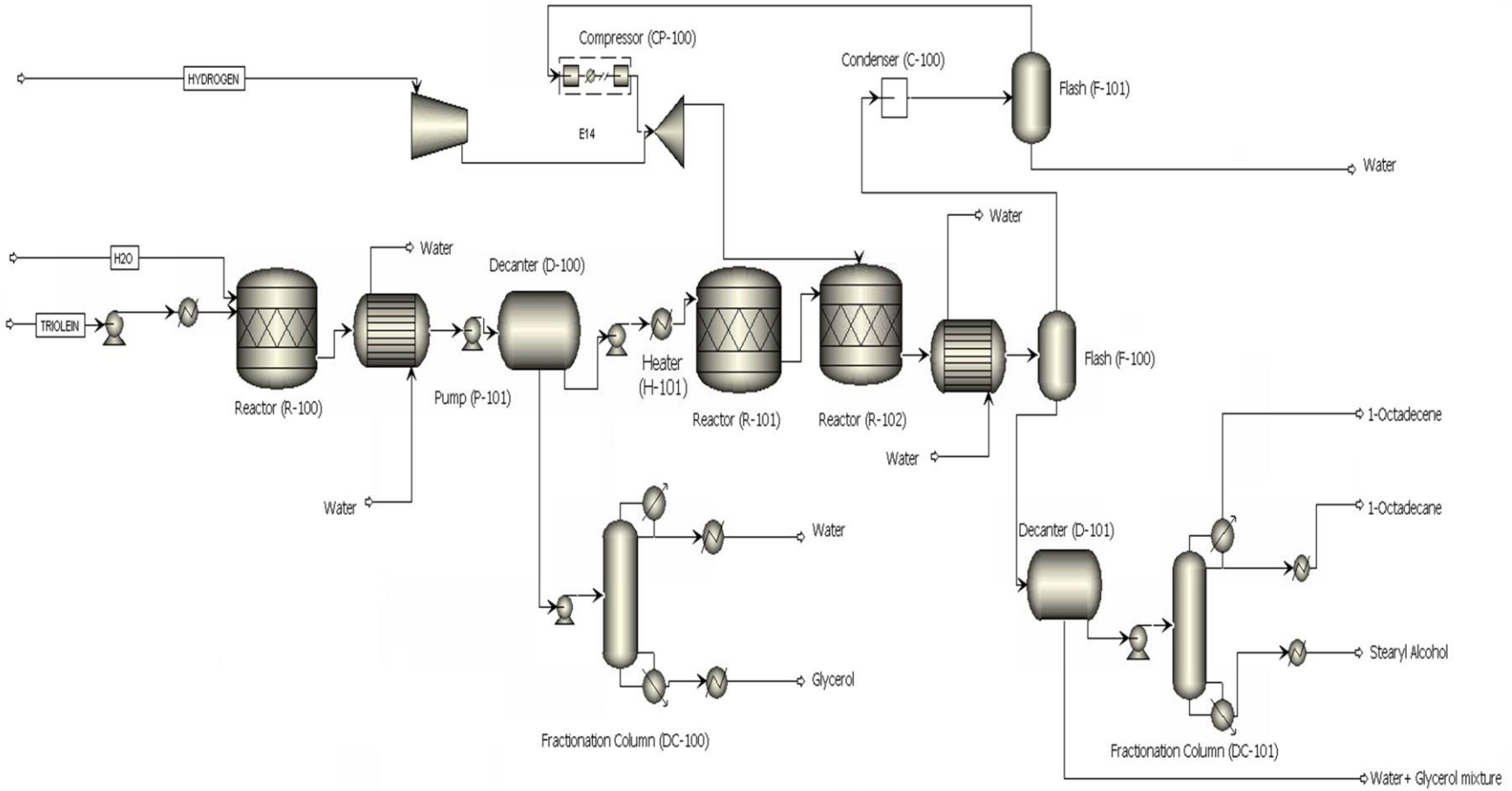

Fig. 7.1. Process flow sheet for hydrodeoxygenation process

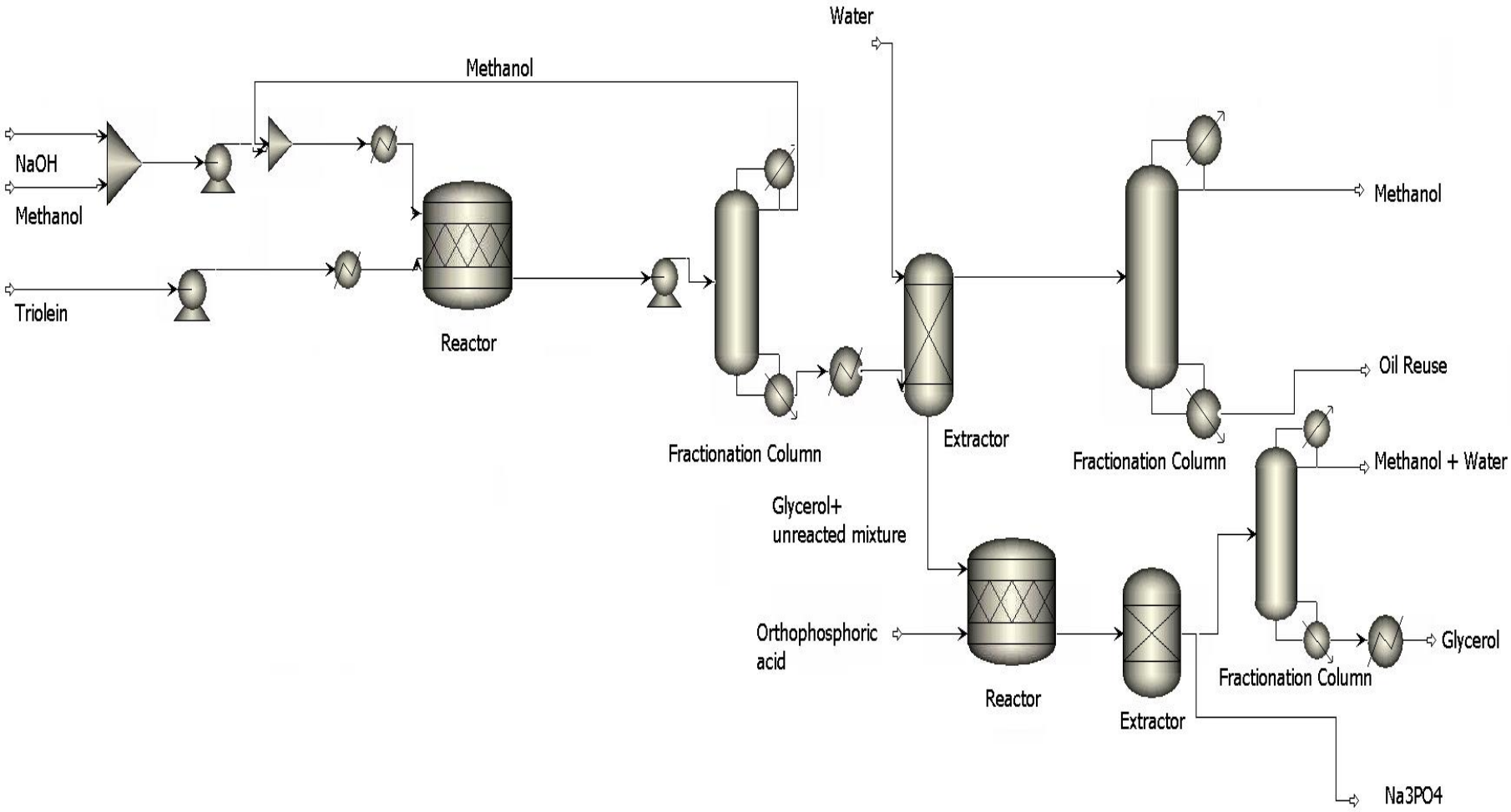

Fig. 7.2. Process flow sheet for transesterification process

All reactors were modeled as stoichiometric reactors with an overall conversion rate of 99%. The first reactor hydrolyzes triolein to oleic acid while the reactors R-101 and R-102 convert oleic acid to a mixture of octadecane and octadecane. The process is influenced by the use of catalysts. For the decanters (D-100 & D-101) employed in the system, Soave – Redlich – Kwong (SRK) property method was used to model mixed polarity blends in liquids better than Non-random two-liquid (NRTL) model (Sanchez et al. 2011).

Hydrogen is supplied in excess to the reactors R-101 and R-102 and therefore, the product mixture contains a substantial amount of hydrogen. Unreacted hydrogen was recovered through the flash vessel (F-100) and condenser system (C-100) and recycled back into the process. Since large temperature variations exist along the process, steam and cooling water supply were maintained in the process to absorb excess heat or to provide heat if necessary. Cooling water supply to the process is assumed to be at 288 K and low pressure steam (0.34 MPa) at 410 K was employed. Water recovered from the processing plant was treated and then recycled back into the system as cooling water. All reactors operate at 573 K and 6.89 MPa. Hydrolysis of triolein to oleic acid takes place in the 1^{st} reactor (R-100). Hydrodeoxygenation of oleic acid takes place in the 2^{nd} and 3^{rd} reactors (R-101 and R-102).

Compressed hydrogen was added to the reactor to maintain a 4:1 molar ratio with the reactants (Oleic Acid in E11; stearyl alcohol in E12). The conversion of oleic acid to stearyl alcohol is assumed to be 100%, while hydrogenation of stearyl alcohol is assumed to have a conversion of 99% based on stearyl alcohol. The final product generated is a mixture of octadecane and 1-octadecene. The selectivity of conversion of stearyl alcohol to octadecane is 0.4 and to 1-octadecene is 0.6. Reactor R-102 was used to convert the residual stearyl alcohol to octadecane and 1-octadecene. Unit C-100 **(**condenser) is used to separate hydrogen and water after flashing.

High purity hydrogen obtained after condensation is compressed and recycled back into the process through reactor R-101 and R-102. The decanters (D-100 and D-101) are used to separate two liquid phases with differing densities from each other. Glycerol is separated from oleic acid through decanter 1 (D-100) while decanter 2 (D-101) is used to remove excess water and residual glycerol from the process mixture. Glycerol obtained must be purified and concentrated further before it can be sold in the market. A fractionation column (DC-100) was used to concentrate and purify glycerol to 99.5% for further use. Glycerol is collected from the reboiler residue stream. The column is operated at a near vacuum conditions to maintain the temperature of the column below 423 K in order to avoid decomposition of glycerol that occurs above 423 K. To lower the pressure of the process stream from the heat exchanger to the pressure of the decanter, a turbine (P-101) is installed to reduce the pressure from 6.89-0.14 MPa as well as to generate electricity. Twenty-five percent of hydrogen remains unreacted and its removal from the process stream is facilitated by flash tanks (F-100 and F-101). The pressure drop associated with the flash vessel also leads to a substantial amount of water vapor being present in the stream which is removed from the system through condenser C-100 to generate 99.8% hydrogen.

Hydrodeoxygenation reactions are favorable and proceed to near completion at a temperature of 573 K. Hence, there is a large scope for heat recovery within the system. Heat is recovered from the exit streams of the reactors using heat exchangers and steam is generated at 0.34 MPa and 412 K. Using design specifications in Aspen Plus, the flow rate of process water to the heat exchangers was set such that the outlet had only 100% saturated steam. Heat exchanger H-101 was simulated as fuel oil fired box type furnaces to achieve the required reactor inlet temperature of 573 K. The liquid feed to the reactors is preheated to avoid any possibility of temperature shocks inside the reactor. All pumps were modeled as single stage centrifugal pumps. To

compress hydrogen to a pressure of 6.89 MPa, a 5 stage compressor (CP-100**)** was used with provisions for intercoolers to keep the temperature of hydrogen below 573 K. The flow of cooling water was adjusted to the intercoolers to ensure that the outlet temperature of hydrogen is same as the reactor temperature. The required product is a mixture of octadecane and octadecene (with purity greater than 99%) that was obtained from the distillate stream from E20. Stearyl alcohol, octadecane, and octadecene have similar boiling points at the room temperature and hence it is difficult to achieve 100% separation, but operating the column at near vacuum conditions helps to increase the purity of the product. The column is simulated as a 7 stage tray tower in Aspen Plus with condenser pressure being set at 0.07 MPa and condenser temperature set at 404 K.

7.2.2 Life-cycle assessment

A traditional LCA is performed from cradle-to-grave which implies that all environmental impacts associated with the production to end usage are accounted. The cradle-to-grave analysis involves the methodology of accounting the gas emissions and cost involved in the growth of canola oil seeds and it is inclusive of all steps until the commercialization of the final product and its end usage. Several LCA models have been developed and applied for the analysis of chemical/biochemical processes. Usually, LCA models such as GREET model are more transparent and allows easier applications. For the different input variables (x), the LCA value and the emissions factor are related by the equation (Eq. 7.4) given below (Krohn and Fripp, 2012).

$$\text{LCA value} = \sum_{x} (\text{Emission factor})_x \text{ x } (\text{Usage rate})_x$$
$$= \text{Input into the biofuel system} \qquad (7.4)$$

The system can be broadly classified into 4 stages

- Production of canola oil
- Transesterification and hydrodeoxygenation of canola oil to produce biofuel
- Storage and transportation of biofuel to dispensing station
- Operation of vehicles

In the case of hydrodeoxygenation and transesterification of triolein, a cradle to grave LCA was performed with the help of GHGenius v4.03 developed by $(S\&T)^2$ consultants. The inventory for the life cycle analysis was generated through the process flow sheets and mass/energy balances obtained from Aspen Plus v.2006 were used as inputs for the life cycle analysis (Aspen Technology Inc., USA). Canola seeds are crushed to obtain canola oil. Canola farming requires the use of fertilizers and some amount of fossil energy as well. The oil obtained is collected and then transported for processing to biofuels. During transesterification, glycerol is generated as a by-product and separated from the reaction mixture and sent for storage. The carbon footprint of the two processes was estimated using GHGenius v 4.03. A comparison was done between biodiesel and green diesel and the results were compared with low sulfur petrodiesel and gasoline for normalized and total GHG emissions.

7.3. Results and Discussion

7.3.1 Sensitivity Analysis

Sensitivity analysis using Aspen Plus v.2006 was performed on the process units. Hydrogen is an important raw material and it cannot be released into the atmosphere. A condenser pressure (C-100) over 0.10 MPa at a constant temperature gives a marginal improvement over the current hydrogen purity of 99%. Higher temperatures at a constant pressure of 0.10 MPa entails a higher concentration of water vapor in the final outlet stream as well as reducing the purity of the outlet hydrogen stream to below 80% for temperatures close to 340 K (Fig. 7.3).

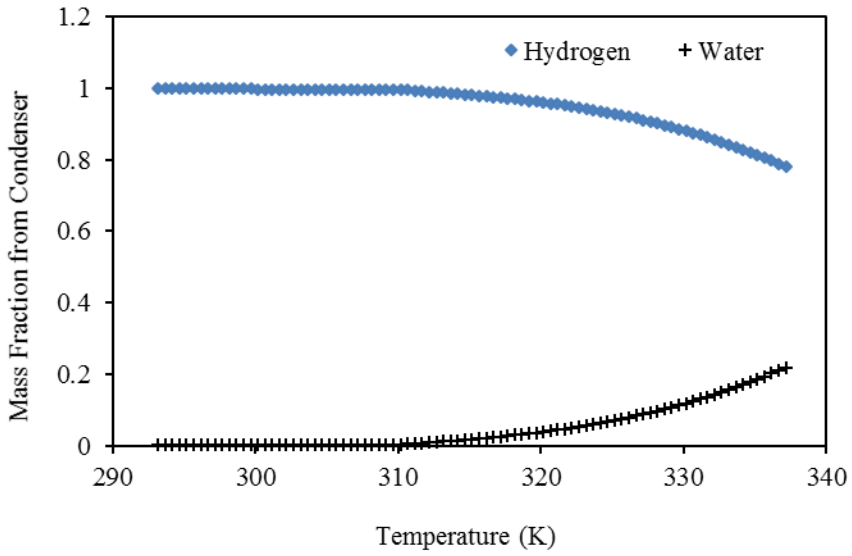

Fig. 7.3. Influence of temperature on fractional removal of hydrogen and water

Temperatures beyond 310 K may result in water build up inside the system which is detrimental to the process. Temperatures above 338 K resulted in a significant amount of octadecane and octadecene vapor being present in the liquid stream and therefore, this temperature should be avoided. Sensitivity analysis on decanter (D-100) was carried out to find the optimal operating temperature for maximum glycerol recovery (Fig. 7.4). The change in glycerol removal rate with temperature was studied to analyze the influence of decanter temperature on the by-product removal. The analysis was performed between a temperature of 293 to 373 K. Maximum recovery is observed at lower temperatures and thus it is preferable to operate the process at low temperatures (293-305 K). A similar analysis was carried out for decanter D-101 and in this case, water is the primary component of interest (Fig. 7.5). Water is an undesired impurity in biofuels and hence must be removed from the process stream. Even though lower temperatures are favorable, the presence of stearyl alcohol in the process mixture governs the minimum temperature of the process, as stearyl alcohol solidifies at a temperature below 330 K. Therefore,

it is preferable to operate at a temperature below 330 K to decant most of the water from the vessel.

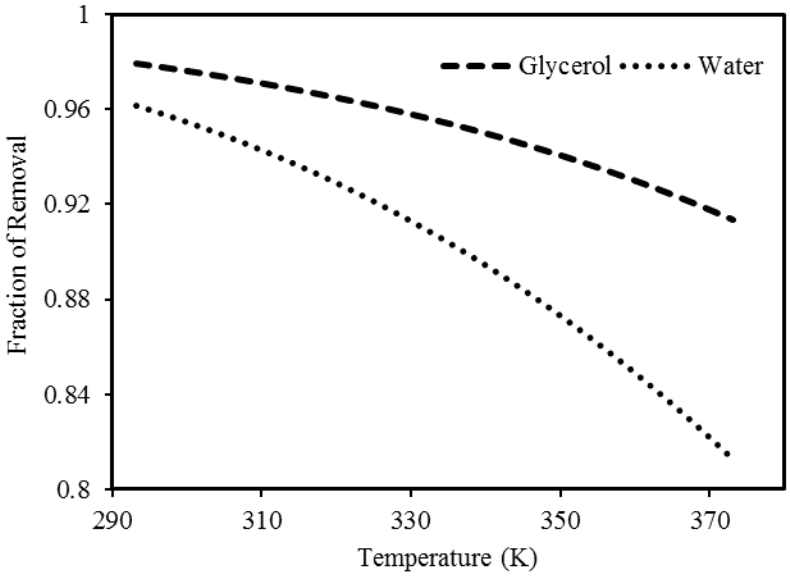

Fig. 7.4. Fraction of glycerol and water removed from the decanter (D-101) as a function of temperature

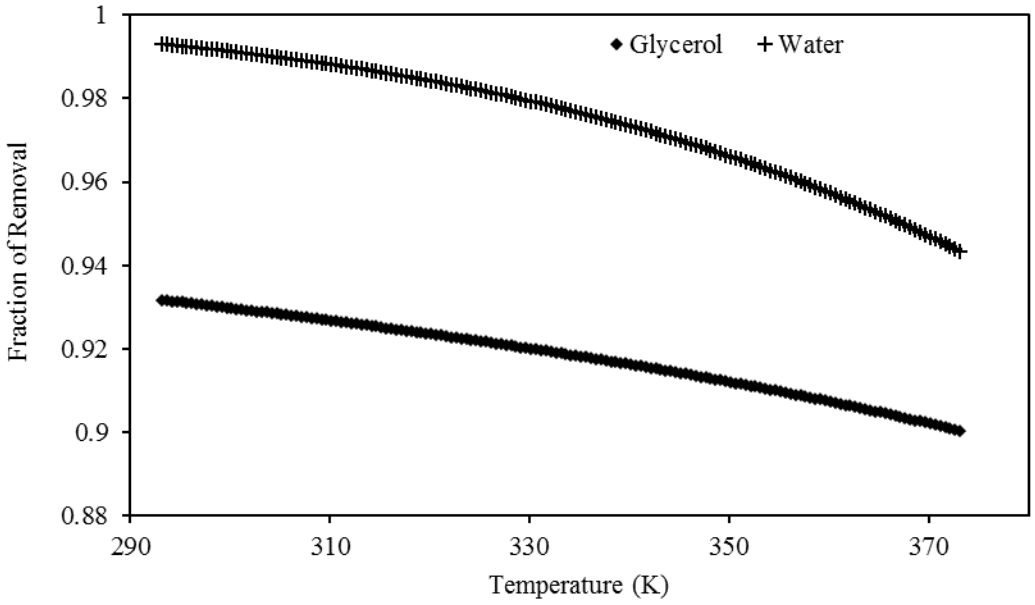

Fig. 7.5. Influence of temperature on removal of glycerol and water from decanter (D-101)

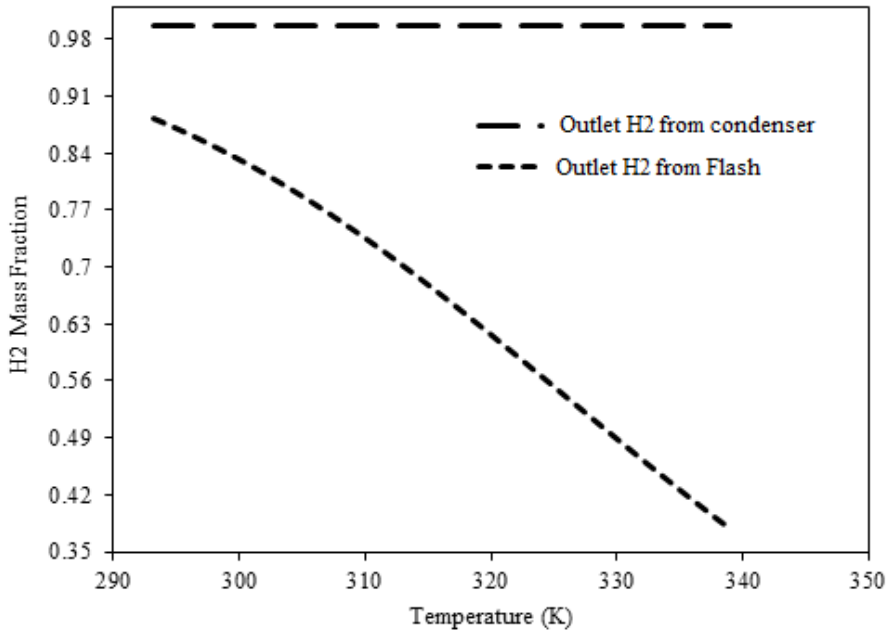

Fig. 7.6. Hydrogen concentration in streams obtained through the flash vessel (F-100) and the condenser (C-100) at different temperatures

Sensitivity analysis on the flash vessel (F-100) was carried out using Aspen Plus to check the effect of flash vessel conditions on the hydrogen recovery process (Fig. 7.6). The analysis was carried out in a temperature range of 293-340 K. Temperatures above 340 K result in vaporization of large quantities of paraffin which is unfavorable while temperatures below 333 K are unfavorable due to solidification of stearyl alcohol. Fig.7.7 indicates the variation in biofuel concentration with the column pressure (DC-101**)**. It could be seen that the product purity was independent (< 0.1% change) with respect to the change in column pressure. Stearyl alcohol, octadecane, and octadecene have similar boiling points at atmospheric pressure and in order to achieve substantial separation, the column has to be operated at a lower pressure (< 0.21 MPa). Fig. 7.8 indicates the variation in the mass fraction of hydrogen with the condenser temperature.

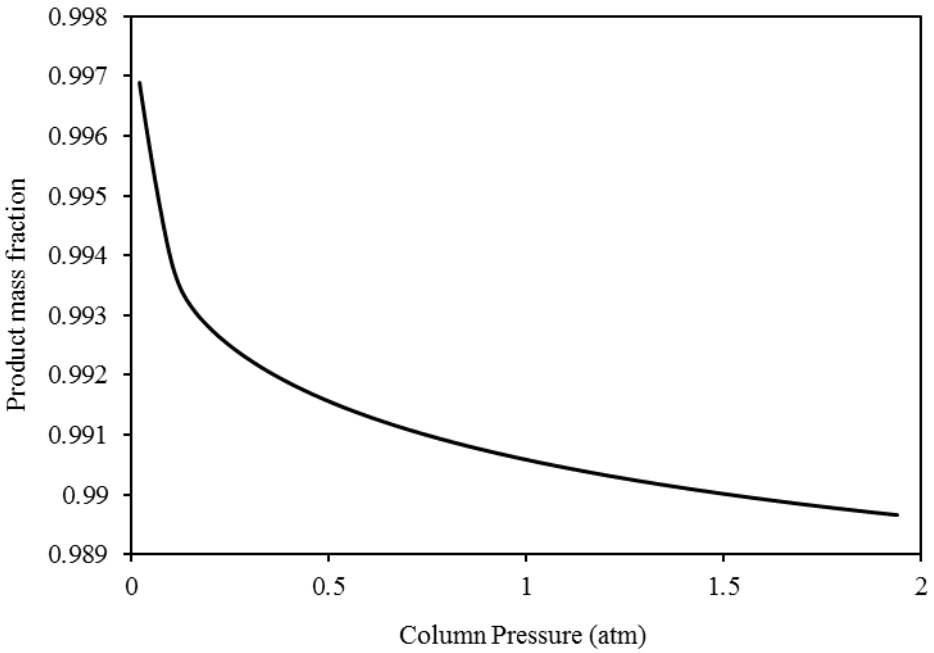

Fig. 7.7. Variation of biofuel concentration with change in average column pressure of the fractionation column

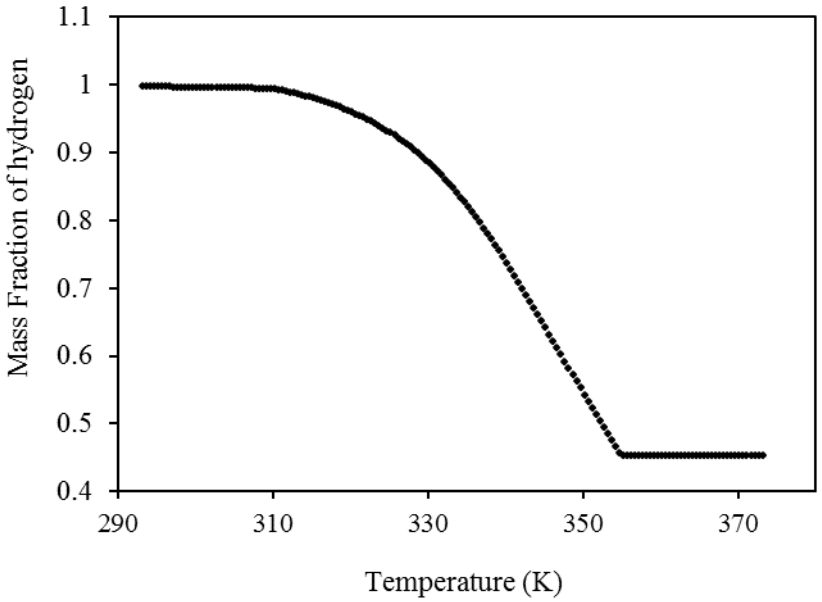

Fig. 7.8. Influence of condenser temperature on hydrogen purity

A drastic reduction in the mass fraction of hydrogen with temperature was seen. This is due to the existence of liquid products in the vapor phase at a higher temperature (> 310 K). Mass fraction of glycerol is found to increase with the decanter temperature (Fig. 7.9). It is evident that the cost of raw material has an influence on the cost of the product (biofuel).

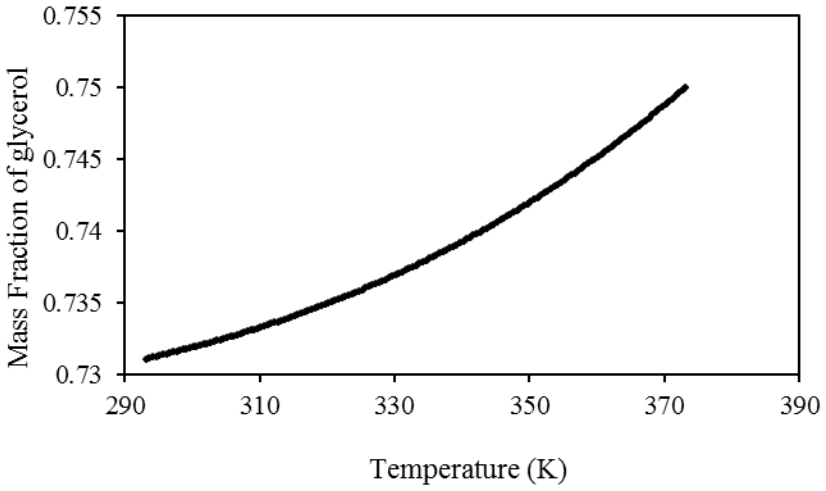

Fig. 7.9. Influence of decanter temperature on glycerol purity

7.3.2 Techno-Economic Assessment

Equipment sizing and economic evaluations were carried out using Aspen Icarus Process Evaluator v.2006. All cost calculations were based on the data available in Q1 2006 and were updated using the CEPCI Index to account for an increase in cost over the years. The calculated costs were based on a base flow rate of 10,000 kg/h of feed oil to the system and an operating factor of 0.9. A provision was also made for the storage of raw materials and products while calculating fixed capital investment (not included in the flow sheet). Sizing of the storage vessels was based on the assumption of on-site storage of 2 weeks' worth of raw materials and 3 weeks' worth of products (Sotoft et al. 2010).

Fixed Capital Investment (FCI) was calculated using Aspen Icarus that includes the components such as Purchased Equipment, Setting of equipment, piping, civil, instrumentation, electrical

fittings, insulation, administrative overheads, contingencies, escalations. The working capital is a fixed percentage of the FCI and the Total Capital Investment (TCI) is the sum of FCI and working capital. The costs were divided into 3 basic units: (1) production costs which include cost of utilities, raw materials, catalysts, operator costs; (2) indirect costs in the form of overheads, insurance and taxes, and (3) other general costs in the form of administrative costs, Research & Development, marketing and depreciation. Table 7.1 indicates the expenditures incurred during hydrodeoxygenation and transesterification process.

The operating costs and the number of operators, overhead insurances were selected based on the information provided by Ulrich and Vasudevan (2004). To ensure the standard basis of comparison, the operating parameters were kept constant for both the process though the reaction mechanism and the feedstock differ. An increase in the price of feedstock from \$0.4/kg to \$1/kg resulted in an increase in biofuel cost by 70% approximately (Fig. 7.9).

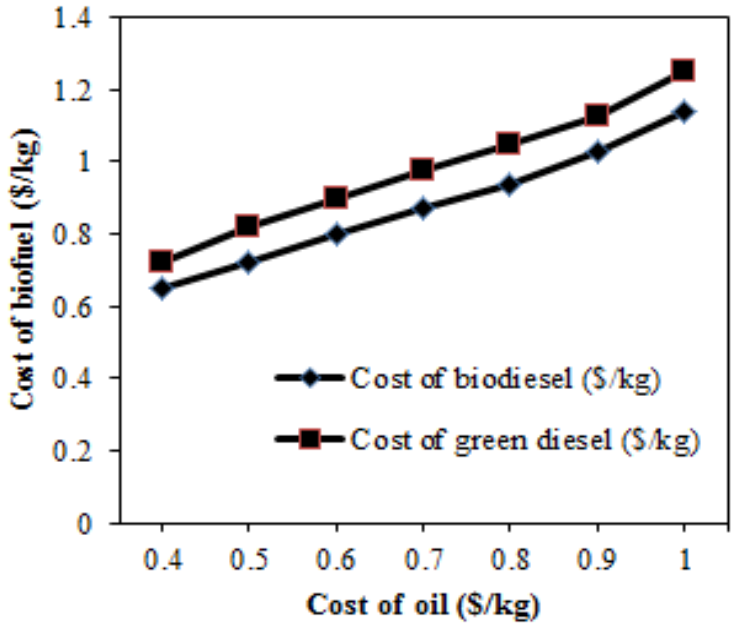

Fig. 7.10. Variation in the cost of biodiesel and green diesel with change in the cost of feed oil

Return on investment is a comparative indicator of the profitability of processes and no significant difference in return on investment was observed between biodiesel and green diesel obtained from hydrodeoxygenation process (Fig. 7.10).

Table 7.1. Costs related to the plant operations

Greendiesel		Biodiesel	
Item	*Cost*	*Item*	*Cost*
Oil	0.35 $/kg	Oil	0.35 $/kg
Hydrogen	5.4 $/kg	Methanol	530 $/tonne
Process Water	1.5 $/ton	Process Water	1.5 $/tonne
Sodium Hydroxide	1.27 $/lb	Catalyst	84 $/kg
Glycerol	2 $/kg	Glycerol	2 $/kg
Biofuel	1.2 $/L	Biofuel	0.89 $/L
Cooling Water	1.26 $/ton	Cooling Water	1.26 $/tonne
Steam (690 kPa)	9.1 $/ton	Steam (690 kPa)	9.1 $/ton
Electricity	7.32 c/kWh	Electricity	7.32 c/kWh
Number of Shifts	5	Number of Shifts	5
Fixed Capital	13 M$	Fixed Capital	12.5 M$
Working Capital	10% of FCI	Working Capital	10% of FCI
Operators	54,000 $/yr.	Operators	54,000 $/yr.
Operating Supplies	15% of maintenance	Operating Supplies	15% of maintenance
Laboratory Charges	20% of	Laboratory Charges	20% of operating
Overheads	70% of total labor	Overheads	70% of total labor
Insurance	2% of FCI	Insurance	2% of FCI
Distribution and marketing	3% of TME	Distribution and	3% of TME
R & D	2% of TME	R & D	2% of TME
Depreciation	10%/year for 10 years	Depreciation	10%/year for 10
Exchange Rate	0.99 US$/CDN$	Exchange Rate	0.99 US$/CDN$

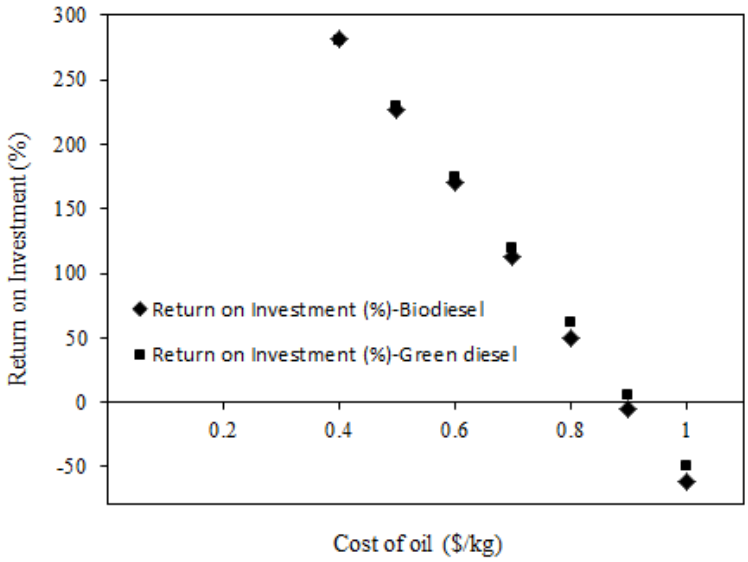

Fig. 7.11. Comparison of return on investment (%) for hydrodeoxygenation and transesterification process

Table 7.2 illustrates the comparison between biodiesel and greendiesel production process on the manufacturing cost and internal rate of return (IRR). Table 7.3 indicates the operator's requirement for different standard units that are used in hydrodeoxygenation and transesterification processes. Transesterification and hydrodeoxygenation processes were found to offer the same internal rate of return indicating that both processes are highly profitable for a venture capitalist. It is evident that, most venture capitalists expect a high internal rate of return (> 150%) and for any start up business, it is highly desirable to design a process that offers IRR of at least 150%.

Table 7.2. Economic comparison of biodiesel and HDO plant

	Biodiesel	Greendiesel
Manufacturing cost ($/kg)	0.61	0.70
Density (kg/m^3)	880	775
IRR	213%	210%

The total manufacturing cost is essentially a sum of all the costs mentioned above subtracted by the revenue from by-products. Total manufacturing expenditure (TME) is related to the production cost using equation (7.5).

TME = Production Cost + Indirect Cost + General Costs – By-product revenue (Gael and Vasudevan, 2004) (7.5)

Materials flow involved in hydrodeoxygenation process is presented in Table 7.4. The payback period is the time in which the TCI is recovered through normal plant operation (Eq. 7.6).

$$\text{Payback Period} = \frac{\text{TCI}}{\text{Total Profit/period}}$$ (Gael and Vasudevan, 2004) (7.6)

The price of oil has a great impact on the cost of biofuel. Table 7.5 indicates the cost associated with the different process units in both hydrodeoxygenation and transesterification process.

Table 7.3. Number of operators for different process units

Equipment			
	No	Operators Req./unit/shift	
Pumps	5	0	0
Decanters	2	0	0
Columns	2	0.3	0.6
Compressors	1	0.1	0.1
Reactors	3	0.3	0.9
Flash Vessels	1	0.05	0.05
Heaters	7	0.05	0.35
Heat Exchangers	2	0.05	0.1
Condensers	1	0.05	0.05
Splitter	1	0.2	0.2
Total No. of operators required			15
No. of Shifts*			5

*5 Shifts include 3 normal shifts and 2 shifts to account for ill employees and employees on holiday.

Table 7.4. Overall stream composition for hydrodeoxygenation process

Stream No.	From	To	Oleic acid	Octadecane	Octadecene	Water	Hydrogen	Triolein	Glycerol	Stearyl alcohol	Mass flow	Temperature	Pressure
											Kg/h	K	atm
		E1											
100		E3	0	0	0	0	0	1	0	0	10000	293	1
	E3	E4											
102			0	0	0	1	0	0	0	0	1000	298	1
	E5	E6											
103			0.87	0	0	0.04	0	0	0.09	0	11000	573.15	64.15
	E10	E11											
105	E11	E12	0.87	0	0	0.04	0	0	0.09	0	11000	370.61	1
	E12	E15											
108			1	0	0	0	0	0	0	0	9606.87	573.15	2
	E17	E14											
109			0	0.17	0.65	0.12	0.005	0	0	0.05	9873	573.15	64.15
		E14											
110	E13	E12	0	0.18	0.67	0.12	0.01	0	0	0.01	9893.03	573.15	64.15
118	E6	E7	0	0	0	0	1	0	0	0	66.87	297.65	1
	E22												
119			0	0	0	0	1	0	0	0	219.29	293	1
	E21												
122			0	0	0	0	1	0	0	0	20.03	360.15	64.05
	E23												
124	E24		0	0	0	0.27	0	0	0.73	0	1393.13	293.15	1

128	E4	0	0	0	1	0	0	0	0	365	308.15	1
129	E15	0	0	0	0.01	0	0	0.99	0	1028.13	300	0.073
131		0	0.21	0.78	0	0	0	0	0	8449.56	300	0.1
132		0	0.14	0.35	0	0	0	0	0.51	134.51	300	1
202		0	0	0	1	0	0	0	0	2252.94	411.58	3.4
204		0	0	0	1	0	0	0	0	2809.78	446.86	3.4
133	E20	0	0.07	0.28	0.54	0.11	0	0	0	0.44	404.37	0.1

Table 7.5. Cost associated with process units

Component ID	*Component Type*	*Equipment Cost (CAD)*	*Total Direct Cost (CAD)*
E1	Centrifugal Pump	3400	31800
E10	Box type process furnace	262000	364100
E11	Jacketed Reactor	48100	160500
E12	Jacketed Reactor	48100	160500
E15	Floating head heat exchanger	29000	94400
E16	Flash Vessel	47300	150800
E17	Floating head heat exchanger	31200	74700
E18	Horizontal Decanter	18000	101400
E19	Centrifugal Pump	3300	26500
E2	Box type process furnace	11700	80600
E20	Tray tower	394600	1279000
E21	Floating head heat exchanger	50100	89800
E22	Floating head heat exchanger	20800	64700
E3	Jacketed Reactor	48100	160500
E4	Floating head heat exchanger	29000	94400
E5	Turbine	4200	31900
E6	Horizontal Decanter	18400	108300
E7	Centrifugal Pump	3300	22400
E8	Centrifugal Pump	3300	23500
E9	Tray tower	139800	513500
S1	Storage Tank	459400	586900
S3	Storage Tank	429200	569900
S2	Storage Tank	79500	178700
E14	Multi-stage Compressor	819800	915700
	Total	3001600	5884500

Though, the materials involved in the process and the operating conditions for both process differ, the cost for equipment was based on the size and the material used. The net contribution of raw materials to the final cost is 74% that means the most of it is spent on procuring oil. Fig. 7.12 represents the distribution of costs in building a hydrotreatment plant for hydrodeoxygenation of canola oil for the production of green diesel.

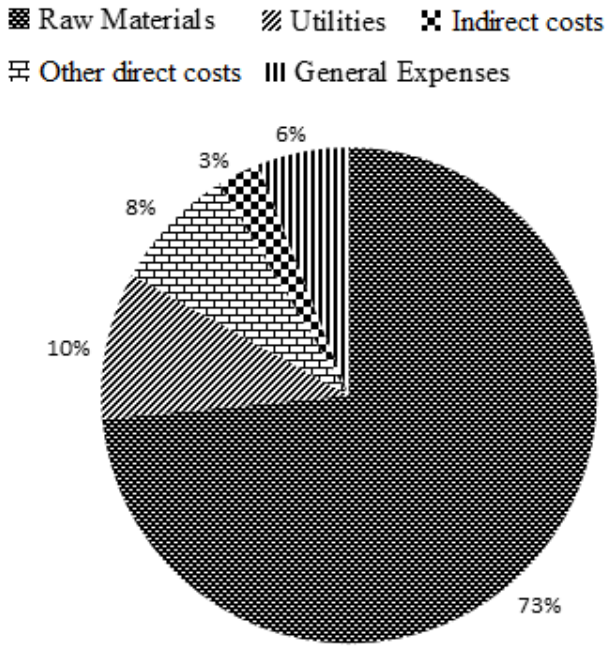

Fig. 7.12. Distribution of cost in the hydrotreatment plant

Profits involved with processes are provided in Tables 7.6 and 7.7. As reported by Canola Council of Canada, biodiesel production capacity of 151 MMLY (metric million liters per year) will yield a total revenue of $151.5 Million and gross profit of $17.6 million per year. In our process design, the plant was designed to process 10,000 kg/h of feed oil which accounts to 87.6 MMLY. Based on our calculations, the profit of $29.1 million can be obtained. One major contributing factor in our design is the credits obtained using glycerol (by product of transesterification process). Table 7.8 indicates the energy expenditures associated with the reactants and products associated with the hydrodeoxygenation reaction. Total energy input

required during hydrodeoxygenation process is 119.36 MW. Cumulatively, the output energy based on the products is 92.24 MW and based on the input and output energy values, it can be seen that, the HDO process is 77% efficient in terms of energy usage.

Table 7.6. Cost break up for producing biodiesel through transesterification

	Annual Cost		Unit Price ($/kg)	
Direct				
Raw Materials				
Methanol	$ 4,583,127		0.063	
Process Water	$ 2,000		0.000	
Orthophosphoric Acid.	$ 414,698		0.006	
Triolein	$ 27,594,000		0.380	
By-Product Credits				
Glycerol	$ 17,344,800		-0.239	
Catalysts / Solvents	$ 1,559,103		0.021	
Operating Labor	$ 810,000		0.011	
Supervisory/Clerical Labor	$ 162,000		0.002	
Utilities				
Steam	$ 206,876		0.003	
Electricity	$ 57,710		0.001	
Cooling Water	$ 5,351,265		0.074	
Maintenance/Repairs	$ 500,000		0.007	
Operating Supplies	$ 75,000		0.001	
Laboratory Charges	$ 243,000		0.003	
Patents and Royalties	$ 121,069		0.002	
Total	$ 24,335,049	$ 24,335,049	0.336	0.336
Indirect				
Overheads	$ 1,030,400		0.014	
Local Taxes	$ 125,000		0.002	
Insurance	$ 125,000		0.002	
Total	$ 1,280,400	$ 25,615,449	0.018	0.353

Total Manufacturing Expense		$ 25,615,449		0.353
General Expenses				
Administrative Costs	$ 257,600		0.004	
Distribution and Selling	$ 768,463		0.011	
R & D	$ 512,309		0.007	
Total	$ 1,538,372	$ 27,153,822	0.021	0.374
Depreciation	$ 1,375,000	$ 28,528,822	0.019	0.393
Revenue				
Biofuel	$ 73,357,036			
Total	$ 73,357,036			
Net Annual Earnings	$ 44,828,214			
Income Taxes	$ 15,689,874		0.216	0.610
Profit	$ 29,138,339			

Table 7.7. Cost break up for producing biodiesel through hydrodeoxygenation

	Annual Cost	Unit Price ($/kg)
Direct		
Raw Materials		
Hydrogen	$ 9,323,618	0.139
Process Water	$ 9,933	0.000
Triolein	$ 27,594,000	0.412
By-Product Credits		
Glycerol	$ 19,272,000	-0.288
Catalysts / Solvents	$ 2,016,000	0.030
Operating Labor	$ 812,250	0.012
Supervisory/Clerical Labor	$ 162,450	0.002
Utilities		
Steam	$ 53,323	0.001

Electricity	$ 866,817		0.013	
Fuel Oil	$ 952,623		0.014	
Cooling Water	$ 2,665,391		0.040	
Maintenance/Repairs	$ 524,000		0.008	
Operating Supplies	$ 78,600		0.001	
Laboratory Charges	$ 162,450		0.002	
Patents and Royalties	$ 129,747		0.002	
Total	$ 26,079,202	$ 26,079,202	0.389	0.389
Indirect				
Overheads	$ 1,049,090		0.016	
Local Taxes	$ 131,000		0.002	
Insurance	$ 131,000		0.002	
Total	$ 1,311,090	$ 27,390,292	0.020	0.409
Total Manufacturing Expense		$ 27,390,292		0.409
General Expenses				
Administrative Costs	$ 262,273		0.004	
Distribution and Selling	$ 684,757		0.010	
R & D	$ 547,806		0.008	
Total	$ 1,494,836	$ 28,885,128	0.022	0.431
Depreciation	$ 1,441,000	$ 30,326,128	0.022	0.453
Revenue				
Biofuel	$ 76,871,543			
Total	$ 76,871,543			
Net Annual Earnings	$ 46,545,415			
Income Taxes	$ 16,290,895		0.243	0.700
Profit	$ 30,254,520			

One major concern is the usage of fuel oil to provide the energy (temperature) required for the hydrodeoxygenation reaction. Usually, HDO reactions are performed at temperatures > 300 °C and a hydrogen pressure of 6.89 MPa. Achieving these reaction conditions requires usage of fuel oil or natural gas in chemical industries. From our analysis, it is observed that major part of the

expenses is made in the production of raw materials which is in agreement with the literature (Vlysidis et al. 2011, Mora et al. 2012). The influence of cost of oil on investment return (%) and cost of the product (green diesel) is shown in Fig. 7.13.

Table 7.8. Energy calculations for hydrodeoxygenation process

Location	Components	Molecular weight	Molar Flow (mol/h)	Energy (Megawatts, MW)
Inlet	Triolein	885.43	11293	107
	Hydrogen	2	118780	9.44
	Fuel oil		156.4	1.90
Outlet	Octadecane	254.49	7068	23.57
	Octadecene	252.48	26307.77	87.16
	Glycerol	92.1	11058	5.08

With an increase in the cost of feedstock from \$0.4/kg to \$0.9/kg, the return on investment decreases drastically (Fig. 7.13). Therefore, it is important to optimize the cost distribution of feedstock to maximize profit and return on investment in the production of green diesel in industrial scale.

7.3.3 Life-cycle assessment based on environmental impacts

The technical assessment of the two processes relates to the estimation of the total energy production and the amount of external energy input to the system required to generate 1 kJ of energy in the form of biodiesel (transesterification) and green diesel (HDO). Tables 7.9 & 7.10 represent the higher heating values (HHV) for reactants and products involved in the transesterification and the hydrodeoxygenation processes respectively. The energy input is calculated HHV of all inputs excluding the feedstock and the final product. Energy efficiency of a process and the HHV of the reactants and the products involved with the process are related by Eq. (7.7).

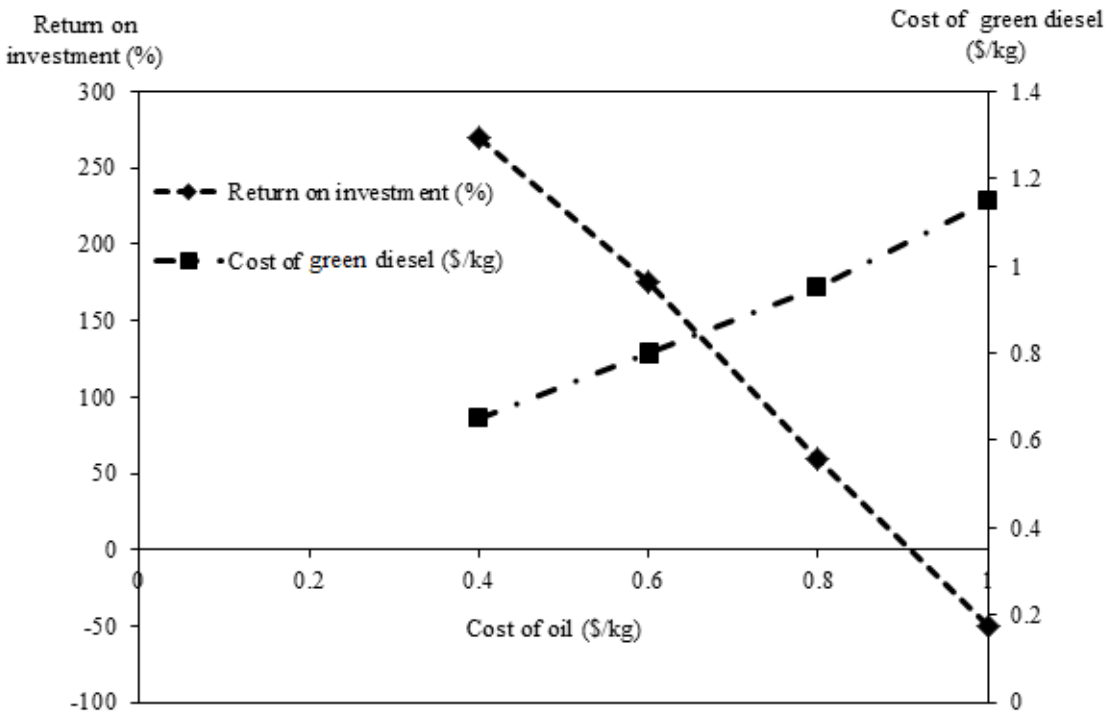

Fig. 7.13. Variation of return on investment (%) and cost of green diesel with cost of oil

Table 7.9. Higher Heating Value (HHV) of feedstock and products for transesterification plant

Component	HHV, kJ/kg
Canola Oil (Feed)	38,520
Methanol(Feed)	23261
Biodiesel (Product)	41,200
Glycerol (Product)	152168

Table 7.10. Higher Heating Value (HHV) of feedstock and products for hydrodeoxygenation plant

Component	HHV, kJ/kg
Canola Oil (Feed)	38,520
Hydrogen (Feed)	286
Stearyl Alcohol (Product)	3.19×10^6
Octadecane (Product)	3.05×10^6
1 – Octadecene (Product)	7.2×10^5

For hydrodeoxygenation process, the external energy supply to generate 1 kJ of product comes out to be 0.132 kJ and the amount of external energy required to produce 1 kJ of biodiesel through transesterification is 0.095 kJ. This data relates to only the production of fuel and not to the various stages that also support the production of fuel. Table 7.11 compares the transesterification and hydrodeoxygenation process on their energy efficiency. It could be seen that, both the processes require a considerable supply of energy. Overall, a total of 1.09 kJ of energy needs to be supplied to generate 1 kJ of green diesel whereas for biodiesel this stands at 1.17 kJ.

$$\text{Energy Efficiency} = \frac{\text{HHV of products + Net Electricity Generated}}{\text{HHV of reactants added to the system}} \quad (7.7)$$

Table 7.11. Comparison of the processes on their energy efficiency

	Biodiesel (Transesterification)	Green diesel (HDO)
Input energy (HHV in Megawatts)	115.9	121.6
Output energy (HHV in Megawatts)	98.5	115.82
Energy requirement ratio	1.17	1.09
Energy efficiency	85%	95%

Paraffins obtained through hydrotreating of vegetable oils have higher energy content as compared to methyl esters and hence are usually better fuels. An overall synthesis energy balance shows that hydrodeoxygenation process is found to be 95% energy efficient whereas the transesterification process had 85% efficiency. Higher (95%) efficiency of the hydrodeoxygenation process can be attributed to the energy content of the products (C_{18} paraffin

and olefins) obtained through hydrotreatment reactions. As mentioned earlier, life cycle assessment gives detailed information on the environmental impact of a process from its genesis to the product commercialization (Fig. 7.14). Glycerol credit obtained through selling glycerol as a by-product is an important part of the cost structure. The price of glycerol is another important factor affecting the price of biodiesel. Depending on the grade of glycerol being produced the impact on the price is different. The glycerol credit obtained for this system is 29 c/kg of biodiesel.

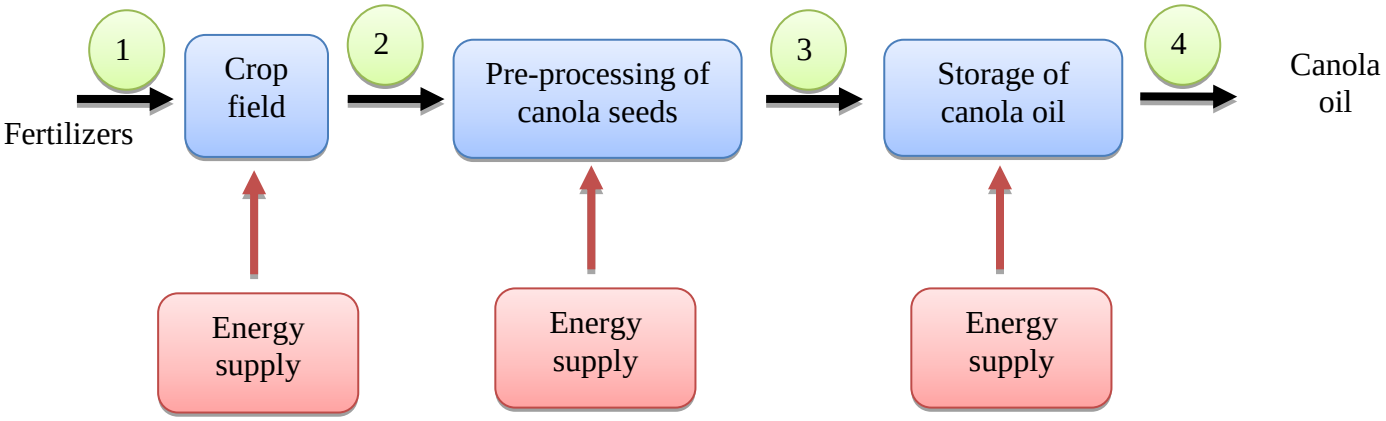

1- Supply of fertilizers to grow canola plant
2- Pre-processing of seeds to produce canola oil
3- Transportation of canola oil to the storage unit
4- Transfer of canola oil to the hydroprocessing/biodiesel unit

Fig. 7.14. Energy expenditures associated with the production of canola oil

Since biodiesel usage still faces an uncertain future and currently has an unstable market, a viable process must have a payback period of fewer than 2 years and processes with a payback period greater than 4 years are considered unviable. If a lesser amount of oil is converted to its

final form of biofuel costs per unit of biofuel escalates to close to $2.3 /kg for 80% conversion of oleic acid to biofuel. For instance, the cost of biofuel is estimated as $2.3/kg for 80% conversion of oleic acid to biofuel. Total capital investment was found to be $14.41 M with a net profit of $3.17 M per year. A decrease in the price of hydrogen in the future due to alternate production methods may make the process more cost efficient.

For the growth of plants, fertilizers are employed that contribute to human toxicity, terrestrial acidification, and pollution of aquatic systems. During pre-processing of canola seeds, chemicals and process units such as crushers and extractors are used that makes a significant contribution to the environmental impact. Fig. 7.15 represents the gram equivalent of CO_2 emissions per kilometer on various factors. The gram equivalent of CO_2 emissions per kilometer is calculated based on average fuel consumption per km for high duty vehicles in Canada and total relative individual GHG emissions (g/km) are represented in Fig. 7.15. It is evident that gasoline and petrol diesel represent higher GHG emissions in comparison to biodiesel and HRD. Petro-diesel, gasoline, hydrotreated renewable diesel (HRD) and biodiesel are compared based on various factors such as feedstock upgrading, feedstock transport and fuel production for their gram equivalent emissions of CO_2. It is evident that most of the CO_2 emissions equivalents are associated with the vehicle operation and production of fuels and fertilizers. Table 7.12 indicates the exact emission values for the different fuels. Comparison of biodiesel and HRD is essential to justify the environmentally benign of either the hydrotreatment or biodiesel plant. Biodiesel production involves lesser CO_2, CO, CH_4 and total VOC emissions in comparison to HRD.

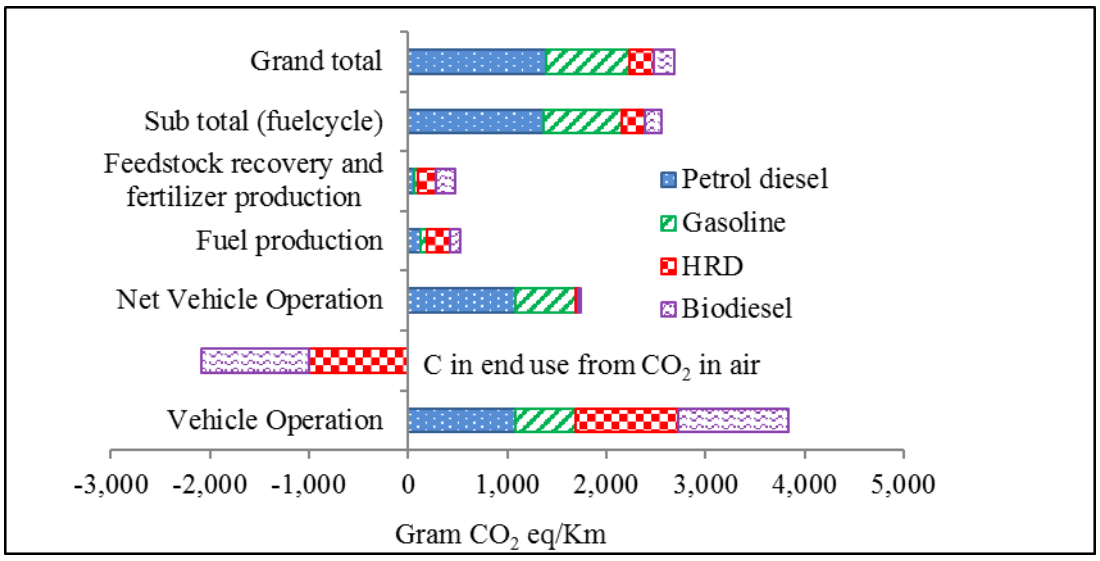

Fig. 7.15. Comparison of petrodiesel, gasoline, hydrotreated diesel and biodiesel on their CO_2 emissions per kilometer

Table 7.12. Comparison of greenhouse gases emissions from petrodiesel, gasoline, HRD (green diesel) and biodiesel

Pollutant	Petrodiesel	Gasoline	HRD	Biodiesel	Total (gram eq/km)
CO_2	1313.9	769.6	143.3	86.1	2312.9
CH_4	2.64	1.72	0.59	0.48	5.43
N_2O	0.058	0.055	0.33	0.34	0.783
CO	0.585	0.794	0.4	0.33	2.109
NO_X	1.47	1.045	3.678	3.863	10.056
Total VOC	0.223	0.485	0.24	0.2	1.148
SO_X	1.365	0.89	0.3	0.4	2.955
CFC's + HFC's	0.001	0.001	0.001	0.001	0.004
PM	0.144	0.108	0.25	0.26	0.762

Fig. 7.16 indicate the relative comparison of biodiesel, green diesel (HRD), gasoline and petrodiesel on the gram equivalent CO_2 emissions associated with transportation of feedstock and operation of vehicles.

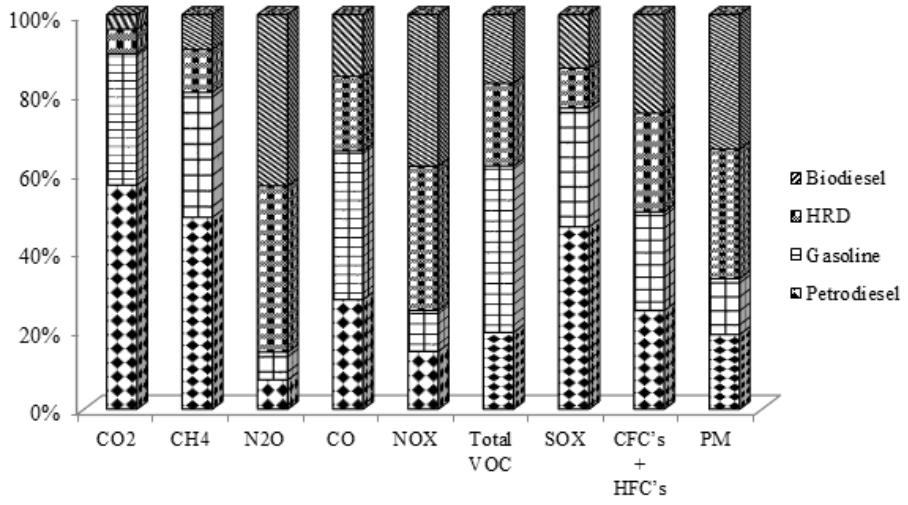

Fig. 7.16. Relative comparison of petrodiesel, gasoline, hydrotreated diesel (HRD) and biodiesel on greenhouse gas emissions

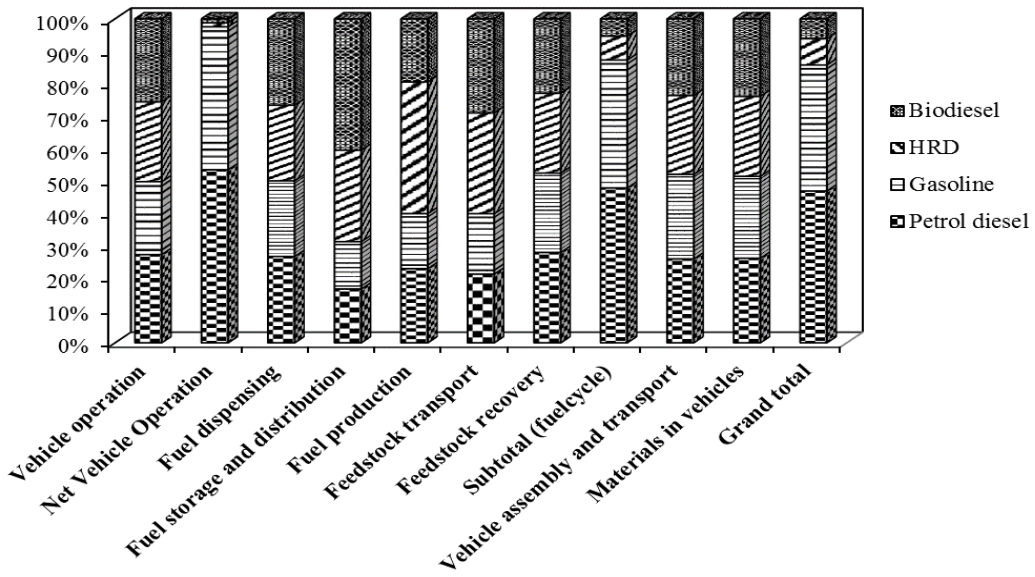

Fig. 7.17. Relative comparison of petrodiesel, gasoline, hydrotreated diesel (HRD) and biodiesel on gram equivalent CO_2 emissions associated with different factors

One interesting finding is that, production of biofuels contributes majorly to emissions in comparison to the fossil fuels. It is evident that, fossil fuels are employed for the transportation of feedstock and fertilizers and also for the operation of the plant. Hence, production of biofuels is directly and indirectly dependent on fossil fuels. However, considering the other factors as indicated in the diagram, it is seen that the overall emissions from biofuels are considerably less than fossil fuels. The principle of computational LCA is based on the following method as prescribed by Heijungs and Sangwon, 2013. Technology matrix (A) or the database of process flows and production processes, and the final output (f) that is desired from the system are related by the Eq. (7.8).

$$s = A^{-1}f \tag{7.8}$$

Matrices' obtained is the scaling vector which when multiplied by the emissions matrix B gives the necessary intensity of emissions caused by the whole system.

$$g = B.s \tag{7.9}$$

Emissions inventory vector (g) and scaling vector (s) are related by Eq. (7.9). Emissions inventory vector (g) defines the emissions caused by the whole system which when multiplied by the characterization matrix Q gives non-normalized environmental impact values (Eq. 7.10).

$$h = Q.g \tag{7.10}$$

The environmental impacts can be divided by regional or world reference impact factors to obtain normalized results which are easier to compare and which can be weighted to obtain a single environmental performance indicator. A comparison was carried out between transesterification and hydrodeoxygenation route and the results are presented below. Reference impact factors are sourced from LCIA ReCiPe v1.08 (Goedkoop et al. 2008; Hischier et al. 2010). World reference emission factors were used for the LCA and the impact factors that were

calculated are : “Global warming potential(GWP), ozone depletion (OD), terrestrial acidification (TA), marine eutrophication (ME), human toxicity (HT), photochemical oxidant formation (POF), freshwater ecotoxicity (FWE), marine ecotoxicity (ME), agricultural land occupation (ALO), water depletion (WD), metal depletion (MD) and fossil depletion (FD)” (Wagner and Lewandowski, 2017). Fig.7.17 represents the comparison of biodiesel and the hydrotreated diesel fuel production plant based on their impact on several environmental factors.

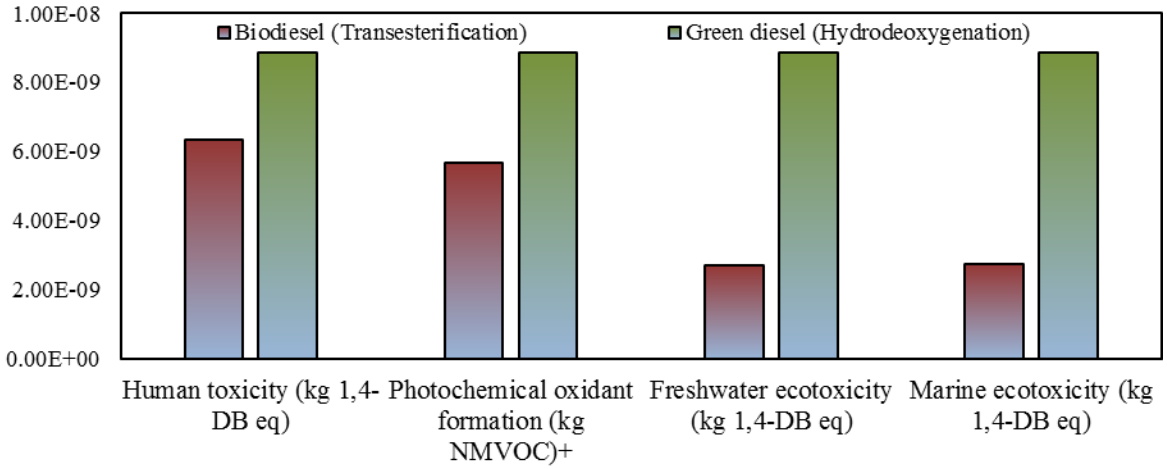

Fig. 7.18. Comparison of biodiesel and green diesel on their environmental impact

In the case of environmental factors such as marine and fresh water toxicity, the impact of biodiesel production plant is less than 40% of the impact caused by the hydrodeoxygenation plant. This is mainly due to the involvement of hydrogen (reactant) during hydrotreatment and also the products such as C_{18} paraffin/olefins and the intermediates such as alcohols and ketones have a great environmental impact on the flora and fauna.

7.3.4 Comparison of CO_2 equivalent emissions

Overall, GHG emissions for hydrotreated renewable diesel (HRD)/green diesel produced by hydrodeoxygenation of canola oil are 81.7% lower than low sulfur petrodiesel and for biodiesel,

the emissions are 85.7% lower than low sulfur petrodiesel. The equivalent results obtained are discussed below based on 1L of fuel production. Fig.7.19 represents the gram equivalent emissions of CO_2 per kilometer with the usage of petrodiesel, gasoline, HRD, and biodiesel. It is evident that the gram equivalent CO_2 emissions associated with the usage of HRD and biodiesel are comparatively less than the emissions involved with the usage of petrodiesel and gasoline. Fig. 7.20 compares the emissions on 'per liter' basis.

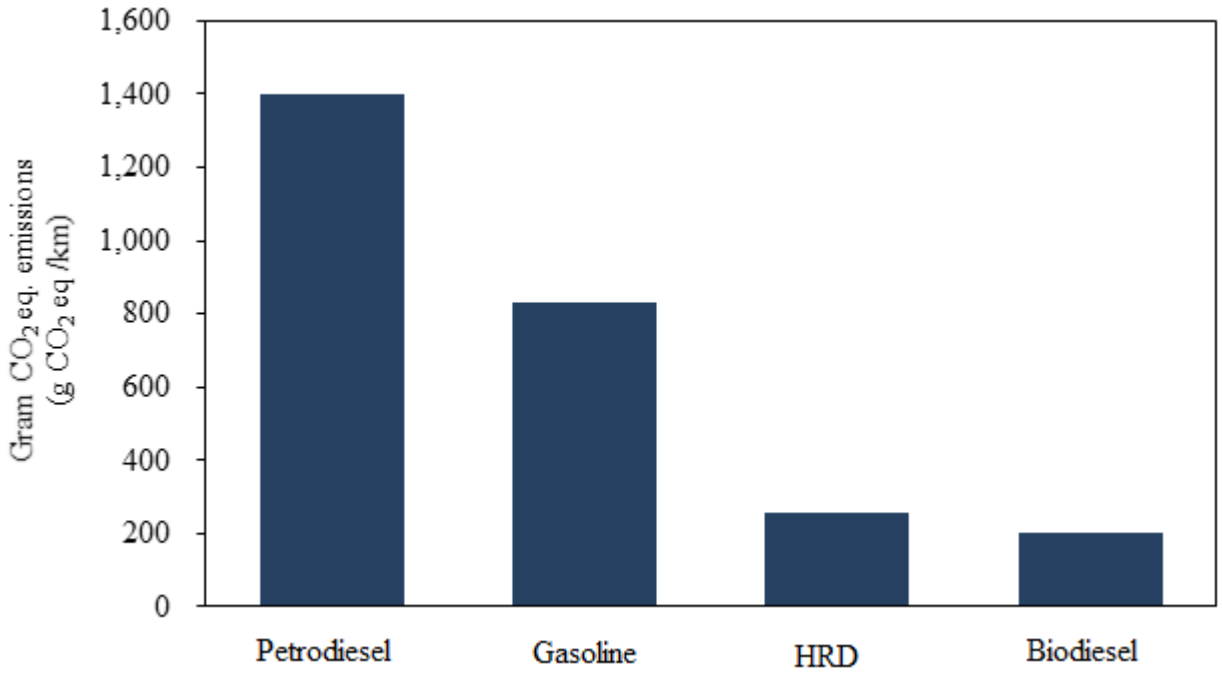

Fig. 7.19. Gram CO_2 eq emissions per km for petrodiesel, gasoline, HRD (green diesel from hydrodeoxygenation) and biodiesel (transesterification)

From Figs. 7.19 and 7.20, it is seen that the emissions involved with the biodiesel are lesser than the HRD. One factor is the involvement of hydrogen and high temperature (> 300°C) / pressure (> 5 MPa) conditions. Moreover, hydrotreatment of vegetable oils yields series of products such as aldehydes, ketones, paraffin and olefins that can attribute to higher CO_2 emissions equivalent in comparison to biodiesel production process.

The gram CO_2 eq emission per liter of fuel for HRD is 610.2 and for biodiesel is 461 which is 84.6% and 88.8% lesser than petrodiesel emissions, respectively. Chloroflurocarbons (CFC) emissions and particulate matter (PM) emissions are nearly the same for both processes. Using 100% hydrotreated diesel or biodiesel requires several engine modifications to enable them to operate properly. Using biofuel blends eliminates the problem of modifying the engine properties as well as extra engine maintenance and oil change.

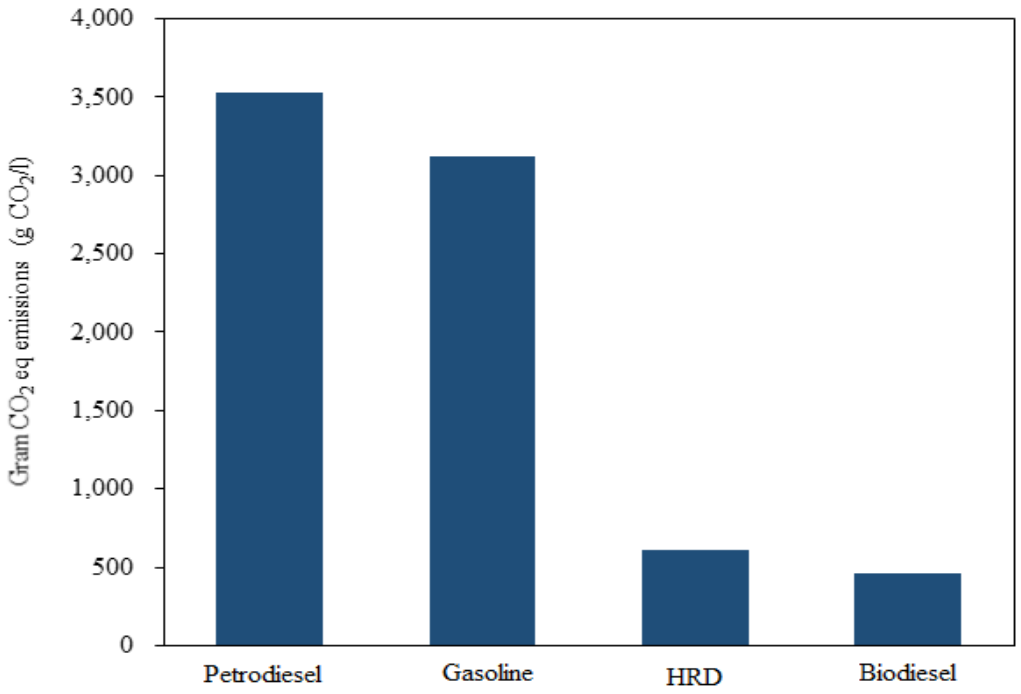

Fig. 7.20. Gram CO_2 eq emissions per liter for petrodiesel, gasoline, HRD (green diesel from hydrodeoxygenation) and biodiesel (transesterification)

Hydrotreated diesel can be added to ASTM D975 standard diesel to a concentration of 50% by volume whereas biodiesel can only be blended to a concentration of 20% in diesel without having to modify engine properties. Environmental impact of B50 HRD and B20 biodiesel are

compared in Fig. 7.21 a & b. It is quite evident that the blend of biodiesel with diesel poses higher environmental impact in comparison to the B50 blend.

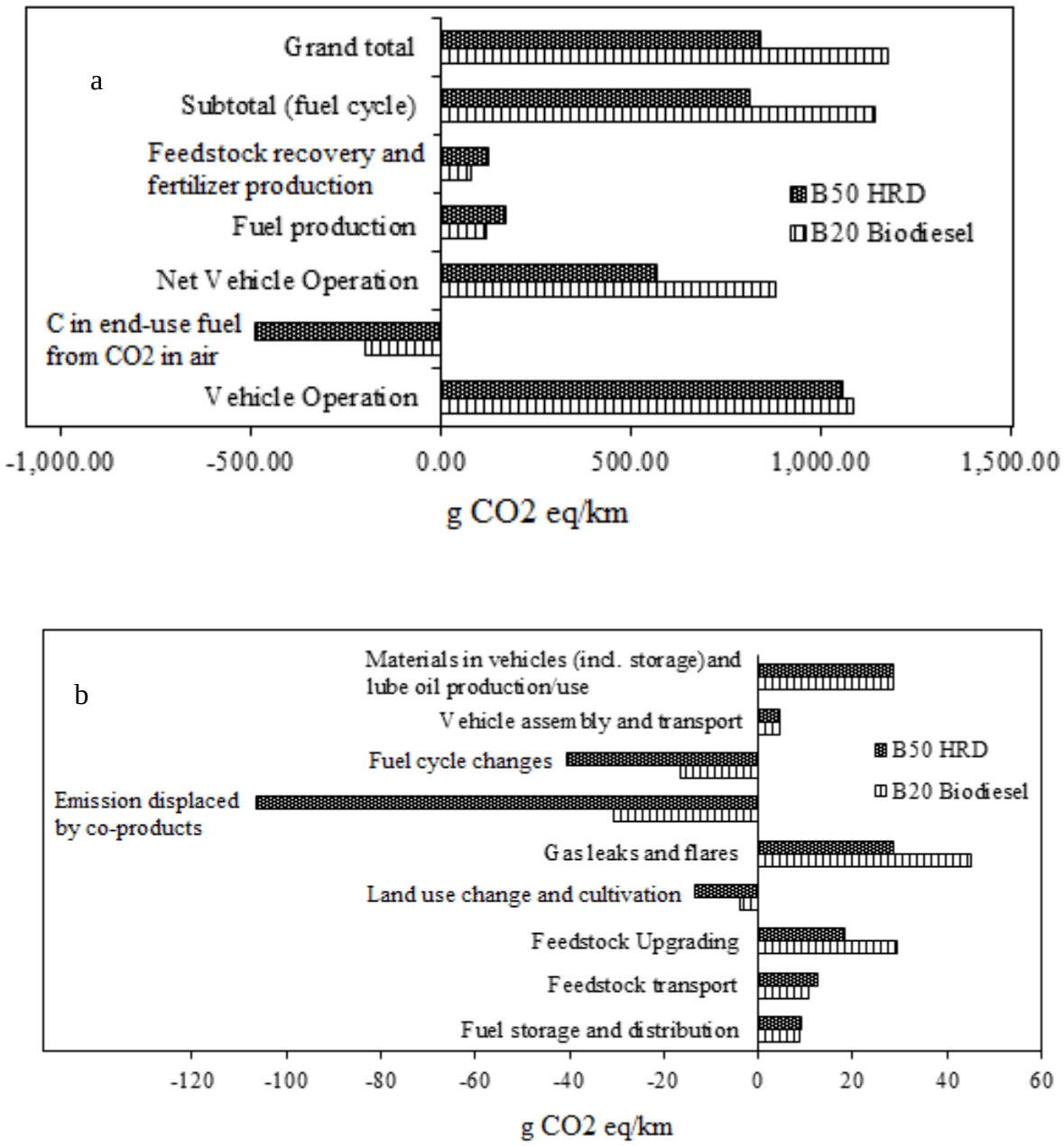

Fig. 7.21. a & b. Comparison of B50 HRD and B20 biodiesel on their environmental impact

In such a scenario, the total g CO_2 eq emissions are lesser for hydrotreated diesel blends compared to biodiesel blends. The second component of the blend in both cases is low sulfur petrodiesel. Therefore, if diesel blends are to be used as a basis for comparison of the two processes, a 50% blend of hydrotreated diesel and gasoline emits 835 g CO_2 eq emissions per liter lesser than a 20% biodiesel blend, thus making it a better alternative fuel for commercial usage.

7.4. Discussion and Conclusions

As the hydrodeoxygenation reaction proceeds to near completion at higher temperatures and pressures, there is a need of a lot of energy. As the process conversion edges downwards, the price edges upwards making the process completely unfeasible and uneconomical at conversions below 95%. The production of biofuel from canola oil through hydrodeoxygenation process is not feasible in the present market condition due to the high cost of raw materials. The fixed production cost for hydrodeoxygenation is 23.4 c/kg and the rest of the cost is due to the cost of raw materials and cost reduction through the sale of glycerol. The hydrotreatment process for the production of green diesel is not commercially feasible for oil prices above $1064/tonne. The process can be more energy efficient if the process has a methodology for energy recovery and reuse.

Over the techno-economic assessment, it was found that the green diesel production pathway is 95% energy efficient while the biodiesel pathway is only 85% energy efficient. A comparison between the production of biodiesel through transesterification and biofuels through HDO reveals that the average emissions of hydro treated diesel are higher than biodiesel but both of them are significantly lower than traditional fossil fuel based low sulfur content petrodiesel and gasoline. Overall the global warming potential (GWP) of HRD is larger than biodiesel, but when

the values obtained are normalized over the total CO_2 emissions in a calendar year, the difference between the two processes is only 0.7%. Comparison of the B50 HRD and B20 biodiesel blend indicates that the total gram equivalent CO_2 emission for the biodiesel blend is higher (~1200 gCO_2 eq/Km) in comparison to B50 HRD blend (~850 gCO_2 eq/Km). From our results, biodiesel production pathway is environmentally benign than the hydrotreatment process owing to its lesser environmental impacts in comparison to green diesel, petrodiesel, and gasoline. Sequestration of CO_2 released as a by-product during hydrodeoxygenation reaction and finding end-usage for the CO_2/CO through reactions such as water-gas shift reaction is essential to increase the environmental credibility of hydrodeoxygenation process. Hydrotreated vegetable oil can be a promising alternative fuel on a commercial scale when blended with diesel. However, considerable research in the area of reaction chemistry, process design and optimization is essential to commercialize the usage of hydrotreated vegetable oils in its pure form.

CHAPTER 8

SUMMARY, CONCLUSIONS, AND RECOMMENDATIONS

8.1 Summary

In this research, FeCu/γ-Al_2O_3 was developed for the hydrodeoxygenation of oleic acid. From the first phases of the work, it was determined that the order of the performance for NiMo on a support for the conversion of oleic acid during HDO and selectivity towards C-18 paraffin: γ-Al_2O_3 > SBA-15> HMS. It is evident that the acidity of the support material plays a vital role in the HDO activity. This work led to the further characterization of this material to understand the HDO reaction mechanism. Raman spectroscopy indicates that Mo is present in the form of clusters and these Mo clusters interact with the support material. The Mo-O coordination distance was found to be 0.18± 0.1nm and Mo-Ni coordination distance was 0.29 ± 0.1nm. The occurrence of particular oxidation states and the coordination environment govern the efficiency of the hydrotreating catalysts. Raman spectroscopy indicates that Mo is present in the form of clusters and these Mo clusters interact with the support material. XRD results indicate that the promoter material (Ni) was well dispersed on the support materials such as γ-Al_2O_3, SBA-15 and HMS.

Comparison of the metal precursors (Mo, V, and W) indicated that molybdenum nitride is the best choice for hydrotreating of oleic acid as it gave higher conversion and product selectivity. Hence, from the continuous flow reactor studies, Mo_2N/γ-Al_2O_3 was found to be the best catalyst. NiMo/γ-Al_2O_3 showed higher conversion (80%) in comparison to NiMo supported on SBA-15 and HMS during the HDO of oleic acid at a reaction temperature of 300°C, a hydrogen pressure of 6.89 MPa and reaction time of 8 h with 8 wt. % catalyst

loading. At higher reaction temperature (>320°C), undesired cracking reactions were observed resulting in the formation of lower carbon number products. Then, at this stage, the catalyst performance of a commercial catalyst for HDO of oleic acid was compared with that of a mixed-metal oxide catalyst (synthesized in the laboratory) and the best catalyst obtained so far in this study. It was found that the performance of mixed metal catalyst (Cu: Zn: Cr: Zr) was superior (HDO conversion~90 %) in comparison to commercial NiMo catalyst (HDO conversion~75 %) and CuNiMo/γ-Al_2O_3 catalyst (HDO conversion~82%) for the HDO of oleic acid. Though the HDO conversion was higher for the mixed oxide catalyst, the product selectivity was better for CuNiMo/γ-Al_2O_3. The comparison of predicted values by Response Surface Methodology (RSM) and Artificial Neural Networks (ANN) with the experimental values was carried out for each experiment for CuNiMo/γ-Al_2O_3 and it was observed that the RSM predicted values are in agreement with the experimental values in the uncertainty range of ±5%. Both models seem to predict the same level of conversion of oleic acid and it is in agreement with the experimental results.

The last part of the work was to compare the techno-economic and life cycle analysis of HDO and transesterification of canola oil. It was concluded that the production of biofuel from canola oil through hydrodeoxygenation process is not feasible in the present market condition due to the high cost of raw materials. The fixed production cost for hydrodeoxygenation is 23.4 c/kg and the rest of the cost is due to the cost of raw materials and cost reduction through the sale of glycerol. The hydrotreatment process for the production of green diesel is not commercially feasible for oil prices above $1064/tonne. The process can be more energy efficient if the process has a methodology for energy recovery and reuse. The gram CO_2 eq emission per liter of fuel for green diesel from HDO is 610 and

for biodiesel is 461 which is 84.6% and 88.8% lesser than petro diesel emissions, respectively. The whole process seems to have high sensitivity to the cost of oil.

8.2 Conclusions

The acidity of the support material was proven to be the most influential parameter in comparison to other physico-chemical properties such as BET surface area and pore volume. HDO reactions are proven to be favored by the higher acidity of support material. Higher temperature (T> 390°C) favored cracking reactions causing a decrease in selectivity towards C-18 paraffin. Better catalytic performance of γ-Al_2O_3 supported catalyst was attributed to the occurrence of distorted tetrahedral-octahedral geometry. In the case of trimetallic catalyst system (CuNiMo/γ-Al_2O_3), the order of influence of process parameters is: reaction temperature>catalyst loading>hydrogen pressure> reaction time. Range analysis and analysis of variance (ANOVA) indicated that the maximum conversion was obtained at a reaction temperature of 325 °C, hydrogen pressure 6.89 MPa, reaction time of 8 h and catalyst loading of 8 wt.%. From the studies using trimetallic catalyst systems, it can be concluded that Cu and Fe as promoters in the above trimetallic catalyst systems are suitable for HDO reactions owing to their affinity towards oxygen and hydrogen activation. FeCu supported on γ-Al_2O_3 was evaluated and its performance was comparable to the existing commercial NiMo catalyst system. The most significant feature of this thesis is the development of novel FeCu supported catalyst system that can actively catalyze HDO reactions at less severe operating conditions and evaluation of techno-economic and life cycle impact of the hydrodeoxygenation process using real feedstock.

8.3 Recommendations for future work

1. Research on the in-situ characterization of the catalysts during hydrodeoxygenation reaction is important and can be a focus of research in future. Also, catalyst development studies for continuous hydrodeoxygenation and long term usage of catalyst needs to be carried out.
2. Studies on the hydrodeoxygenation of real feedstock using continuous fixed-bed reactors should be carried out to check the efficiency of the prepared catalysts in this research and also to develop insights on the continuous biofuels production by hydrodeoxygenation reactions.
3. Studies on the influence of monometallic catalysts such as Cu/γ-Al_2O_3 and Fe/γ-Al_2O_3, and the influence of various synthesis parameters such as metal loading, pH and calcination temperature on catalyst structure and their impacts on HDO activity are recommended.
4. Engine tests on the biofuels produced by hydrodeoxygenation reaction are recommended.
5. Due to the fluctuations in the vegetable oil price, studies on the influence of the cost of vegetable oil on the operational cost, cash-flow analysis and overall profitability of the process needs to be carried out. HDO of vegetable oils can produce CO_2/CO and it is important to develop an end usage for these by products by integrating a CO_2 capture technology with the hydrodeoxygenation unit, and studies on the environmental and economic credibility of such an integrated refinery are essential.
6. Studies on HDO of algal oils to produce diesel range of products and jet fuels is of potential interest in future.

REFERENCES

Alvarado-Morales, M., Boldrin, A., Karakashev, D. B., Holdt, S. L., Angelidaki, I., Astrup, T., "Life cycle assessment of biofuel production from brown seaweed in Nordic conditions", Bioresource Technology, 129, 92–99 (2013).

Arun, N., Sharma, R. V., Dalai, A. K., "Green diesel synthesis by hydrodeoxygenation of bio-based feedstocks: Strategies for catalyst design and development", Renewable and Sustainable Energy Reviews, 48, 240-255 (2015).

Arun, N., Maley, J., Chen, N., Sammynaiken, R., Hu, Y., Dalai, A.K. NiMo nitride supported on γ-Al_2O_3 for hydrodeoxygenation of oleic acid: Novel characterization and activity study (2017) Catalysis Today, 291, pp. 153-159.

Ardiyanti, A.R., Khromova, S.A, Venderbosch, R.H, Yakovlev, V.A, Heeres, H.J., "Catalytic hydrotreatment of fast-pyrolysis oil using non-sulfided bimetallic Ni-Cu catalysts on a δ-Al_2O_3 support", Applied Catalysis B: Environmental, 117– 118, 105–117 (2012).

Aspen Plus User Guide, Version 10.2, Copyright (c) 1981-2000 by Aspen Technology, Inc.

Assen, N., Voll, P., Peters, M., Bardow, A., "Life cycle assessment of CO2 capture and utilization: a tutorial review", Chemical Society Reviews, 43, 7982-7994 (2014).

Ayodele, O.B., Farouk, H.U., Mohammed, J., Uemura, Y., Daud, W.M.A.W, "Hydrodeoxygenation of oleic acid into n- and iso-paraffin biofuel using zeolite supported fluoro-oxalate modified molybdenum catalyst: Kinetics study", Journal of the Taiwan Institute of Chemical Engineers, 50, 142–152 (2015).

Ayodele, O.B., Farouk, H.U., Mohammed, J., Uemura, Y., Daud, W.M.A.W., "Effect of precursor acidity on zeolite supported Pd catalyst properties and hydrodeoxygenation

activity for the production of biofuel", Journal of Molecular Catalysis A: Chemical 400, 179–186 (2015).

Azadi, P., Inderwildi. O. R, Farnood, R., King, D. A., "Liquid fuels, hydrogen and chemicals from lignin: A critical review", Renewable and Sustainable Energy Reviews, 21, 506-523 (2013).

Ben, H., Mu, W., Deng Y, Ragauskas, A. J., "Production of renewable gasoline from aqueous phase hydrogenation of lignin pyrolysis oil", Fuel, 103, 1148–1153 (2013).

Black, M. J., Whittaker, C., Hosseini, S., Diaz-Chavez, R., Woods, J., Murphy, R. J., "Life Cycle Assessment and sustainability methodologies for assessing industrial crops, processes and end products", Industrial Crops and Products, 34, 1332–1339 (2011).

Bu, Q., Lei, H., Zacher, A.H., Wang, L., Ren, S., Liang, J., Wei, Y., Liu, Y., Tang, J., Zhang, Qin, Ruan, R., "A review of catalytic hydrodeoxygenation of lignin-derived phenols from biomass pyrolysis", Bioresource Technology, 124, 470–477 (2012).

Bui, V. N, Laurenti, D., Afanasiev, P., Geantet, C., "Hydrodeoxygenation of guaiacol with CoMo catalysts. Part I: Promoting effect of cobalt on HDO selectivity and activity", Applied Catalysis B: Environmental, 101, 239–245 (2011).

Bykova, M. V, Ermakov, D. Y, Kaichev, V. V, Bulavchenko, O. A, Saraev, A. A, Lebedev, M. Y, Yakovlev, V. A., "Ni-based sol–gel catalysts as promising systems for crude bio-oil upgrading: Guaiacol hydrodeoxygenation study", Applied Catalysis B: Environmental, 113–114, 296– 307 (2012).

Case, P., Wheeler, M. C., DeSisto, W. J., "Formate assisted pyrolysis of pine sawdust for in-situ oxygen removal and stabilization of bio-oil", Bioresource technology, 173, 177–184 (2014).

Cerny, R., Kubu, M., Kubicka, D., "The effect of oxygenates structure on their deoxygenation over USY zeolite", Catalysis Today, 204, 46–53 (2013).

Chen, N., Gong, S., Qian, E.W., "Effect of reduction temperature of NiMoO3-x/SAPO-11 on its catalytic activity in hydrodeoxygenation of methyl laurate" Applied Catalysis B: Environmental, 174-175, 253-263 (2015).

Cherubini, F., Strømman, A. H., "Life cycle assessment of bioenergy systems: State of the art and future challenges" Bioresource Technology, 102, 437–445 (2011).

Chiappero, M., Do, P. T. M, Crossley, S., Lobban, L. L., Resasco, D. E, "Direct conversion of triglycerides to olefins and paraffins over noble metal supported catalysts", Fuel, 90, 1155–1165 (2011).

Chiaramonti, D., Bonini, M., Fratini, E., Tondi, G., Gartner, K., Bridgewater, A. V, Grimm, H. P, Soldaini, I., Webster, A., Baglioni, P., "Development of emulsions from biomass pyrolysis liquid and diesel and their use in engines – Part 1: emulsion production", Biomass and Bioenergy, 25, 85-99 (2003).

Chiu, C., Genest, A., Borgna, A., Ro, N., "Hydrodeoxygenation of Guaiacol over Ru (0001): A DFT Study", ACS Catalysis, 4, 4178–4188 (2014).

Choi, J. S, Bugli, G., Mariadassou, G. D., "Influence of the Degree of Carburization on the Density of Sites and Hydrogenating Activity of Molybdenum Carbides", Journal of Catalysis, 193, 238-247 (2000).

Choudhary, T. V, Phillips, C. B., "Renewable fuels via catalytic hydrodeoxygenation", Applied Catalysis A: General, 397, 1-12 (2011).

Clarens, A. F., Resurreccion, E. P., White, M. A., Colosi, L. M., "Environmental life cycle comparison of algae to other bioenergy feedstocks", Environmental Science and Technology, 44, 1813–1819 (2010).

Jiang, D. T., Chen, N., Sheng, W., "Wiggler-base hard X-ray spectroscopy beamline at CLS" AIP Proceedings, 879, 800–803 (2007).

Damartzis, T., Zabaniotou, A., "Thermochemical conversion of biomass to second generation biofuels through integrated process design-A Review", Renewable and Sustainable Energy Reviews, 15, 366-378 (2011).

De, S., Saha, B., Luque, R., "Hydrodeoxygenation processes: Advances on catalytic transformations of biomass-derived platform chemicals into hydrocarbon fuels", Bioresource Technology, 178, 108–118 (2015).

Dickinson, J. G., Poberezny, J. T., Savage, P. E., "Deoxygenation of benzofuran in supercritical water over a platinum catalyst", Applied Catalysis B: Environmental, 123-124, 357-366 (2012).

Dickinson, J.G., Savage, P.E., "Development of NiCu Catalysts for Aqueous-Phase Hydrodeoxygenation", ACS Catalysis, 4, 2605–2615 (2014).

Dmytryshyn, S. L, Dalai, A. K, Chaudhari, S. T, Mishra, H. K, Reaney, M. J, "Synthesis and characterization of vegetable oil derived esters: evaluation for their diesel additive properties", Bioresource Technology, 92, 55–64 (2004).

Do, P. T. M., Foster, A. J., Chen, J., Lobo, R.F., "Bimetallic effects in the hydrodeoxygenation of meta-cresol on γ-Al_2O_3 supported Pt–Ni and Pt–Co catalysts", Green Chemistry, 14, 1388-1397 (2012).

Donnis, B., Egeberg, R. G., Blom, P., Knudsen, K. G., "Hydroprocessing of bio-oils and oxygenates to hydrocarbons. Understanding the reaction routes" Topics in Catalysis, 52, 229-240 (2009).

Duan, P., Savage, R. E., "Catalytic hydrotreatment of crude algal bio-oil in supercritical water", Applied Catalysis B: Environmental, 104, 136-143 (2011).

Duan, Y., Wu, Y., Zhang, Q., Ding, R., Chen, Y., Liu, J., Yang, M., "Towards conversion of octanoic acid to liquid hydrocarbon via hydrodeoxygenation over Mo promoter nickel-based catalyst", Journal of Molecular Catalysis A: Chemical, 398, 72–78 (2015).

Dupont, C., Lemeur, R., Daudin, A., Raybaud, P., "Hydrodeoxygenation pathways catalyzed by MoS2 and NiMoS active phases: A DFT study", Journal of Catalysis, 279, 276-286 (2011).

Stavitski, E., Weckhuysen, B. M., "Infrared and Raman imaging of heterogeneous catalysts", Chemical Society Reviews, 39, 4615–4625 (2010).

Echeandia, S., Arias, P. L., Barrio, V. L., Pawelec, B., Fierro, J. L. G., "Synergy effect in the HDO of phenol over Ni–W catalysts supported on active carbon: Effect of tungsten precursors", Applied Catalysis B: Environmental, 101, 1–12 (2010).

Elliott, D. C., Hart, T. R., "Catalytic hydroprocessing of chemical models for bio-oil", Energy & Fuels, 23, 631-637 (2009).

Elliott, D. C., "Historical Developments in Hydroprocessing Bio-oils", Energy & Fuels, 21, 1792-1815 (2007).

Fargione, J., Hill, J., Tilman, D., Polasky, F., Hawthorne, P., "Land clearing and the biofuel carbon debt", Science, 319, 1235-1238 (2008).

Ferdous, D., Dalai, A. K., Adjaye, J., "A series of NiMo/γ-Al_2O_3 catalysts containing boron and phosphorus Part II. Hydrodenitrogenation and hydrodesulfurization using heavy gas oil derived from Athabasca bitumen", Applied Catalysis A: General, 260, 153–162 (2004).

Ferrari, M., Delmon, B., Grange, P., "Influence of the impregnation order of molybdenum and cobalt in carbon-supported catalysts for hydrodeoxygenation reactions", Carbon, 40, 497–511 (2002).

Filley, J., Roth, C., "Vanadium catalyzed guaiacol deoxygenation", Journal of Molecular Catalysis A: General, 139, 245–252 (1999).

Foteinis, S., Kouloumpis, V., Tsoutsos, T., "Life cycle analysis for bioethanol production from sugar beet crops in Greece", Energy Policy, 39, 4834–4841 (2011).

Frauwallner, M. L, Lopez-Linares, F., Lara-Romero, J., Scott, C. E., Ali, V., Hernandez, E,, Pereira-Almao, P., "Toluene hydrogenation at low temperature using a molybdenum carbide catalyst" Applied Catalysis A: General, 394, 62–70 (2011).

Furimsky, E., "Metal carbides and nitrides as potential catalysts for hydroprocessing-Review", Applied Catalysis A: General, 240, 1-28 (2003).

GHGenius, Model Version 4.01a; $(S\&T)^2$ Consultants Inc. for Natural Resources Canada: Delta, British Columbia, 2012.

Heijungs, R., Sangwon, S., "The computational structure of life cycle assessment", Kluwer Academic Publishers, Dordrecht, The Netherlands (2013).

Hada, K., Nagai, M., Omi, S., " XPS and TPR studies of Nitrided Molybdena-Alumina", The Journal of Physical Chemistry B, 104, 2090-2098 (2000).

Hinakuma, S., Yamashita, N., katsuhara, Y., Kogami, H., Machida, M., "CO oxidation activity of thermally stable Fe–Cu/CeO_2 catalysts prepared by dual-mode arc-plasma process", Catalysis Science & Technology, 5, 3945-3952.

Hu, H., Wachs, I. E., "Catalytic properties of supported molybdenum oxide catalysts: In situ Raman and methanol oxidation studies". The Journal of Physical Chemistry, 99, 10911–10924 (1995).

Hsu, D. D., "Life cycle assessment of gasoline and diesel produced via fast pyrolysis and hydroprocessing", Biomass and Bioenergy, 45, 41–47 (2012).

Kadam, K. L., "Environmental implications of power generation via coal microalgae cofiring", Energy, 27, 905-922 (2002).

Kauffman, N., Hayes, D., Brown, R., "A life cycle assessment of advanced biofuel production from a hectare of corn", Fuel. 90, 3306–3314 (2011).

Kim, U. J., Furtado, C. A, Liu, X.,Chen, G., Eklund, P. C., "Raman and IR Spectroscopy of Chemically Processed Single-Walled Carbon Nanotubes", Journal of the American Chemical Society, 127, 15437-15445 (2005).

Lamberti, C., Borfecchia, E., van Bokhoven, J. A. and Fernández-García, M. (2016) XAS Spectroscopy: Related Techniques and Combination with Other Spectroscopic and Scattering Methods, in X-Ray Absorption and X-Ray Emission Spectroscopy: Theory and Applications (eds J. A. Van Bokhoven and C. Lamberti), John Wiley & Sons, Ltd, Chichester, UK. doi: 10.1002/9781118844243.ch12

Miskolczi, N., Buyong, F., Angyal, A., Williams, P. T, Bartha, L., "Two stages catalytic pyrolysis of refuse derived fuel: Production of biofuel via syncrude", Bioresource Technology, 101, 8881-8890 (2010).

Mohammad, M., Kandaramath, T., Yaakob, Z., Chandra, Y., "Overview on the production of paraffin based-biofuels via catalytic hydrodeoxygenation", Renewable and Sustainable Energy Reviews, 22, 121-132 (2013).

Nava, R., Ortega, R. A., Alonso, G., Ornelas, C., Pawelec, B., Fierro, J. L. G., "CoMo/Ti-SBA-15 catalysts for dibenzothiophene desulfurization", Catalysis Today, 127, 70–84 (2007).

Requena, J. F. S., Guimaraes, A. C., Alpera, S. Q., Gangas, E. R., Hernandez-navarro, S., Gracia, L. M. N., Martin-Gil, J., Cuesta, H. F., "Life Cycle Assessment (LCA) of the biofuel production process from sunflower oil, rapeseed oil and soybean oil", Fuel Processing Technology, 92, 190–199 (2011).

Roiaini, M., Ardiannie, T., Norhayati, H., " Physicochemical properties of canola oil, olive oil and palm olein blends", International Food Research Journal, 22, 1227-1233 (2015).

Saidi, M., Samimi, F., Karimipourfard, D., Nimmanwudipong, T., Gates, B.C., Rahimpour, M.R., 2014. Upgrading of lignin-derived bio-oils by catalytic hydrodeoxygenation. Energy & Environmental Science, 7, 103-129.

Sharma, R. V., Das, U., Sammynaiken, R., Dalai, A. K., "Liquid phase chemo-selective catalytic hydrogenation of furfural to furfuryl alcohol", Applied Catalysis A: General, 454, 127-136 (2013).

Toor, S. S., Rosendahl, L., Rudolf, A., "Hydrothermal liquefaction of biomass: A review of subcritical water technologies", Energy, 36, 2328-2342 (2011).

Trimm, D. L. Design of Industrial catalysts, Elsevier Scientific publishing company, 1980.

Ulrich, G.D., Vasudevan, P.T. Chemical Engineering Process Design and Economics (2004).

Wagner, M., Lewandowski, I., "Relevance of environmental impact categories for perennial biomass production", GCB Bioenergy, 9, 215–228 (2017).

Wang, W., Yang, Y., Luo, H., Liu, W., “Effect of additive (Co, La) for Ni-Mo-B amorphous catalyst and its hydrodeoxygenation properties”, Catalysis Communications, 11, 803-807 (2010).

Wu, X., Leung, D. Y. C.,” Optimization of biodiesel production from camelina oil using orthogonal experiment", Applied Energy, 88, 11, 3615-3624 (2011).

Xiong, W. M., Fu, Y., Zeng, F. X., Guo, Q. X., “An in situ reduction approach for bio-oil hydroprocessing”, Fuel Processing Technology, 92, 1599–1605 (2011).

Yan, X., Inderwildi, O. R., King, D. A., “Biofuels and synthetic fuels in the US and China: A review of Well-to-Wheel energy use and greenhouse gas emissions with the impact of land-use change”, Energy and Environmental Science, 3, 190-197 (2010).

Zhao, C., He, J., Lemonidou, A. A., Li, X., Lercher, J. A., “Aqueous-phase hydrodeoxygenation of bio-derived phenols to cycloalkanes”, Journal of Catalysis, 280, 8–16 (2011).

APPENDICES

Appendix A: Conversion and Selectivity Sample Calculation

Oxygen Removal (Conversion)

The extent of oxygen removal was calculated for each experiment to determine the conversion of the liquid feed.

$$\%HDO = \frac{\left(x_0^{IN} - x_O^{OUT-ADJ}\right)}{x_O^{IN}} * 100$$

$$\%HDO = \frac{\left(x_0^{IN} - x_O^{OUT-ADJ}\right)}{x_O^{IN}} * 100$$

Where,

x_O^{IN} = Weight percent of oxygen in the liquid entering the reactor

$x_O^{OUT-ADJ}$ = Adjusted weight percent of oxygen in the liquid exiting the reactor

Alkane/Olefin Yield / Diesel Fuel Yield (Selectivity)

The product selectivity was described in terms of liquid yield during the process optimization. A sample calculation and results are as follows, beginning by calculating the normalized organic liquid yield (OLY_N {g/100g}):

$$OLY_N = OLY * \frac{M^{OUT}}{M^{IN}} * 100$$

Where,

OLY = Organic liquid yield fed

M^{OUT} = Total mass exiting the reactor

M^{IN} = Total mass entering the reactor

Appendix B: Copyrights Form

Title: Green diesel synthesis by hydrodeoxygenation of bio-based feedstocks: Strategies for catalyst design and development

Author: Naveenji Arun,Rajesh V. Sharma,Ajay K. Dalai

Publication: Renewable and Sustainable Energy Reviews

Publisher: Elsevier

Date: August 2015

Logged in as:
Naveenji Arun
Account #:
3000671553

LOGOUT

Order Completed

Thank you for your order.

This Agreement between Naveenji Arun ("You") and Elsevier ("Elsevier") consists of your license details and the terms and conditions provided by Elsevier and Copyright Clearance Center.

Your confirmation email will contain your order number for future reference.

Printable details.

License Number	4100830725925
License date	May 02, 2017
Licensed Content Publisher	Elsevier
Licensed Content Publication	Renewable and Sustainable Energy Reviews
Licensed Content Title	Green diesel synthesis by hydrodeoxygenation of bio-based feedstocks: Strategies for catalyst design and development
Licensed Content Author	Naveenji Arun,Rajesh V. Sharma,Ajay K. Dalai
Licensed Content Date	August 2015
Licensed Content Volume	48
Licensed Content Issue	n/a
Licensed Content Pages	16
Type of Use	reuse in a thesis/dissertation
Portion	full article
Format	both print and electronic
Are you the author of this Elsevier article?	Yes
Will you be translating?	No
Order reference number	
Title of your thesis/dissertation	Development of Novel catalysts for the hydrodeoxygenation of vegetable oils

Expected completion date	May 2017
Estimated size (number of pages)	200
Elsevier VAT number	GB 494 6272 12
Requestor Location	Naveenji Arun Box 184, 103 Cumberland Ave. S Saskatoon, SK S7N 1L6 Canada Attn: Naveenji Arun
Total	0.00 USD

ORDER MORE CLOSE WINDOW

Copyright Clearance Center RightsLink®

Account Info Help

Title: NiMo nitride supported on γ-Al2O3 for hydrodeoxygenation of oleic acid: Novel characterization and activity study

Author: Naveenji Arun,Jason Maley,Ning Chen,Ramaswami Sammynaiken,Yongfeng Hu,Ajay K. Dalai

Publication: Catalysis Today

Publisher: Elsevier

Date: Available online 29 April 2017

Logged in as:
Naveenji Arun
Account #: 3000671553
LOGOUT

Order Completed

Thank you for your order.

This Agreement between Naveenji Arun ("You") and Elsevier ("Elsevier") consists of your order details and the terms and conditions provided by Elsevier and Copyright Clearance Center.

License number	Reference confirmation email for license number
License date	Jun, 05 2017
Licensed Content Publisher	Elsevier
Licensed Content Publication	Catalysis Today
Licensed Content Title	NiMo nitride supported on γ-Al2O3 for hydrodeoxygenation of oleic acid: Novel characterization and activity study
Licensed Content Author	Naveenji Arun,Jason Maley,Ning Chen,Ramaswami Sammynaiken,Yongfeng Hu,Ajay K. Dalai
Licensed Content Date	Available online 29 April 2017
Licensed Content Volume	n/a

Licensed Content Issue	n/a
Licensed Content Pages	1
Type of Use	reuse in a thesis/dissertation
Portion	full article
Format	both print and electronic
Are you the author of this Elsevier article?	Yes
Will you be translating?	No
Order reference number	
Title of your thesis/dissertation	Development of Novel catalysts for the hydrodeoxygenation of vegetable oils
Expected completion date	May 2017
Estimated size (number of pages)	200
Elsevier VAT number	GB 494 6272 12
Requestor Location	Naveenji Arun Box 184, 103 Cumberland Ave. S Saskatoon, SK S7N 1L6 Canada Attn: Naveenji Arun
Billing Type	Invoice
Billing address	Naveenji Arun Box 184, 103 Cumberland Ave. S Saskatoon, SK S7N 1L6 Canada Attn: Naveenji Arun
Total	0.00 USD

CLOSE WINDOW

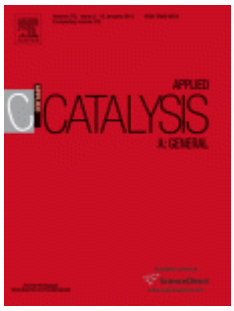

Title: Liquid phase chemo-selective catalytic hydrogenation of furfural to furfuryl alcohol

Author: Rajesh V. Sharma,Umashankar Das,Ramaswami Sammynaiken,Ajay K. Dalai

Publication: Applied Catalysis A: General

Publisher: Elsevier

Date: 15 March 2013

Order Completed

Thank you for your order.

This Agreement between Naveenji Arun ("You") and Elsevier ("Elsevier") consists of your license details and the terms and conditions provided by Elsevier and Copyright Clearance Center.

Your confirmation email will contain your order number for future reference.

Printable details.

License Number	4100911069798
License date	May 02, 2017
Licensed Content Publisher	Elsevier
Licensed Content Publication	Applied Catalysis A: General
Licensed Content Title	Liquid phase chemo-selective catalytic hydrogenation of furfural to furfuryl alcohol
Licensed Content Author	Rajesh V. Sharma,Umashankar Das,Ramaswami Sammynaiken,Ajay K. Dalai
Licensed Content Date	15 March 2013
Licensed Content Volume	454
Licensed Content Issue	n/a
Licensed Content Pages	10
Type of Use	reuse in a thesis/dissertation
Portion	excerpt
Number of excerpts	2
Format	both print and electronic
Are you the author of this Elsevier article?	No
Will you be translating?	No
Order reference number	
Title of your thesis/dissertation	Development of Novel catalysts for the hydrodeoxygenation of vegetable oils
Expected completion date	May 2017
Estimated size (number of pages)	200

Elsevier VAT number	GB 494 6272 12
Requestor Location	Naveenji Arun Box 184, 103 Cumberland Ave. S Saskatoon, SK S7N 1L6 Canada Attn: Naveenji Arun
Total	0.00 USD

ORDER MORE CLOSE WINDOW

Copyright Clearance Center RightsLink® Home Account Info Help

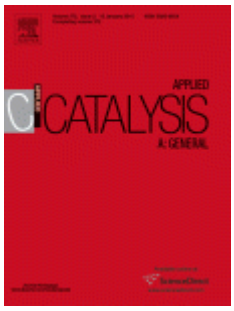

Title: Metal carbides and nitrides as potential catalysts for hydroprocessing
Author: Edward Furimsky
Publication: Applied Catalysis A: General
Publisher: Elsevier
Date: 10 February 2003

Logged in as:
Naveenji Arun
Account #:
3000671553
LOGOUT

Order Completed

Thank you for your order.

This Agreement between Naveenji Arun ("You") and Elsevier ("Elsevier") consists of your license details and the terms and conditions provided by Elsevier and Copyright Clearance Center.

Your confirmation email will contain your order number for future reference.

Printable details.

License Number	4100911222325
License date	May 02, 2017
Licensed Content Publisher	Elsevier
Licensed Content Publication	Applied Catalysis A: General
Licensed Content Title	Metal carbides and nitrides as potential catalysts for hydroprocessing
Licensed Content Author	Edward Furimsky
Licensed Content Date	10 February 2003
Licensed Content Volume	240
Licensed Content Issue	1-2
Licensed Content Pages	28
Type of Use	reuse in a thesis/dissertation
Portion	excerpt
Number of excerpts	1
Format	both print and electronic
Are you the author of this Elsevier article?	No

Will you be translating?	No
Order reference number	
Title of your thesis/dissertation	Development of Novel catalysts for the hydrodeoxygenation of vegetable oils
Expected completion date	May 2017
Estimated size (number of pages)	200
Elsevier VAT number	GB 494 6272 12
Requestor Location	Naveenji Arun Box 184, 103 Cumberland Ave. S Saskatoon, SK S7N 1L6 Canada Attn: Naveenji Arun
Total	0.00 USD

ORDER MORE CLOSE WINDOW

Copyright Clearance Center RightsLink®

Home Account Info Help

Title: Life cycle assessment of biodiesel production in China

Author: Sai Liang,Ming Xu,Tianzhu Zhang

Publication: Bioresource Technology

Publisher: Elsevier

Date: February 2013

Logged in as:
Naveenji Arun
Account #: 3000671553

LOGOUT

Permission Request Submitted

Your request is now under review.
You will be notified of the decision via email.
Please print this request for your records.

Printable details.

Order Number	501265716
Order Date	May 02, 2017
Licensed Content Publisher	Elsevier
Licensed Content Publication	Bioresource Technology
Licensed Content Title	Life cycle assessment of biodiesel production in China
Licensed Content Author	Sai Liang,Ming Xu,Tianzhu Zhang
Licensed Content Date	February 2013

Licensed Content Volume	129
Licensed Content Issue	n/a
Licensed Content Pages	6
Type of Use	reuse in a thesis/dissertation
Portion	figures/tables/illustrations
Number of figures/tables/illustrations	3
Format	both print and electronic
Are you the author of this Elsevier article?	No
Will you be translating?	No

Order reference number	
Original figure numbers	Table 1
Title of your thesis/dissertation	Development of Novel catalysts for the hydrodeoxygenation of vegetable oils
Expected completion date	May 2017
Estimated size (number of pages)	200
Elsevier VAT number	GB 494 6272 12
Requestor Location	Naveenji Arun Box 184, 103 Cumberland Ave. S Saskatoon, SK S7N 1L6 Canada Attn: Naveenji Arun
Total	Not Available

ORDER MORE CLOSE WINDOW

Title: Fuel production by hydrotreating of triglycerides on NiMo/Al2O3/F catalyst

Author: Sándor Kovács,Tamás Kasza,Artur Thernesz,Ilona Wálhné Horváth,Jenő Hancsók

Publication: Chemical Engineering Journal

Publisher: Elsevier

Date: 1 December 2011

Order Completed

Thank you for your order.

This Agreement between Naveenji Arun ("You") and Elsevier ("Elsevier") consists of your license details and the terms and conditions provided by Elsevier and Copyright Clearance Center.

Your confirmation email will contain your order number for future reference.

Printable details.

License Number	4100821094887
License date	May 02, 2017
Licensed Content Publisher	Elsevier
Licensed Content Publication	Chemical Engineering Journal
Licensed Content Title	Fuel production by hydrotreating of triglycerides on NiMo/Al2O3/F catalyst
Licensed Content Author	Sándor Kovács,Tamás Kasza,Artur Thernesz,Ilona Wálhné Horváth,Jenő Hancsók
Licensed Content Date	1 December 2011
Licensed Content Volume	176
Licensed Content Issue	n/a
Licensed Content Pages	7
Type of Use	reuse in a thesis/dissertation
Portion	figures/tables/illustrations
Number of figures/tables/illustrations	1
Format	both print and electronic
Are you the author of this Elsevier article?	No
Will you be translating?	No
Order reference number	
Original figure numbers	Fig. 8
Title of your thesis/dissertation	Development of Novel catalysts for the hydrodeoxygenation of vegetable oils
Expected completion date	May 2017
Estimated size (number of pages)	200
Elsevier VAT number	GB 494 6272 12
Requestor Location	Naveenji Arun Box 184, 103 Cumberland Ave. S Saskatoon, SK S7N 1L6 Canada Attn: Naveenji Arun
Total	0.00 USD

ORDER MORE CLOSE WINDOW

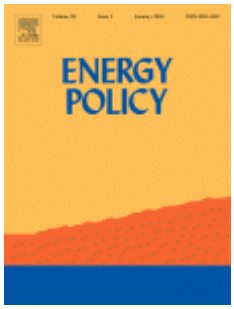

Title: Methods of dealing with co-products of biofuels in life-cycle analysis and consequent results within the U.S. context

Author: Michael Wang,Hong Huo,Salil Arora

Publication: Energy Policy

Publisher: Elsevier

Date: October 2011

Order Completed

Thank you for your order.

This Agreement between Naveenji Arun ("You") and Elsevier ("Elsevier") consists of your license details and the terms and conditions provided by Elsevier and Copyright Clearance Center.

Your confirmation email will contain your order number for future reference.

Printable details.

License Number	4100821351325
License date	May 02, 2017
Licensed Content Publisher	Elsevier
Licensed Content Publication	Energy Policy
Licensed Content Title	Methods of dealing with co-products of biofuels in life-cycle analysis and consequent results within the U.S. context
Licensed Content Author	Michael Wang,Hong Huo,Salil Arora
Licensed Content Date	October 2011
Licensed Content Volume	39
Licensed Content Issue	10
Licensed Content Pages	11
Type of Use	reuse in a thesis/dissertation
Portion	figures/tables/illustrations
Number of figures/tables/illustrations	1
Format	both print and electronic
Are you the author of this Elsevier article?	No
Will you be translating?	No
Order reference number	
Original figure numbers	Table 1
Title of your thesis/dissertation	Development of Novel catalysts for the hydrodeoxygenation of vegetable oils
Expected completion date	May 2017
Estimated size (number of pages)	200
Elsevier VAT number	GB 494 6272 12
Requestor Location	Naveenji Arun Box 184, 103 Cumberland Ave. S Saskatoon, SK S7N 1L6 Canada Attn: Naveenji Arun
Total	0.00 USD

ORDER MORE CLOSE WINDOW

Title: Biofuels and synthetic fuels in the US and China: A review of Well-to-Wheel energy use and greenhouse gas emissions with the impact of land-use change

Author: Xiaoyu Yan,Oliver R. Inderwildi,David A. King

Publication: Energy & Environmental Science

Publisher: Royal Society of Chemistry

Date: Nov 12, 2009

Order Completed

Thank you for your order.

This Agreement between Naveenji Arun ("You") and Royal Society of Chemistry ("Royal Society of Chemistry") consists of your license details and the terms and conditions provided by Royal Society of Chemistry and Copyright Clearance Center.

Your confirmation email will contain your order number for future reference.

Printable details.

License Number	4100830041478
License date	May 02, 2017
Licensed Content Publisher	Royal Society of Chemistry
Licensed Content Publication	Energy & Environmental Science
Licensed Content Title	Biofuels and synthetic fuels in the US and China: A review of Well-to-Wheel energy use and greenhouse gas emissions with the impact of land-use change
Licensed Content Author	Xiaoyu Yan,Oliver R. Inderwildi,David A. King
Licensed Content Date	Nov 12, 2009
Licensed Content Volume	3
Licensed Content Issue	2
Type of Use	Thesis/Dissertation
Requestor type	academic/educational
Portion	figures/tables/images
Number of figures/tables/images	3
Distribution quantity	50
Format	print and electronic
Will you be translating?	no
Order reference number	
Title of the thesis/dissertation	Development of Novel catalysts for the hydrodeoxygenation of vegetable oils

Expected completion date	May 2017
Estimated size	200
Requestor Location	Naveenji Arun Box 184, 103 Cumberland Ave. S Saskatoon, SK S7N 1L6 Canada Attn: Naveenji Arun
Billing Type	Invoice
Billing address	Naveenji Arun Box 184, 103 Cumberland Ave. S Saskatoon, SK S7N 1L6 Canada Attn: Naveenji Arun
Total	0.00 USD

ORDER MORE CLOSE WINDOW

Copyright Clearance Center RightsLink®

Home Account Info Help

Title: Catalytic cracking of edible and non-edible oils for the production of biofuels
Author: Niken Taufiqurrahmi,Subhash Bhatia
Publication: Energy & Environmental Science
Publisher: Royal Society of Chemistry
Date: Mar 2, 2011

Logged in as:
Naveenji Arun
Account #: 3000671553
LOGOUT

Order Completed

Thank you for your order.

This Agreement between Naveenji Arun ("You") and Royal Society of Chemistry ("Royal Society of Chemistry") consists of your license details and the terms and conditions provided by Royal Society of Chemistry and Copyright Clearance Center.

Your confirmation email will contain your order number for future reference.

Printable details.

License Number	4100830189165
License date	May 02, 2017
Licensed Content Publisher	Royal Society of Chemistry
Licensed Content Publication	Energy & Environmental Science
Licensed Content Title	Catalytic cracking of edible and non-edible oils for the production of biofuels
Licensed Content Author	Niken Taufiqurrahmi,Subhash Bhatia
Licensed Content Date	Mar 2, 2011
Licensed Content Volume	4
Licensed Content Issue	4
Type of Use	Thesis/Dissertation
Requestor type	academic/educational
Portion	figures/tables/images
Number of figures/tables/images	3
Distribution quantity	50
Format	print and electronic
Will you be translating?	no
Order reference number	
Title of the thesis/dissertation	Development of Novel catalysts for the hydrodeoxygenation of vegetable oils
Expected completion date	May 2017
Estimated size	200
Requestor Location	Naveenji Arun Box 184, 103 Cumberland Ave. S Saskatoon, SK S7N 1L6 Canada Attn: Naveenji Arun
Billing Type	Invoice
Billing address	Naveenji Arun Box 184, 103 Cumberland Ave. S Saskatoon, SK S7N 1L6 Canada Attn: Naveenji Arun
Total	0.00 USD

ORDER MORE CLOSE WINDOW

Title: Biofuels: a technological perspective

Author: Rafael Luque,Lorenzo Herrero-Davila,Juan M. Campelo,James H. Clark,Jose M. Hidalgo,Diego Luna,Jose M. Marinas,Antonio A. Romero

Publication: Energy & Environmental Science

Publisher: Royal Society of Chemistry

Date: Sep 5, 2008

Order Completed

Thank you for your order.

This Agreement between Naveenji Arun ("You") and Royal Society of Chemistry ("Royal Society of Chemistry") consists of your license details and the terms and conditions provided by Royal Society of Chemistry and Copyright Clearance Center.

Your confirmation email will contain your order number for future reference.

Printable details.

License Number	4100830278125
License date	May 02, 2017
Licensed Content Publisher	Royal Society of Chemistry
Licensed Content Publication	Energy & Environmental Science
Licensed Content Title	Biofuels: a technological perspective
Licensed Content Author	Rafael Luque,Lorenzo Herrero-Davila,Juan M. Campelo,James H. Clark,Jose M. Hidalgo,Diego Luna,Jose M. Marinas,Antonio A. Romero
Licensed Content Date	Sep 5, 2008
Licensed Content Volume	1
Licensed Content Issue	5
Type of Use	Thesis/Dissertation
Requestor type	academic/educational
Portion	figures/tables/images
Number of figures/tables/images	3
Distribution quantity	50
Format	print and electronic
Will you be translating?	no
Order reference number	
Title of the thesis/dissertation	Development of Novel catalysts for the hydrodeoxygenation of vegetable oils
Expected completion date	May 2017
Estimated size	200
Requestor Location	Naveenji Arun Box 184, 103 Cumberland Ave. S

	Saskatoon, SK S7N 1L6 Canada Attn: Naveenji Arun
Billing Type	Invoice
Billing address	Naveenji Arun Box 184, 103 Cumberland Ave. S Saskatoon, SK S7N 1L6 Canada Attn: Naveenji Arun
Total	0.00 USD

ORDER MORE CLOSE WINDOW

Title: Liquid phase chemo-selective catalytic hydrogenation of furfural to furfuryl alcohol

Author: Rajesh V. Sharma,Umashankar Das,Ramaswami Sammynaiken,Ajay K. Dalai

Publication: Applied Catalysis A: General

Publisher: Elsevier

Date: 15 March 2013

Logged in as:
Naveenji Arun
Account #:
3000671553
LOGOUT

Order Completed

Thank you for your order.

This Agreement between Naveenji Arun ("You") and Elsevier ("Elsevier") consists of your license details and the terms and conditions provided by Elsevier and Copyright Clearance Center.

Your confirmation email will contain your order number for future reference.

Printable details.

License Number	4123780943366
License date	Jun 07, 2017
Licensed Content Publisher	Elsevier
Licensed Content Publication	Applied Catalysis A: General
Licensed Content Title	Liquid phase chemo-selective catalytic hydrogenation of furfural to furfuryl alcohol
Licensed Content Author	Rajesh V. Sharma,Umashankar Das,Ramaswami Sammynaiken,Ajay K. Dalai
Licensed Content Date	Mar 15, 2013
Licensed Content Volume	454
Licensed Content Issue	n/a

Licensed Content Pages	10
Type of Use	reuse in a thesis/dissertation
Portion	excerpt
Number of excerpts	2
Format	both print and electronic
Are you the author of this Elsevier article?	No
Will you be translating?	No
Order reference number	
Title of your thesis/dissertation	Development of Novel catalysts for the hydrodeoxygenation of vegetable oils
Expected completion date	May 2017
Estimated size (number of pages)	200
Elsevier VAT number	GB 494 6272 12
Requestor Location	Naveenji Arun Box 184, 103 Cumberland Ave. S Saskatoon, SK S7N 1L6 Canada Attn: Naveenji Arun
Total	0.00 USD

ORDER MORE CLOSE WINDOW

Copyright Clearance Center RightsLink®

Home | Account Info | Help

Title: Biomass as renewable feedstock in standard refinery units. Feasibility, opportunities and challenges

Author: Juan Antonio Melero,Jose Iglesias,Alicia Garcia

Publication: Energy & Environmental Science

Publisher: Royal Society of Chemistry

Date: Mar 30, 2012

Logged in as:
Naveenji Arun
Account #: 3000671553
LOGOUT

Order Completed

Thank you for your order.

This Agreement between Naveenji Arun ("You") and Royal Society of Chemistry ("Royal Society of Chemistry") consists of your license details and the terms and conditions provided by Royal Society of Chemistry and Copyright Clearance Center.

Your confirmation email will contain your order number for future reference.

Printable details.

License Number	4100830427319
License date	May 02, 2017
Licensed Content Publisher	Royal Society of Chemistry
Licensed Content Publication	Energy & Environmental Science
Licensed Content Title	Biomass as renewable feedstock in standard refinery units. Feasibility, opportunities and challenges
Licensed Content Author	Juan Antonio Melero,Jose Iglesias,Alicia Garcia
Licensed Content Date	Mar 30, 2012
Licensed Content Volume	5
Licensed Content Issue	6
Type of Use	Thesis/Dissertation
Requestor type	academic/educational
Portion	figures/tables/images
Number of figures/tables/images	3
Distribution quantity	50
Format	print and electronic
Will you be translating?	no
Order reference number	
Title of the thesis/dissertation	Development of Novel catalysts for the hydrodeoxygenation of vegetable oils
Expected completion date	May 2017
Estimated size	200
Requestor Location	Naveenji Arun Box 184, 103 Cumberland Ave. S Saskatoon, SK S7N 1L6 Canada Attn: Naveenji Arun
Billing Type	Invoice
Billing address	Naveenji Arun Box 184, 103 Cumberland Ave. S Saskatoon, SK S7N 1L6 Canada Attn: Naveenji Arun
Total	0.00 USD

ORDER MORE CLOSE WINDOW

Title: Analysis of biofuels production from sugar based on three criteria: Thermodynamics, bioenergetics, and product separation

Author: Wei-Dong Huang,Y.-H. Percival Zhang

Publication: Energy & Environmental Science

Publisher: Royal Society of Chemistry

Date: Dec 16, 2010

Order Completed

Thank you for your order.

This Agreement between Naveenji Arun ("You") and Royal Society of Chemistry ("Royal Society of Chemistry") consists of your license details and the terms and conditions provided by Royal Society of Chemistry and Copyright Clearance Center.

Your confirmation email will contain your order number for future reference.

Printable details.

License Number	4100830618352
License date	May 02, 2017
Licensed Content Publisher	Royal Society of Chemistry
Licensed Content Publication	Energy & Environmental Science
Licensed Content Title	Analysis of biofuels production from sugar based on three criteria: Thermodynamics, bioenergetics, and product separation
Licensed Content Author	Wei-Dong Huang,Y.-H. Percival Zhang
Licensed Content Date	Dec 16, 2010
Licensed Content Volume	4
Licensed Content Issue	3
Type of Use	Thesis/Dissertation
Requestor type	academic/educational
Portion	figures/tables/images
Number of figures/tables/images	3
Distribution quantity	50
Format	print and electronic
Will you be translating?	no
Order reference number	
Title of the thesis/dissertation	Development of Novel catalysts for the hydrodeoxygenation of vegetable oils
Expected completion date	May 2017
Estimated size	200
Requestor Location	Naveenji Arun Box 184, 103 Cumberland Ave. S

	Saskatoon, SK S7N 1L6 Canada Attn: Naveenji Arun
Billing Type	Invoice
Billing address	Naveenji Arun Box 184, 103 Cumberland Ave. S Saskatoon, SK S7N 1L6 Canada Attn: Naveenji Arun
Total	0.00 USD

ORDER MORE CLOSE WINDOW

Copyright Clearance Center RightsLink® Home Account Info Help

Title: Food waste as a valuable resource for the production of chemicals, materials and fuels. Current situation and global perspective

Author: Carol Sze Ki Lin,Lucie A. Pfaltzgraff,Lorenzo Herrero-Davila,Egid B. Mubofu,Solhy Abderrahim,James H. Clark,Apostolis A. Koutinas,Nikolaos Kopsahelis,Katerina Stamatelatou,Fiona Dickson,Samarthia Thankappan,Zahouily Mohamed,Robert Brocklesby,Rafael Luque

Publication: Energy & Environmental Science

Publisher: Royal Society of Chemistry

Date: Oct 30, 2012

Logged in as:
Naveenji Arun
Account #:
3000671553
LOGOUT

Order Completed

Thank you for your order.

This Agreement between Naveenji Arun ("You") and Royal Society of Chemistry ("Royal Society of Chemistry") consists of your license details and the terms and conditions provided by Royal Society of Chemistry and Copyright Clearance Center.

Your confirmation email will contain your order number for future reference.

Printable details.

License Number	4100830810054
License date	May 02, 2017
Licensed Content Publisher	Royal Society of Chemistry
Licensed Content Publication	Energy & Environmental Science
Licensed Content Title	Food waste as a valuable resource for the production of chemicals, materials and fuels. Current situation and global perspective
Licensed Content Author	Carol Sze Ki Lin,Lucie A. Pfaltzgraff,Lorenzo Herrero-Davila,Egid B. Mubofu,Solhy Abderrahim,James H. Clark,Apostolis A. Koutinas,Nikolaos Kopsahelis,Katerina Stamatelatou,Fiona Dickson,Samarthia Thankappan,Zahouily Mohamed,Robert Brocklesby,Rafael Luque
Licensed Content Date	Oct 30, 2012
Licensed Content Volume	6
Licensed Content Issue	2
Type of Use	Thesis/Dissertation
Requestor type	academic/educational
Portion	figures/tables/images
Number of figures/tables/images	3
Distribution quantity	50
Format	print and electronic
Will you be translating?	no
Order reference number	
Title of the thesis/dissertation	Development of Novel catalysts for the hydrodeoxygenation of vegetable oils
Expected completion date	May 2017
Estimated size	200
Requestor Location	Naveenji Arun Box 184, 103 Cumberland Ave. S Saskatoon, SK S7N 1L6 Canada Attn: Naveenji Arun
Billing Type	Invoice
Billing address	Naveenji Arun Box 184, 103 Cumberland Ave. S Saskatoon, SK S7N 1L6 Canada Attn: Naveenji Arun
Total	0.00 USD

ORDER MORE CLOSE WINDOW

Title: Conversion of Triglycerides to Hydrocarbons Over Supported Metal Catalysts

Author: Tonya Morgan

Publication: Topics in Catalysis
Publisher: Springer
Date: Jan 1, 2010

LOGOUT

Order Completed

Thank you for your order.

This Agreement between Naveenji Arun ("You") and Springer ("Springer") consists of your license details and the terms and conditions provided by Springer and Copyright Clearance Center.

Your confirmation email will contain your order number for future reference.

Printable details.

License Number	4100831021737
License date	May 02, 2017
Licensed Content Publisher	Springer
Licensed Content Publication	Topics in Catalysis
Licensed Content Title	Conversion of Triglycerides to Hydrocarbons Over Supported Metal Catalysts
Licensed Content Author	Tonya Morgan
Licensed Content Date	Jan 1, 2010
Licensed Content Volume	53
Licensed Content Issue	11
Type of Use	Thesis/Dissertation
Portion	Figures/tables/illustrations
Number of figures/tables/illustrations	1
Author of this Springer article	No
Order reference number	
Original figure numbers	Fig. 6
Title of your thesis / dissertation	Development of Novel catalysts for the hydrodeoxygenation of vegetable oils
Expected completion date	May 2017
Estimated size(pages)	200
Requestor Location	Naveenji Arun Box 184, 103 Cumberland Ave. S Saskatoon, SK S7N 1L6 Canada Attn: Naveenji Arun
Billing Type	Invoice
Billing address	Naveenji Arun Box 184, 103 Cumberland Ave. S Saskatoon, SK S7N 1L6 Canada Attn: Naveenji Arun
Total	0.00 USD

ORDER MORE CLOSE WINDOW

Title: Life cycle assessment of sugarcane ethanol and palm oil biodiesel joint production

Author: Simone Pereira Souza,Márcio Turra de Ávila,Sérgio Pacca

Publication: Biomass and Bioenergy

Publisher: Elsevier

Date: September 2012

Order Completed

Thank you for your order.

This Agreement between Naveenji Arun ("You") and Elsevier ("Elsevier") consists of your license details and the terms and conditions provided by Elsevier and Copyright Clearance Center.

Your confirmation email will contain your order number for future reference.

Printable details.

License Number	4100831208254
License date	May 02, 2017
Licensed Content Publisher	Elsevier
Licensed Content Publication	Biomass and Bioenergy
Licensed Content Title	Life cycle assessment of sugarcane ethanol and palm oil biodiesel joint production
Licensed Content Author	Simone Pereira Souza,Márcio Turra de Ávila,Sérgio Pacca
Licensed Content Date	September 2012
Licensed Content Volume	44
Licensed Content Issue	n/a
Licensed Content Pages	10
Type of Use	reuse in a thesis/dissertation
Portion	figures/tables/illustrations
Number of figures/tables/illustrations	1
Format	both print and electronic
Are you the author of this Elsevier article?	No
Will you be translating?	No
Order reference number	
Original figure numbers	Fig. 3
Title of your thesis/dissertation	Development of Novel catalysts for the hydrodeoxygenation of vegetable oils
Expected completion date	May 2017
Estimated size (number of pages)	200
Elsevier VAT number	GB 494 6272 12
Requestor Location	Naveenji Arun Box 184, 103 Cumberland Ave. S

	Saskatoon, SK S7N 1L6 Canada Attn: Naveenji Arun
Total	0.00 USD

ORDER MORE CLOSE WINDOW

Title: Life cycle assessment of sugarcane ethanol and palm oil biodiesel joint production

Author: Simone Pereira Souza,Márcio Turra de Ávila,Sérgio Pacca

Publication: Biomass and Bioenergy

Publisher: Elsevier

Date: September 2012

Logged in as:
Naveenji Arun
Account #:
3000671553
LOGOUT

Order Completed

Thank you for your order.

This Agreement between Naveenji Arun ("You") and Elsevier ("Elsevier") consists of your license details and the terms and conditions provided by Elsevier and Copyright Clearance Center.

Your confirmation email will contain your order number for future reference.

Printable details.

License Number	4100831278539
License date	May 02, 2017
Licensed Content Publisher	Elsevier
Licensed Content Publication	Biomass and Bioenergy
Licensed Content Title	Life cycle assessment of sugarcane ethanol and palm oil biodiesel joint production
Licensed Content Author	Simone Pereira Souza,Márcio Turra de Ávila,Sérgio Pacca
Licensed Content Date	September 2012
Licensed Content Volume	44
Licensed Content Issue	n/a
Licensed Content Pages	10
Type of Use	reuse in a thesis/dissertation
Portion	figures/tables/illustrations
Number of figures/tables/illustrations	1
Format	both print and electronic
Are you the author of this Elsevier article?	No
Will you be translating?	No
Order reference number	
Original figure numbers	Fig. 2

Title of your thesis/dissertation	Development of Novel catalysts for the hydrodeoxygenation of vegetable oils
Expected completion date	May 2017
Estimated size (number of pages)	200
Elsevier VAT number	GB 494 6272 12
Requestor Location	Naveenji Arun Box 184, 103 Cumberland Ave. S Saskatoon, SK S7N 1L6 Canada Attn: Naveenji Arun
Total	0.00 USD

ORDER MORE CLOSE WINDOW

Copyright Clearance Center RightsLink®

Home | Account Info | Help

Title: Life cycle assessment of CO2 capture and utilization: a tutorial review

Author: Niklas von der Assen,Philip Voll,Martina Peters,André Bardow

Publication: Chemical Society Reviews

Publisher: Royal Society of Chemistry

Date: Jan 20, 2014

Logged in as:
Naveenji Arun
Account #:
3000671553

LOGOUT

Order Completed

Thank you for your order.

This Agreement between Naveenji Arun ("You") and Royal Society of Chemistry ("Royal Society of Chemistry") consists of your license details and the terms and conditions provided by Royal Society of Chemistry and Copyright Clearance Center.

Your confirmation email will contain your order number for future reference.

Printable details.

License Number	4100831421589
License date	May 02, 2017
Licensed Content Publisher	Royal Society of Chemistry
Licensed Content Publication	Chemical Society Reviews
Licensed Content Title	Life cycle assessment of CO2 capture and utilization: a tutorial review
Licensed Content Author	Niklas von der Assen,Philip Voll,Martina Peters,André Bardow
Licensed Content Date	Jan 20, 2014
Licensed Content Volume	43

Licensed Content Issue	23
Type of Use	Thesis/Dissertation
Requestor type	academic/educational
Portion	figures/tables/images
Number of figures/tables/images	3
Distribution quantity	100
Format	print and electronic
Will you be translating?	no
Order reference number	
Title of the thesis/dissertation	Development of Novel catalysts for the hydrodeoxygenation of vegetable oils
Expected completion date	May 2017
Estimated size	200
Requestor Location	Naveenji Arun Box 184, 103 Cumberland Ave. S Saskatoon, SK S7N 1L6 Canada Attn: Naveenji Arun
Billing Type	Invoice
Billing address	Naveenji Arun Box 184, 103 Cumberland Ave. S Saskatoon, SK S7N 1L6 Canada Attn: Naveenji Arun
Total	0.00 USD

ORDER MORE CLOSE WINDOW

Copyright Clearance Center RightsLink®

Home | Account Info | Help

Title: Sustainability assessment of novel chemical processes at early stage: application to biobased processes

Author: Akshay D. Patel,Koen Meesters,Herman den Uil,Ed de Jong,Kornelis Blok,Martin K. Patel

Publication: Energy & Environmental Science

Publisher: Royal Society of Chemistry

Date: Jun 14, 2012

Logged in as:
Naveenji Arun
Account #: 3000671553
LOGOUT

Order Completed

Thank you for your order.

This Agreement between Naveenji Arun ("You") and Royal Society of Chemistry ("Royal Society of Chemistry") consists of your license details and the terms and conditions provided by Royal Society of Chemistry and Copyright Clearance Center.

Your confirmation email will contain your order number for future reference.

Printable details.

License Number	4100831492368
License date	May 02, 2017
Licensed Content Publisher	Royal Society of Chemistry
Licensed Content Publication	Energy & Environmental Science
Licensed Content Title	Sustainability assessment of novel chemical processes at early stage: application to biobased processes
Licensed Content Author	Akshay D. Patel,Koen Meesters,Herman den Uil,Ed de Jong,Kornelis Blok,Martin K. Patel
Licensed Content Date	Jun 14, 2012
Licensed Content Volume	5
Licensed Content Issue	9
Type of Use	Thesis/Dissertation
Requestor type	academic/educational
Portion	figures/tables/images
Number of figures/tables/images	3
Distribution quantity	100
Format	print and electronic
Will you be translating?	no
Order reference number	
Title of the thesis/dissertation	Development of Novel catalysts for the hydrodeoxygenation of vegetable oils
Expected completion date	May 2017
Estimated size	200
Requestor Location	Naveenji Arun Box 184, 103 Cumberland Ave. S Saskatoon, SK S7N 1L6 Canada Attn: Naveenji Arun
Billing Type	Invoice
Billing address	Naveenji Arun Box 184, 103 Cumberland Ave. S Saskatoon, SK S7N 1L6 Canada Attn: Naveenji Arun
Total	0.00 USD

ORDER MORE CLOSE WINDOW

Title: Life cycle assessment of biodiesel production in China

Author: Sai Liang,Ming Xu,Tianzhu Zhang

Publication: Bioresource Technology

Publisher: Elsevier

Date: February 2013

Permission Request Submitted

Your request is now under review.
You will be notified of the decision via email.
Please print this request for your records.

Printable details.

Order Number	501265733
Order Date	May 02, 2017
Licensed Content Publisher	Elsevier
Licensed Content Publication	Bioresource Technology
Licensed Content Title	Life cycle assessment of biodiesel production in China
Licensed Content Author	Sai Liang,Ming Xu,Tianzhu Zhang
Licensed Content Date	February 2013
Licensed Content Volume	129
Licensed Content Issue	n/a
Licensed Content Pages	6
Type of Use	reuse in a thesis/dissertation
Portion	figures/tables/illustrations
Number of figures/tables/illustrations	1
Format	both print and electronic
Are you the author of this Elsevier article?	No
Will you be translating?	No
Order reference number	
Original figure numbers	Table 1
Title of your thesis/dissertation	Development of Novel catalysts for the hydrodeoxygenation of vegetable oils
Expected completion date	May 2017
Estimated size (number of pages)	200
Elsevier VAT number	GB 494 6272 12
Requestor Location	Naveenji Arun Box 184, 103 Cumberland Ave. S Saskatoon, SK S7N 1L6 Canada

	Attn: Naveenji Arun
Total	Not Available

ORDER MORE CLOSE WINDOW

Copyright Clearance Center RightsLink®

Home | Account Info | Help

Title: Life cycle assessment of bioenergy systems: State of the art and future challenges

Author: Francesco Cherubini,Anders Hammer Strømman

Publication: Bioresource Technology

Publisher: Elsevier

Date: January 2011

Logged in as:
Naveenji Arun
Account #:
3000671553

LOGOUT

Permission Request Submitted

Your request is now under review.
You will be notified of the decision via email.
Please print this request for your records.

Printable details.

Order Number	501265734
Order Date	May 02, 2017
Licensed Content Publisher	Elsevier
Licensed Content Publication	Bioresource Technology
Licensed Content Title	Life cycle assessment of bioenergy systems: State of the art and future challenges
Licensed Content Author	Francesco Cherubini,Anders Hammer Strømman
Licensed Content Date	January 2011
Licensed Content Volume	102
Licensed Content Issue	2
Licensed Content Pages	15
Type of Use	reuse in a thesis/dissertation
Portion	figures/tables/illustrations
Number of figures/tables/illustrations	1
Format	both print and electronic
Are you the author of this Elsevier article?	No
Will you be translating?	No
Order reference number	
Original figure numbers	Fig.2
Title of your thesis/dissertation	Development of Novel catalysts for the hydrodeoxygenation of vegetable oils
Expected completion date	May 2017
Estimated size (number	200

of pages)	
Elsevier VAT number	GB 494 6272 12
Requestor Location	Naveenji Arun Box 184, 103 Cumberland Ave. S Saskatoon, SK S7N 1L6 Canada Attn: Naveenji Arun
Total	Not Available

ORDER MORE CLOSE WINDOW

Copyright Clearance Center RightsLink®

Home Account Info Help

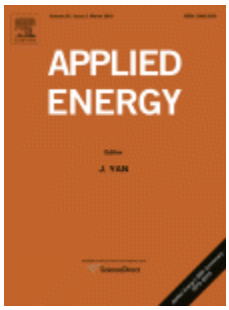

Title: Optimization of biodiesel production from camelina oil using orthogonal experiment
Author: Xuan Wu,Dennis Y.C. Leung
Publication: Applied Energy
Publisher: Elsevier
Date: November 2011

Logged in as:
Naveenji Arun
Account #:
3000671553
LOGOUT

Order Completed

Thank you for your order.

This Agreement between Naveenji Arun ("You") and Elsevier ("Elsevier") consists of your license details and the terms and conditions provided by Elsevier and Copyright Clearance Center.

Your confirmation email will contain your order number for future reference.

Printable details.

License Number	4100910826261
License date	May 02, 2017
Licensed Content Publisher	Elsevier
Licensed Content Publication	Applied Energy
Licensed Content Title	Optimization of biodiesel production from camelina oil using orthogonal experiment
Licensed Content Author	Xuan Wu,Dennis Y.C. Leung
Licensed Content Date	November 2011
Licensed Content Volume	88

Licensed Content Issue	11
Licensed Content Pages	10
Type of Use	reuse in a thesis/dissertation
Portion	excerpt
Number of excerpts	3
Format	both print and electronic
Are you the author of this Elsevier article?	No
Will you be translating?	No
Order reference number	
Title of your thesis/dissertation	Development of Novel catalysts for the hydrodeoxygenation of vegetable oils
Expected completion date	May 2017
Estimated size (number of pages)	200
Elsevier VAT number	GB 494 6272 12
Requestor Location	Naveenji Arun Box 184, 103 Cumberland Ave. S Saskatoon, SK S7N 1L6 Canada Attn: Naveenji Arun
Total	0.00 USD

ORDER MORE CLOSE WINDOW

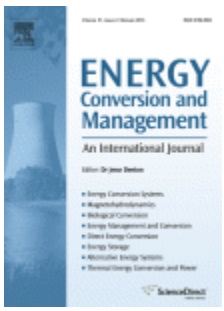

Title: Optimization of sunflower oil ethanolysis catalyzed by calcium oxide: RSM versus ANN-GA

Author: Jelena M. Avramović,Ana V. Veličković,Olivera S. Stamenković,Katarina M. Rajković,Petar S. Milić,Vlada B. Veljković

Publication: Energy Conversion and Management

Publisher: Elsevier

Date: 15 November 2015

Order Completed

Thank you for your order.

This Agreement between Naveenji Arun ("You") and Elsevier ("Elsevier") consists of your license details and the terms and conditions provided by Elsevier and Copyright Clearance Center.

Your confirmation email will contain your order number for future reference.

Printable details.

License Number	4100910947763
License date	May 02, 2017
Licensed Content Publisher	Elsevier
Licensed Content Publication	Energy Conversion and Management
Licensed Content Title	Optimization of sunflower oil ethanolysis catalyzed by calcium oxide: RSM versus ANN-GA
Licensed Content Author	Jelena M. Avramović,Ana V. Veličković,Olivera S. Stamenković,Katarina M. Rajković,Petar S. Milić,Vlada B. Veljković
Licensed Content Date	15 November 2015
Licensed Content Volume	105
Licensed Content Issue	n/a
Licensed Content Pages	8
Type of Use	reuse in a thesis/dissertation
Portion	excerpt
Number of excerpts	3
Format	both print and electronic
Are you the author of this Elsevier article?	No
Will you be translating?	No
Order reference number	
Title of your thesis/dissertation	Development of Novel catalysts for the hydrodeoxygenation of vegetable oils
Expected completion date	May 2017
Estimated size (number of pages)	200
Elsevier VAT number	GB 494 6272 12
Requestor Location	Naveenji Arun Box 184, 103 Cumberland Ave. S Saskatoon, SK S7N 1L6 Canada Attn: Naveenji Arun
Total	0.00 USD

ORDER MORE CLOSE WINDOW